FOSSIL ENERGY

DOE/BC/14883-10
(DE95000135)

SURFACTANT-ENHANCED ALKALINE FLOODING FOR LIGHT OIL RECOVERY

1993-1994

By
Darsh T. Wasan

March 1995

Performed Under Contract No. DE-AC22-92BC14883

Illinois Institute of Technology
Chicago, Illinois

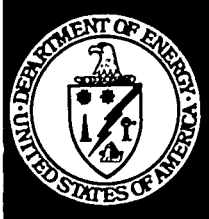

Bartlesville Project Office
U. S. DEPARTMENT OF ENERGY
Bartlesville, Oklahoma

DOE/BC/14883-10
Distribution Category UC-122

SURFACTANT-ENHANCED ALKALINE FLOODING FOR LIGHT OIL RECOVERY

1993-1994

By
Darsh T. Wasan

March 1995

Work Performed Under Contract No. DE-AC22-92BC14883

Prepared for
U.S. Department of Energy
Assistant Secretary for Fossil Energy

Jerry Casteel, Project Manager
Bartlesville Project Office
P.O. Box 1398
Bartlesville, OK 74005

Prepared by
Illinois Institute of Technology
10 West 33rd St.
Chicago, IL 60616

TABLE OF CONTENTS

LIST OF FIGURES

CHAPTER ONE

CHAPTER TWO

CHAPTER THREE

LIST OF TABLES

CHAPTER TWO

EXECUTIVE SUMMARY

In this report, we present the results of our experimental and theoretical studies in surfactant-enhanced alkaline flooding for light oil recovery. The overall objective of this work is to develop a very cost-effective method for formulating a successful surfactant-enhanced alkaline flood by appropriately choosing mixed alkalis which form inexpensive buffers to obtain the desired pH (between 8.5 and 12.0) for ultimate spontaneous emulsification and ultralow interfacial tension. In addition, we have (1) investigated the effect of surfactant on the equilibrium and transient interfacial tension, (2) investigated the kinetics of oil removal from a silica surface, and (3) developed a theoretical interfacial activity model for determining equilibrium interfacial tension. The results of the studies conducted during the course of this project are summarized below.

The effect of added surfactant in alkali/acidic oil systems

An experimental investigation of the buffered surfactant-enhanced alkaline flooding system chemistry was undertaken to determine the influence of various species present on interfacial tension as a function of pH and ionic strength. Phase behavior tests that monitor the extent of emulsification are sufficient to determine the region of low interfacial tension. Optimization of interfacial tension by adjustment of the ionic strength alone may not necessarily provide the lowest interfacial tension under the best conditions. The pH should be simultaneously optimized along with ionic strength to allow better control over attainment of low interfacial tension. The dominant mechanism by which added surfactant aids in the reduction of interfacial tension is the formation of mixed micelles with the ionized acid. Although added surfactant partitioning from the influence of the unionized acid and ionic strength will affect interfacial behavior, the formation of mixed micelles plays a dominant role. Middle phase formation is possible with a low acid oil using a petroleum sulfonate at a proper pH and ionic strength.

Fluid-solid interaction: optical imaging by differential and common interferometry

A new experimental technique has been developed and used to determine the three-phase

contact angle and to study the three-phase contact angle kinetics using common and differential interferometry. It has been found that for most systems studied, the contact angle increases with time until the crude oil droplet separates from the silica surface. The addition of surfactant causes the kinetics of separation to be slower. With smaller drops, the three-phase contact angle reaches its equilibrium value faster. It was also observed that water penetrates between the crude oil and silica surface to form a water film which helps the crude oil to separate from the silica surface.

Interactions in acidic oil/Alkaline-surfactant solutions: Theoretical Studies

This chapter describes predictive models developed for computing the interfacial tension of a system chosen to model acidic light crude oil in contact with alkaline solution of a surfactant. The bulk phase concentrations and specific adsorptions of the various surface active components are computed based on the pseudo-phase separation theory and the mass action model for mixed micelle formation. Non-ideality due to mixing of two types of surface active components, namely the generated soap and the added surfactant, is modeled by the regular solution approximation. The model was used to analyse experimental data where the sodium ion concentration was kept constant by the addition of NaCl. The increase in the number of micelles with alkali concentration causes the actual sodium ion concentration to decrease. Its effect on the electrostatic contribution to the surface pressure is examined in this model. The model also accounts for surfactant partitioning into the oil phase.

PUBLICATIONS

1-1. "The Effect of Added Surfacant on Interfacial Tension and Spontaneous Emulsification in Alkali/Acidic Oil Systems", Rudin, J., Bernard, C., and Wasan, D.T., *Industrial and Engineering Chemistry Research*, **33**, 1150-1158 (1994).

1-2. "Oscillatory Deep Channel Interfacial Rheometer," Nagarajan, R. and D.T. Wasan, *Rev. of Scientific Instruments*, **65**, 2675 (1994).

1-3. "Coalescence of Single Drops at a Liquid-Liquid Interface in the Presence of Surfactants/Polymers," Aderangi, N. and D.T. Wasan, *Chemical Engineering Comm.*, (1994)(in Press).

1-4. "A Controlled Drop Tensiometer for Measuring Dynamic Interfacial Tension and Film Tension," Nagarajan, R., Koczo, K., Erdos, E., and D.T. Wasan, *A.I.Ch.E. Journal*, (1994)(in Press).

1-5. "Study of Dynamic Interfacial Mechanisms For Demulsification of Water-in-Oil Emulsions," Kim, Y.H., D.T. Wasan, and P.J. Breen, *Colloids and Surfaces*, (1994)(in Press).

1-6. "Automatic Apparatus for Measuring Interfacial and Film Tension Under Static and Dynamic Conditions," Soos, J.M., K. Koczo, E. Erdos and D.T. Wasan, *Rev. of Scientific Instruments*, (1994)(in Press).

CHAPTER 1

The Effect of Added Surfactant in Alkali/Acidic Oil Systems

INTRODUCTION

Rudin and Wasan (1993) have shown in the absence of added surfactant that the interfacial tension is sensitive to the pH, and when ionic strength is high, interfacial tension goes through a deep minimum. This minimum is caused by the simultaneous adsorption of ionized and unionized acid upon the interface. With this understanding that the pH is just as important as ionic strength in affecting interfacial tension and extent of emulsification, a practical method was developed (Rudin and Wasan, 1993) to cost-effectively buffer the aqueous alkaline pH in an intermediate range (pH of 9 to 12) by using mixed alkalis.

The investigation of surfactant-enhanced alkali/acidic crude oil interactions with relation to improved oil recovery has been addressed by several investigators (Martin et al., 1985; Nelson et al., 1984; French and Burtchfield, 1990; Schuler et al., 1986). It has been shown that small amounts of surfactant, normally less than 0.5 wt%, together with an alkaline additive can produce ultralow interfacial tension (i.e., a high interfacial activity) against an acidic crude oil, improving oil recovery. Many investigators (Martin et al., 1985; Nelson et al., 1984; French and Burtchfield, 1990; Schuler et al., 1986) have shown that there is a beneficial synergistic effect of combining alkali with surfactant in lowering interfacial tension and improving oil recovery. It is still unknown whether transient (initial) interfacial tension or equilibrium interfacial tension is more important or both in improving oil recovery. What is known is that oil recovery is higher with the combination of surfactant and alkali than with either taken alone, and the addition of a mobility control polymer can make the alkali/surfactant/polymer process several times less expensive than the micellar/polymer flood, recovering the same amount of oil (Surkalo, 1990). The surfactant-enhanced alkaline flooding process as well as the alkaline flooding process are

classically interpreted on the basis of salinity. However, all fail to consider the effect of pH, and as a result, the process is explained solely in terms of the effect of ionic strength. This reasoning can lead the researcher to misinterpret the results or cause confusion in designing meaningful formulations to be injected into the oil reservoir.

The alkali, as explained by Krumrine et al. (1982a) and (1982b), serves a dual role. First, interfacial tension is lowered by the generation of soaps, which reduce capillary forces and facilitate oil displacement. Second, surfactant retention is reduced by the alkali by imparting a negative charge on the rock surface, thus providing a larger supply of surfactant for sustaining high interfacial activity. Falcone et al. (1982) has shown that not only is surfactant adsorption reduced, but it is minimal in the intermediate pH range of 9-12. When divalent ions are present, the alkali precipitates as a multivalent hydroxide, reducing the detrimental effect of divalent ions on surfactant solubility and at the same time plugging the pores with improvement in areal sweep efficiency.

The addition of surfactant to the alkaline solution certainly improves oil recovery. However, the exact role that the surfactant plays in its synergism with the alkali and how to take advantage of this synergism in designing floods for maximum oil production is still unknown. In this chapter, alkali/acidic oil interactions are investigated in order to better understand the mechanisms involved in improving oil recovery by surfactant-enhanced alkaline flooding.

MATERIALS AND EXPERIMENTS

In this study, two crude oils containing natural organic acids were contacted with an alkaline pH aqueous solution. One crude oil used in this investigation is a Long Beach crude oil

obtained from THUMS Long Beach Company, having an acid number of 1.0 determined from ASTM procedure D-664 and an API gravity of 24.9. It was centrifuged at 40,000 G's for 30 minutes remove water and clays. The viscosity of the crude oil after centrifuging was 52 cp at 25 °C and the interfacial tension against deionized water was 24.5 dyne/cm. The other crude oil used was obtained from SURTEK from Adena field located in Morgan County, Colorado. It is a light oil with an API gravity of 41.95, a viscosity of 3.75 cp at 25 °C, and an acid number less than 0.002.

The alkaline solutions were a mixture of sodium hydroxide, sodium chloride, and Trona, which is an industrial grade chemical being 94% sodium bicarbonate. All alkalis were obtained from Fisher Scientific Co., except Trona, which was obtained from Kerr-McGee Chemical Company.

Two preformed surfactants were also added to the alkaline solution. Petroleum sulfonates, Petrostep B-100 and Petrostep B-105 (55% active) were obtained from Stepan Chemical Company, and the surfactant solutions were made on a 100% active basis.

Pre-equilibrated samples were made by stirring equal volumes of aqueous and oil phases for at least 6 hours and allowing them to equilibrate for one week or more. The spinning drop technique was employed to measure both equilibrium and transient (non-equilibrated) interfacial tensions. Equilibrium interfacial tension readings were made when the interfacial tension had reached a steady value, ranging from 0.5 to 8.0 hrs. The volumetric ratio of water to oil in the spinning drop tensiometer is about 140. If all the acid that is in the oil drop went into the water phase during transient interfacial tension measurements, the concentration of ionized acid would be 0.12 mol/m^3. Percent transmittance was measured using a Beckman spectrophotometer set

at 600 nm with deionized water as the reference. The pH was measured using an Orion microprocessor analyzer/901 with a Ross combination electrode designed for low sodium error. All experiments were performed at 25 ± 1 °C.

Throughout this study, the solutions were made by diluting an equimolar ratio of Trona/NaOH (referred to as 20/20) with either the same molarity of Trona plus NaCl to keep the total sodium constant or the same molarity of NaOH plus enough NaCl the keep the total sodium constant. By changing the ratio of Trona/NaOH the pH is changed so that we get lower pH's by adding the Trona plus NaCl solution to the 20/20 mixture or higher pH's by adding the NaOH plus NaCl solution to the 20/20 mixture. The buffering ability was investigated by diluting a solution of constant molar ratio of Trona/NaOH, containing 343 mol/m^3 total sodium, with 343 mol/m^3 NaCl. It should be noted that 343 mol/m^3 total sodium is about 2.0 wt% Trona/NaOH mixture.

RESULTS AND DISCUSSION

As described in the previous papers by Rudin and Wasan (1992a), (1992b) and (1992c), the naturally occurring organic acids in the oil when extracted into the aqueous phase will form mixed micelles. Each species will have its own critical micelle concentration (CMC), however, the CMC of the mixture will be an effective CMC for the system. The petroleum sulfonates used in this study are a blend of various chain lengths. So, the CMC of the sulfonate is an effective CMC for the system. This also holds true when ionized acid and sulfonates form mixed micelles. Throughout this chapter, the usage of CMC usually refers to the effective CMC of the system.

Effect of pH

Figures 1-1a and 1-1b show the transient interfacial tension as a function of pH for 0.1% Petrostep B-100 at 343 mol/m^3 sodium ions. By adding surfactant, the transient interfacial tension levels off to about 0.025 dyne/cm, whereas with no added surfactant the interfacial tension has a sharp increase to about 1 dyne/cm. As pH increases to higher values, the transient minimum disappears, and interfacial tension is at a higher value for all times. This higher tension is most likely due to the ionized acid being not as an effective reducer of interfacial tension as is the added surfactant. As a result, there may be more ionized acid (relative to added surfactant) in monomer form in the bulk (because of mixed micelles) at higher pH, causing interfacial tension to level off at a higher value. The higher interfacial tension at higher pH may also result from less available unionized acid to contribute to a higher surface pressure.

Figure 1-2 shows the comparison of the transient interfacial tension at 400 seconds for 343 mol/m^3 sodium ions with and without 0.1% Petrostep B-100. By adding Petrostep B-100, the minimum shifts to lower pH, and the interfacial tension is low over a larger range of pH. A lower pH is advantageous in that alkali consumption by rock dissolution will be reduced (Martin et al., 1985; Nelson et al., 1984; French and Burchfield, 1990; Holm and Robertson, 1981; ΩSouthwick and Nelson, 1984). It is also interesting to note that the interfacial tension with and without added surfactant approaches the same value. This is to be expected, because ionized acid is becoming the dominating species at higher pH.

The extent of emulsification at equilibrium, where it is measured as the percent transmittance of the aqueous phase is shown in Figure 1-3. The same trends observed in the transient interfacial tension are observed here. The lower the transient interfacial tension, the

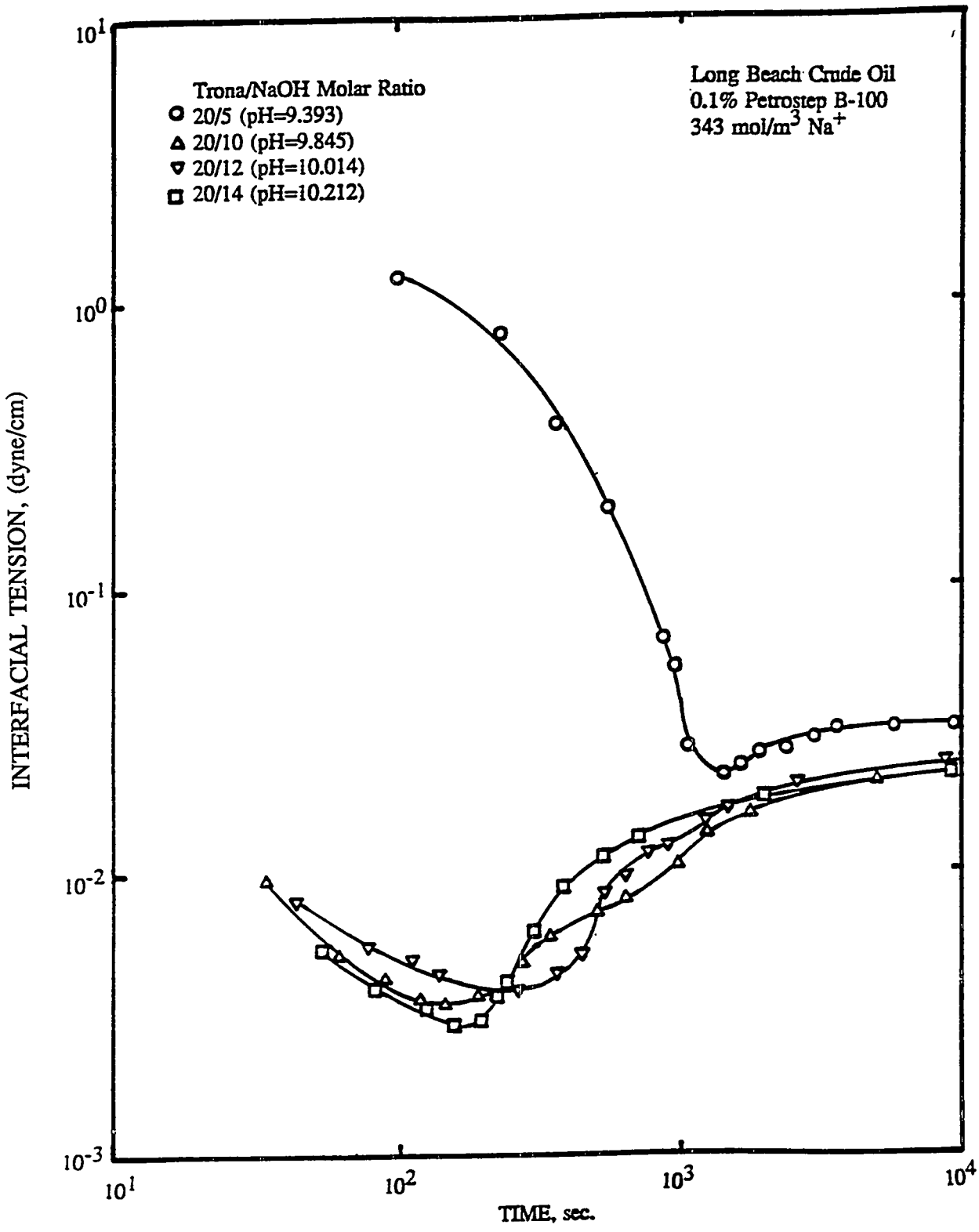

Figure 1-1a. Effect of pH on Transient Interfacial Tension with Petrostep B-100.

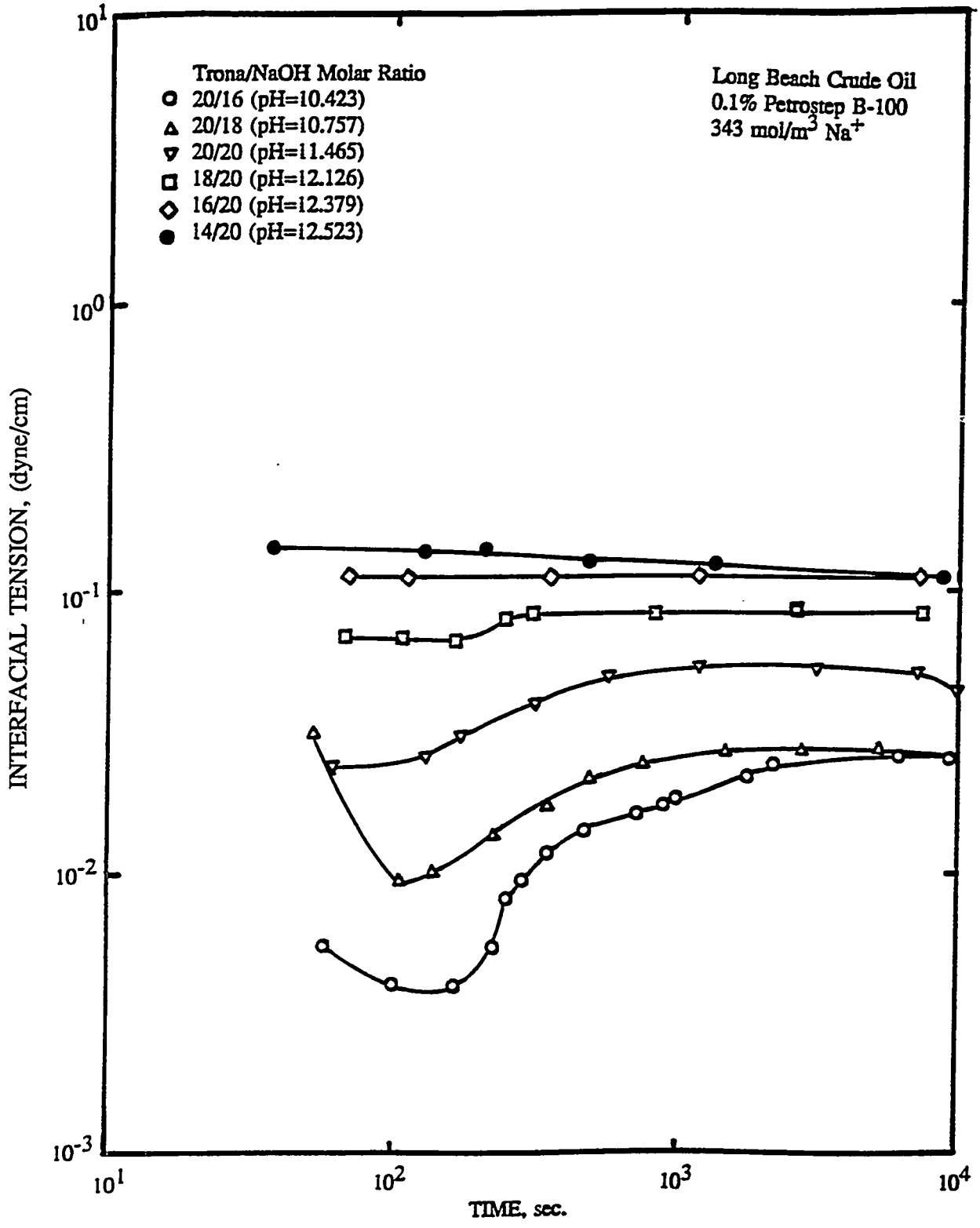

Figure 1-1b. Effect of pH on Transient Interfacial Tension with Petrostep B-100.

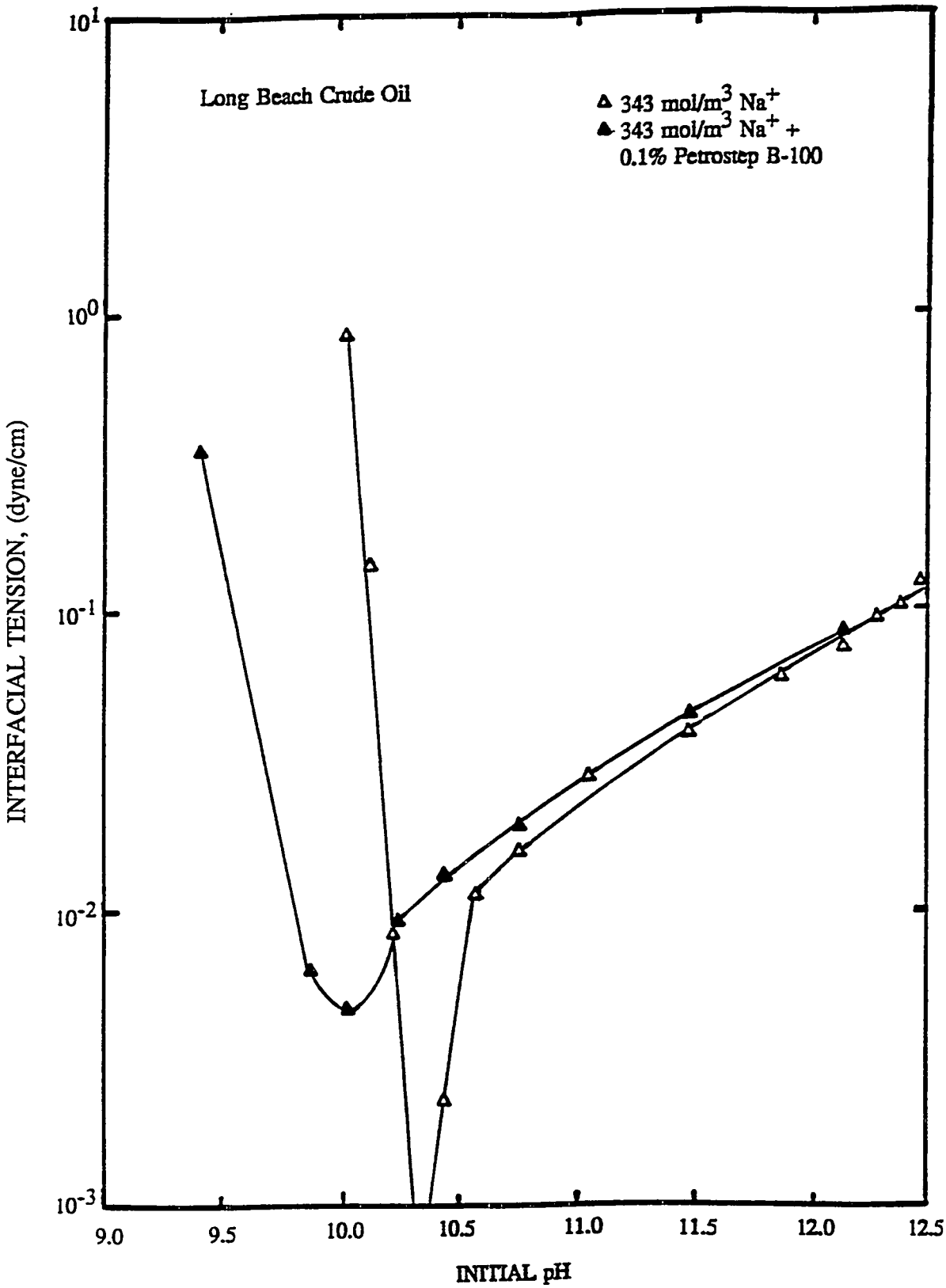

Figure 1-2. Effect of pH on Transient Interfacial Tension with and without Petrostep B-100 at 400 Seconds.

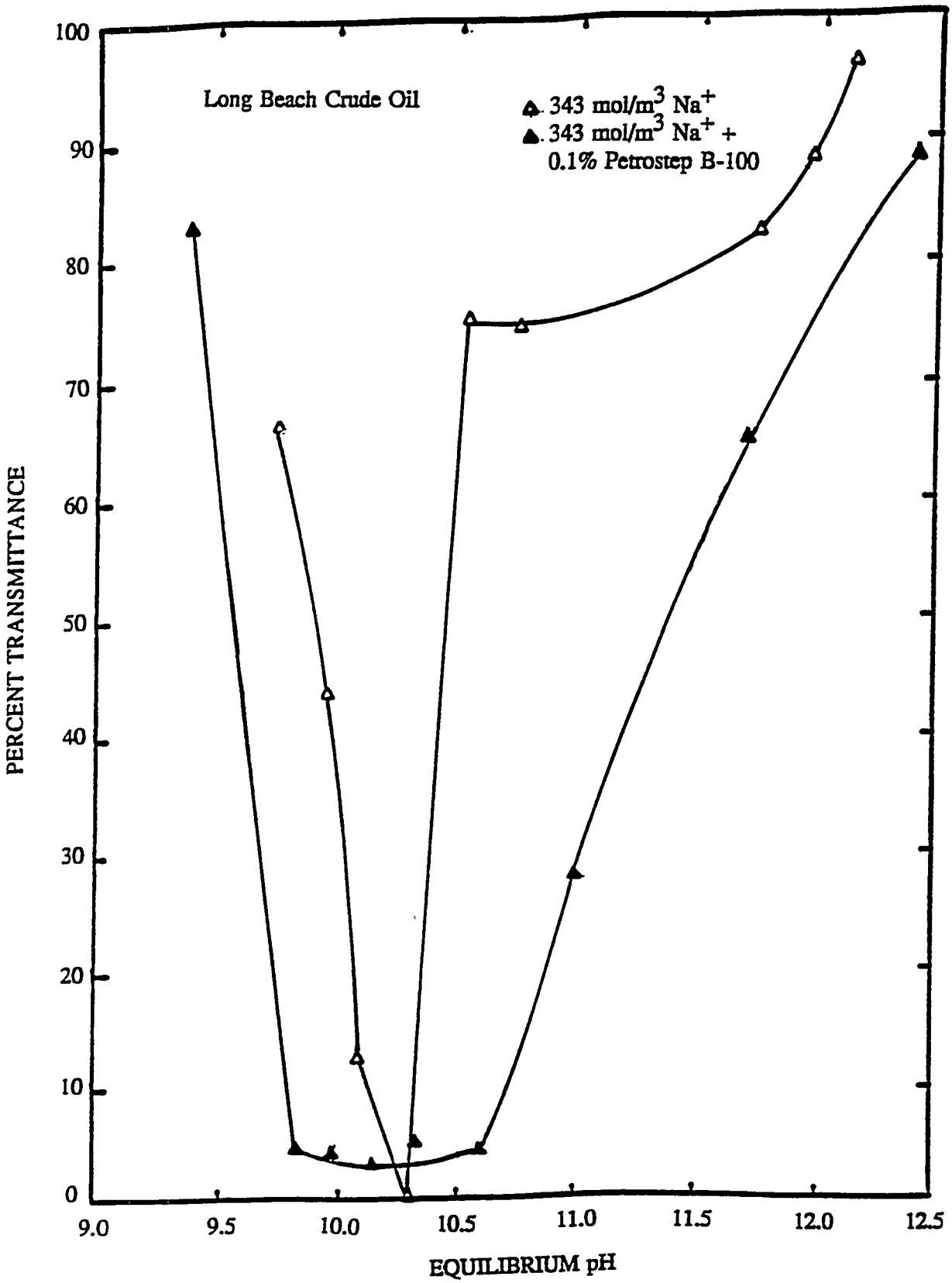

Figure 1-3. Effect of pH on the Extent of Emulsification with and without Petrostep B-100.

more emulsion will be produced during the spontaneous emulsification process.

Figure 1-4 shows the effect of surfactant on the equilibrium interfacial tension. By adding 0.1% Petrostep B-100, the minimum shifts to lower pH and interfacial tension is greatly reduced. Before a pH of about 10.6, the added surfactant takes the place of the ionized acid so that not as much acid needs to be ionized, resulting in the shift of the minimum. The lowering of interfacial tension is likely caused by a synergism between the added surfactant, ionized and unionized acid in forming mixed micelles and a mixed adsorbed interfacial layer. After a pH of about 11.0, where most of the acid has been ionized, the ionized acid is the dominating species, resulting in the same interfacial tension with and without added surfactant.

Buffering Ability

Figure 1-5 shows the buffering ability for 343 mol/m^3 sodium ions with 0.1% added surfactant at 20/16 molar ratio Trona/NaOH. The concentration of surfactant and total sodium was kept constant as the Trona/NaOH mixture was diluted. The buffering ability appears to be good from 2.0% down to 0.05%.

The effect of the buffer is now evident. The alkalinity (i.e., alkali concentration) should be high enough so that the pH remains is as close as possible to the optimal pH when dilution occurs. It should be pointed out here that equilibrium pH should be used instead of initial pH when comparing various equilibrium properties of the system, such as interfacial tension, emulsion stability and viscosity, etc. This is because equilibrium pH (i.e., equilibrium hydrogen ion) is the thermodynamic variable of the system that controls the extent of acid ionization, which in turn controls the various properties of the system. The use of equilibrium pH alleviates the

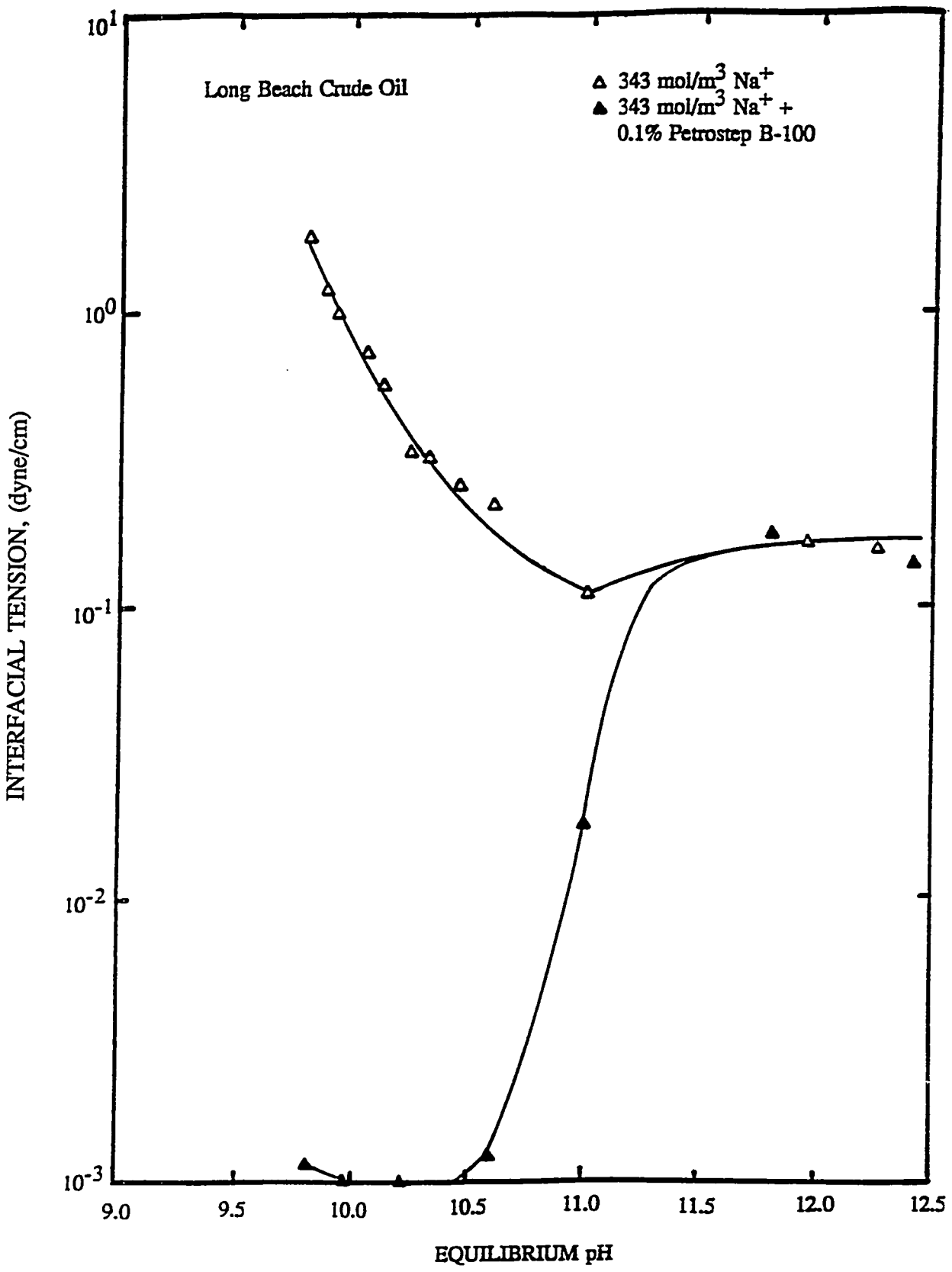

Figure 1-4. Equilibrium Interfacial Tension with and without Petrostep B-100.

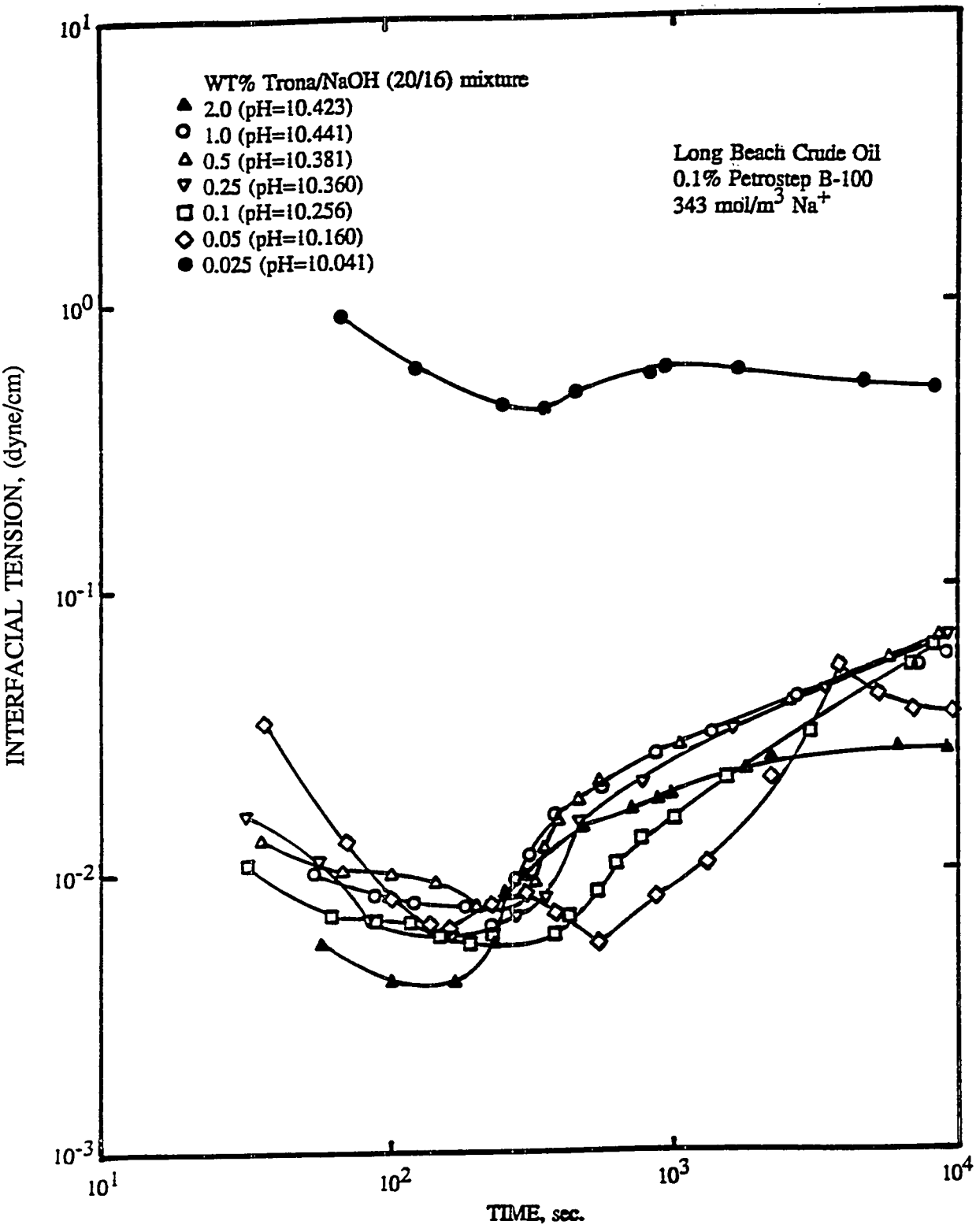

Figure 1-5. **Buffering Ability for 20/16 Trona/NaOH Molar Ratio with Petrostep B-100.**

necessity for considering the role of alkalinity. This is especially helpful when comparing between different types of alkalis or between other parameters, such as ionic strength, added surfactant, added alcohol, etc. However, in comparing results for transient interfacial tension, the initial pH is used. Since the ratio of the volume of water to oil in the spinning drop tensiometer is approximately 100, the initial pH is considered to be very close to the equilibrium pH, because the small amount of ionized acid will not alter the initial pH much, especially in the presence of the buffer.

Effect Ionic Strength

Figure 1-6 shows the transient interfacial tension as a function of pH at 400 seconds and three levels of sodium ions with 0.1% Petrostep B-105. By increasing the sodium ion concentration, the minimum in interfacial tension shifts to lower pH and the region for ultralow interfacial tension becomes wider. The same trend is observed without added surfactant. It then seems reasonable that the shifting trend with respect to ionic strength is connected with the extraction of the acid rather than the presence of the added surfactant. The added surfactant forms mixed micelles with the ionized and unionized acid, and as a result, interfacial tension is lower than without it. The presence of the added surfactant does cause the minimum to be at a slightly higher pH, however.

Figure 1-7 shows the percent transmittance of the aqueous phase as a function of the equilibrium pH and four levels of sodium ions with 0.1% Petrostep B-105. This figure represents the extent of emulsification caused by spontaneous emulsification. As sodium ions are increased, the region for spontaneous emulsification shifts to lower pH like that observed in Figure 1-6.

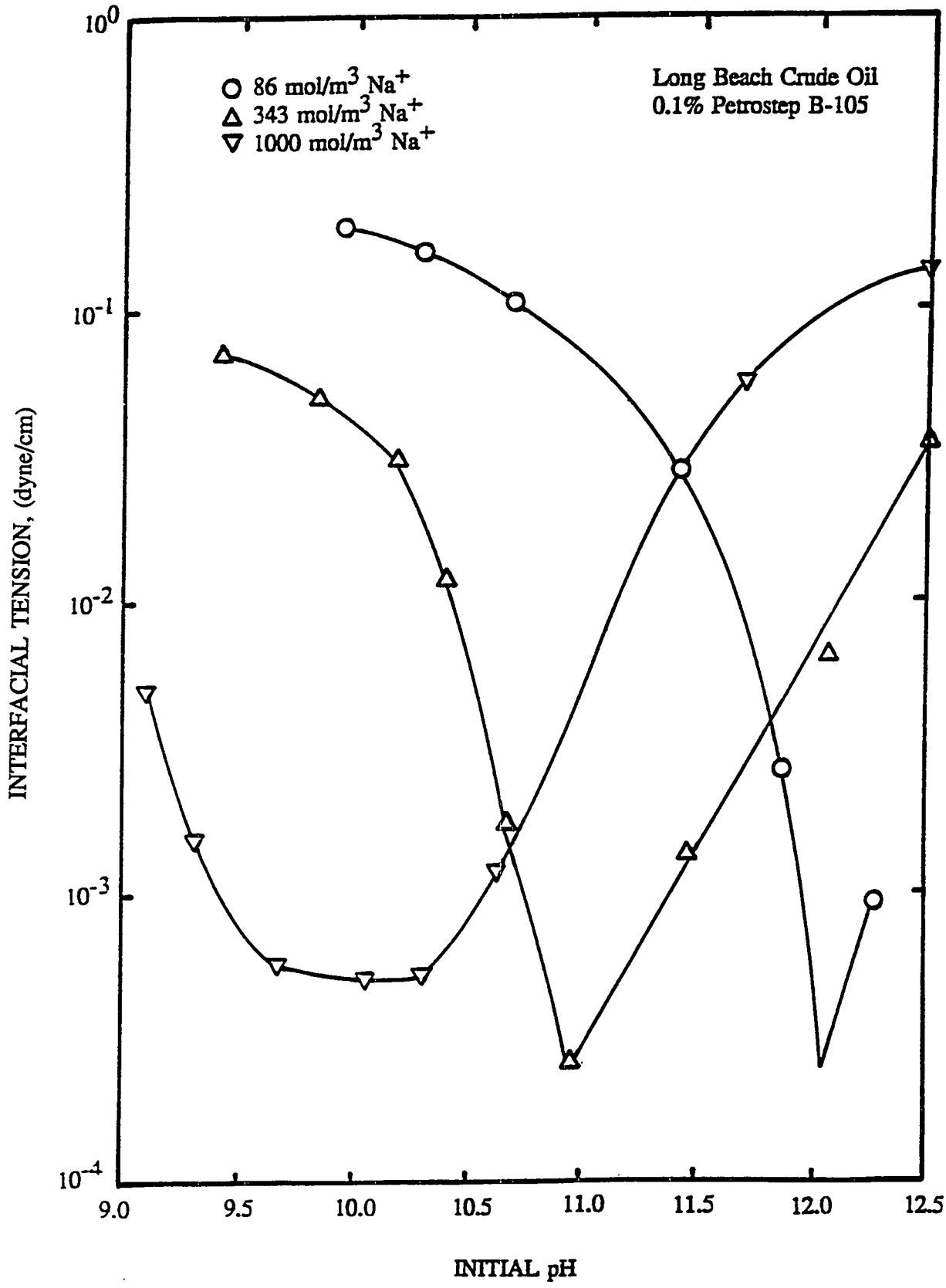

Figure 1-6. Effect of pH and Ionic Strength on Transient Interfacial Tension with Petrostep B-105 at 400 Seconds.

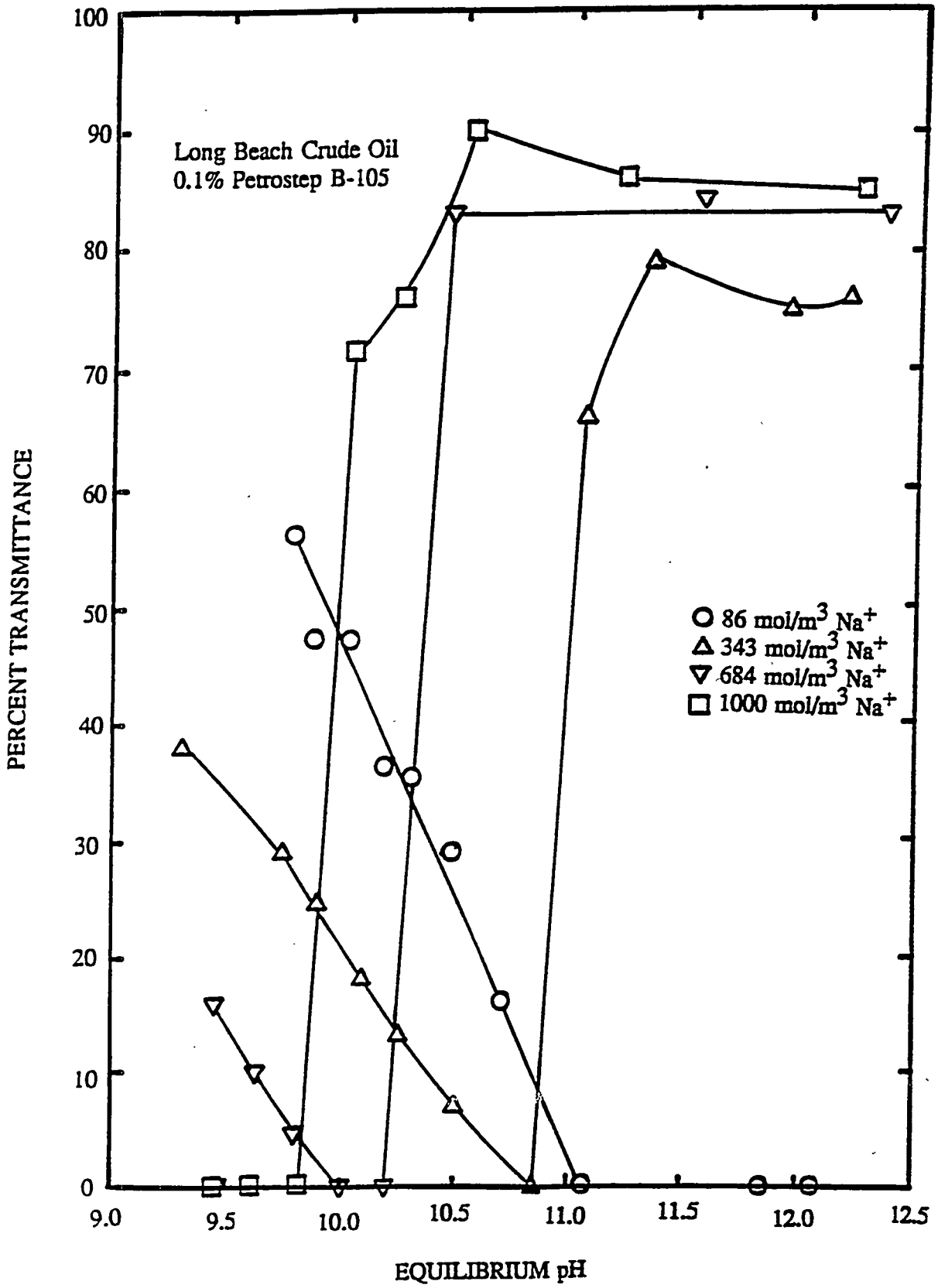

Figure 1-7. Effect of pH and Ionic Strength on the Extent of Emulsification with Petrostep B-105.

This similarity is not surprising since the extent of emulsification is connected with the transient interfacial tension. The viscosity of the water-in-oil emulsion is not very different from that for pure water, which is probably due to very little oil (i.e., an amount less than 0.3 vol%) being emulsified into the water. This viscosity however would not provide a means for mobility control. The in-situ generated oil-in-water emulsion could possibly alter the effective viscosity of the aqueous solution by forming ordered structures while flowing through the narrow pores. Further investigation is necessary to confirm this concept. It is very unlikely, however, that these small emulsions (e.i., less than 0.5 microns) could plug the pores and provide the emulsification and entrapment mechanism for improved oil recovery.

Figure 1-8 shows the equilibrium interfacial tension as a function of the equilibrium pH for four different sodium ion concentrations with 0.1% Petrostep B-105. By increasing the concentration of sodium ions, the minimum is shifted to lower pH, just like in Figures 1-6 and 1-7. It should also be noted that the addition of Petrostep B-105 caused a shifting of the minimum to a higher pH, whereas Petrostep B-100 caused a shifting of the minimum to a lower pH. It is clearly seen that something is happening for all ionic strengths at the system pK_a, where the pH is 10.6. Before this pH, the minimum for 86, 684 and 1000 mol/m^3 total sodium could be influenced by the presence of unionized acid. However, the minimum for the 343 mol/m^3 occurs slightly after this pH, and 86 mol/m^3 sodium has a second minimum occurring much after the pH of 10.6. This suggests that the mixed micelle formation, which regulates the relative amounts of the individual monomeric species, is controlling the lowering of interfacial tension at higher pH for lower ionic strength. If partitioning was controlling the process, then a decrease in ionic strength would cause more surfactant in the aqueous phase, requiring less

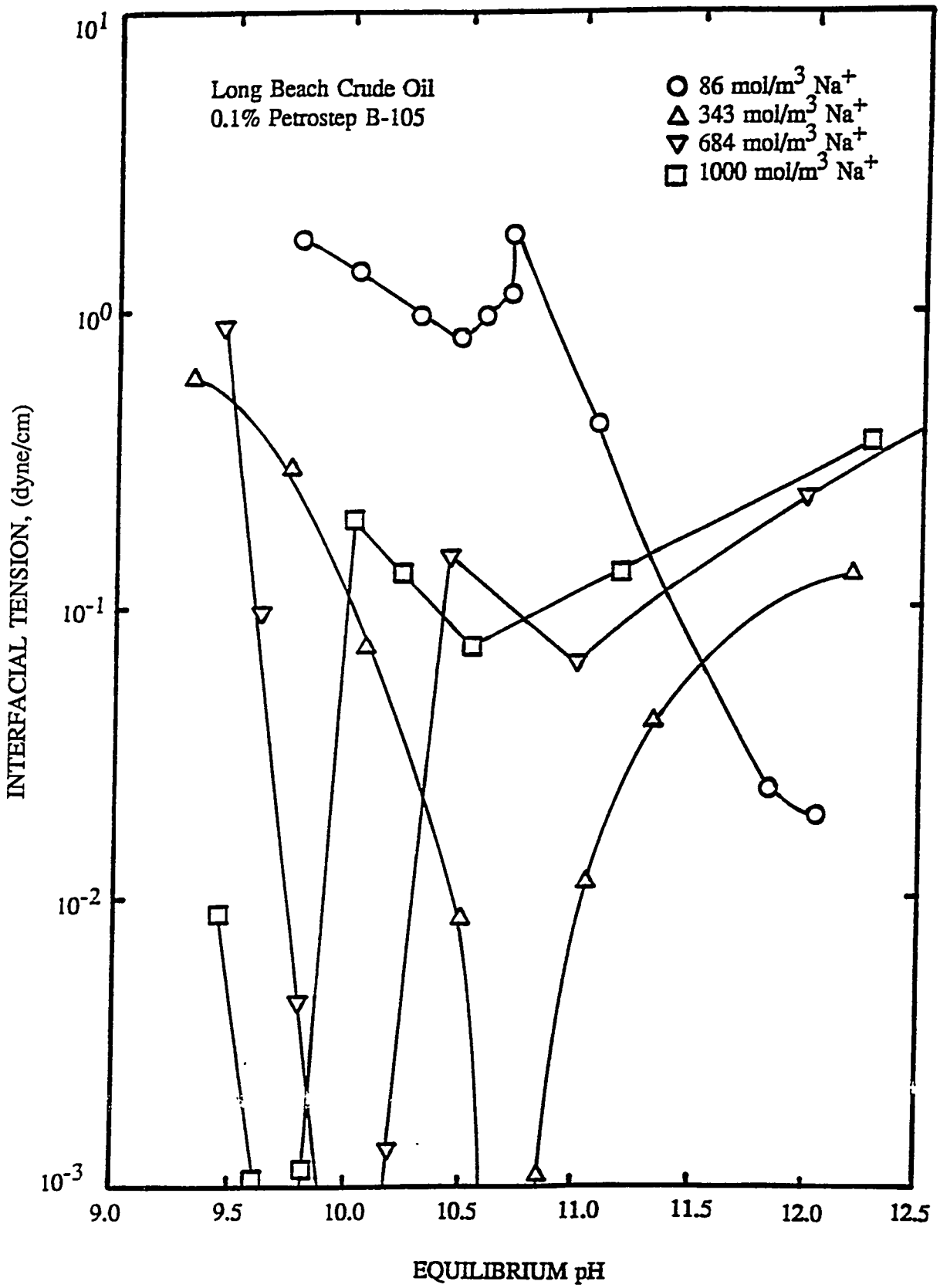

Figure 1-8. Effect of pH and Ionic Strength on the Equilibrium Interfacial Tension with Petrostep B-105.

ionized acid, resulting in the minimum occurring at lower pH. However, the opposite is observed here. For a more in-depth discussion, see Rudin (1991).

It can also be seen in Figure 1-8 that the interfacial tension is going through a minimum with respect to ionic strength when pH is kept constant. This effect appears to be the same as that in surfactant flooding where an increase in ionic strength causes the surfactant to partition into the oil. When the partition coefficient is unity, then interfacial tension in minimized. However, based on the foregoing discussion, increasing ionic strength appears to affect interfacial tension by decreasing the CMC of the mixed surfactant solution rather than partitioning the surfactant into the oil phase.

Without added surfactant, spontaneous emulsification was lost at all pHs when the ionic strength was 1000 mol/m^3. However, by the addition of 0.1% Petrostep B-105 to the 1000 mol/m^3 sodium ions system, spontaneous emulsification is restored and ultralow interfacial tensions are present in a specific pH range. This method shows that the way to tailor the floodwater to high salinity reservoirs is by choosing the pH which corresponds to ultralow interfacial tension.

At the minimum in interfacial tension, a linear relationship exists between the equilibrium pH and the log of the sodium ion concentration as shown in Figure 1-9. This is likely due to the shifting of the CMC of the mixed micelles of added surfactant, ionized, and unionized acid. As a result, less ionized acid is needed at high ionic strength.

Figure 1-10 shows the surface tension of the aqueous phase which has been pre-equilibrated with oil as a function of pH at various levels of ionic strength. This shows that the combination of ionized acid and added surfactant does not partition out of the aqueous phase

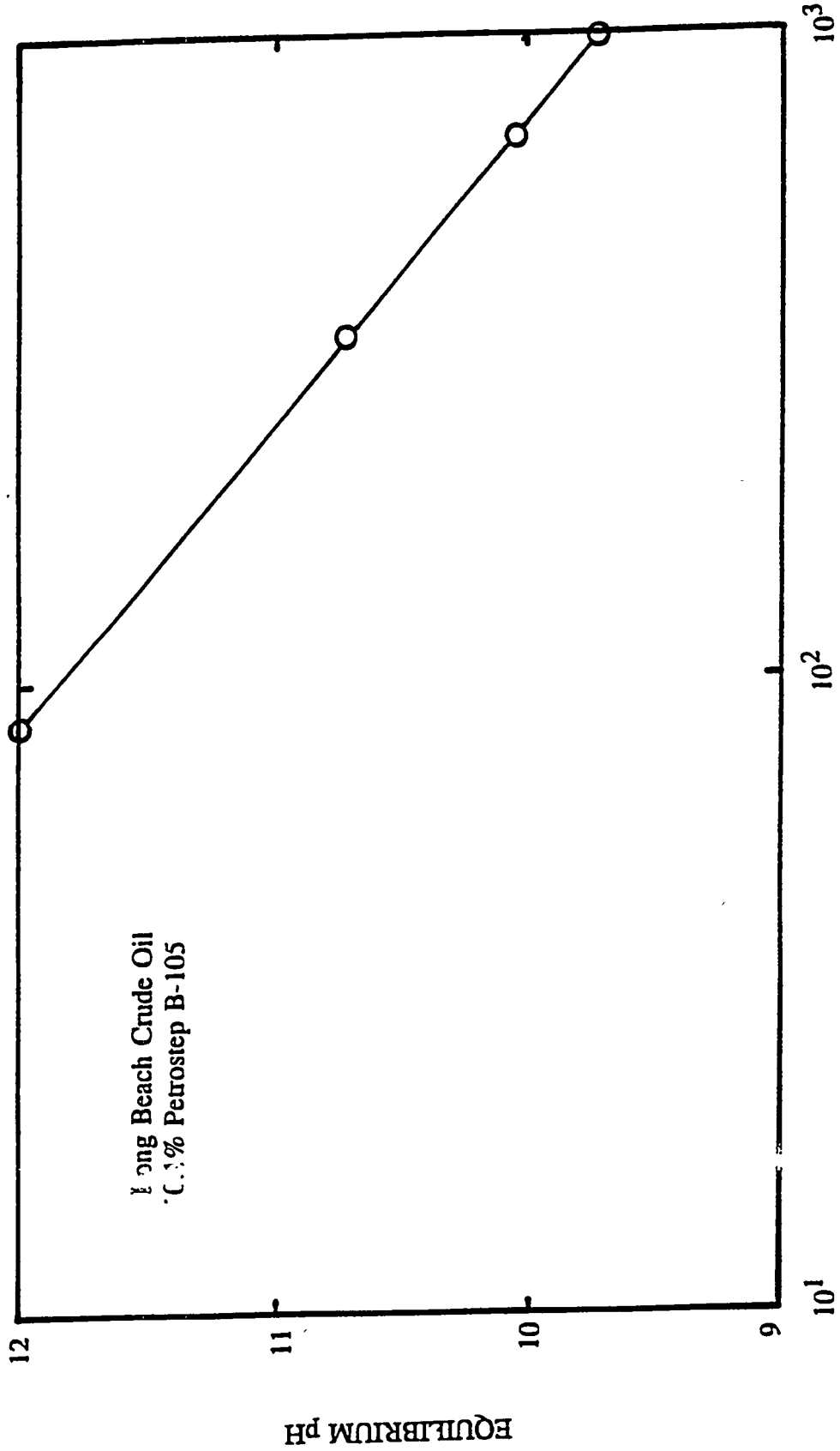

Figure 1-9. Relationship Between Equilibrium pH and Ionic Strength at the Minimum in Interfacial Tension with Petrostep B-105.

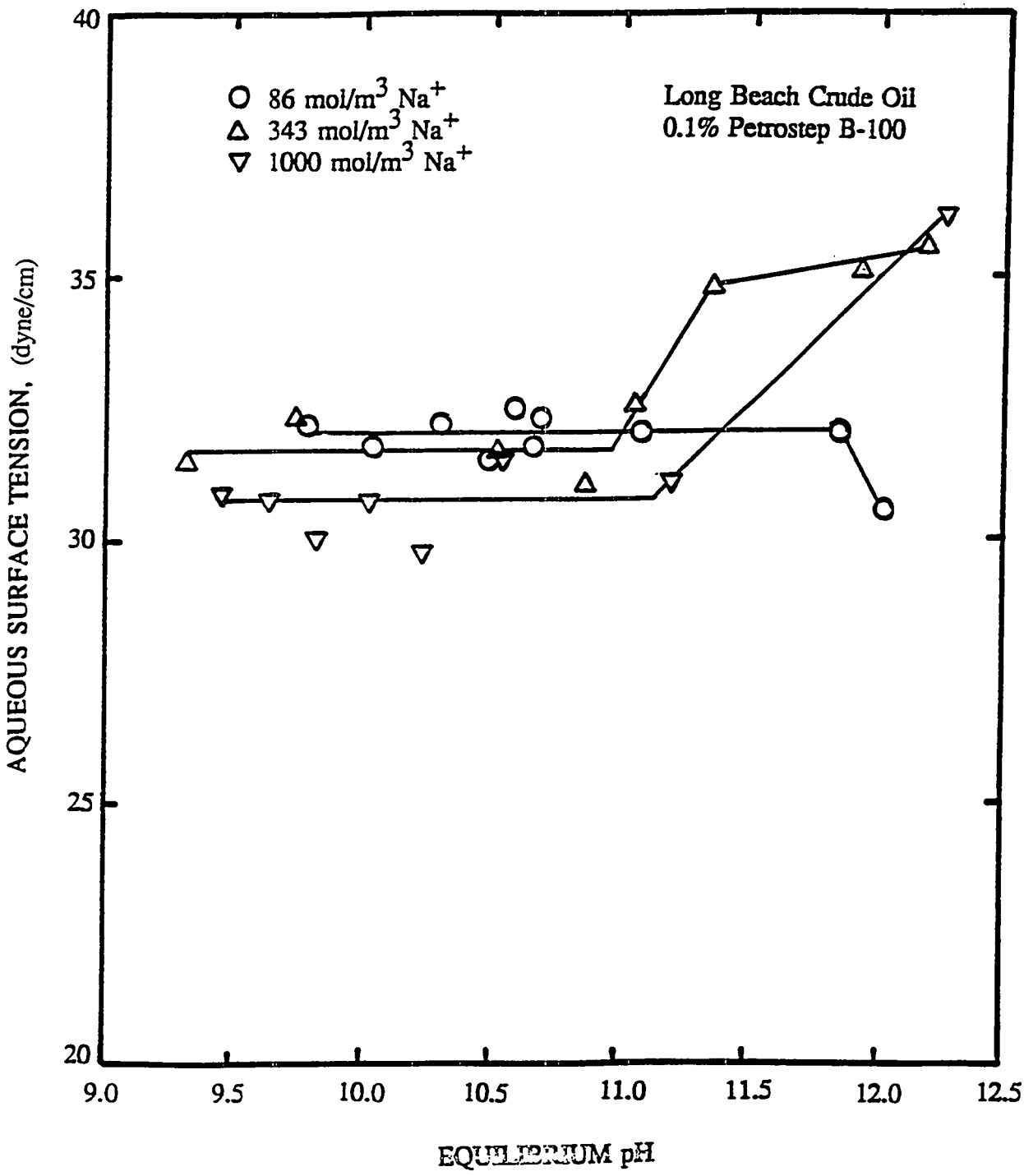

Figure 1-10. Contacted Aqueous Surface Tension as a Function of pH and Ionic Strength with Petrostep B-105.

below their mixed solution CMC. The slight increase in surface tension for 343 and 1000 mol/m^3 sodium is probably due to a change in the monomer-micelle equilibrium. The ionized acid and added surfactant are not expected to partition out of the aqueous phase from increase in pH.

The surface tension of the contacted aqueous phase as a function of NaCl with no added alkali at 0.1% Petrostep B-105 is shown in Figure 1-11. With no added alkali in the system, the CMC of Petrostep B-105 is 0.1% at 343 mol/m^3 sodium and 86 mol/m^3 sodium is below the CMC. In Figure 1-10, we saw that with the combination of ionized acid and added surfactant, the system was above the CMC for 86 mol/m^3 sodium. This indicates that the addition of ionized acid to the added surfactant results in a lower CMC than the added surfactant alone. Clearly, mixed micelle formation plays a key role in affecting the surface properties of the system. For ionic strengths below 343 mol/m^3, 0.1% Petrostep B-105 is below its CMC. However, the ionized acid is above its CMC. This may explain why interfacial tension goes ultralow at 86 mol/m^3 sodium when the pH is greater than 10.6.

The CMC of Petrostep B-105 (in a non-contacted system) is determined to be 0.001% at 343 mol/m^3 sodium (see Figure 1-12). The increase in CMC to 0.1% at 343 mol/m^3 sodium (see Figure 1-11) by contacting with the crude oil, clearly shows that the longer chain length surfactant species have partitioned into the oil phase.

Effect of Surfactant Concentration and Type

An increase in the concentration of added surfactant causes a shifting of the minimum in percent transmittance and interfacial tension to a higher pH as shown in Figures 1-13 and 1-14.

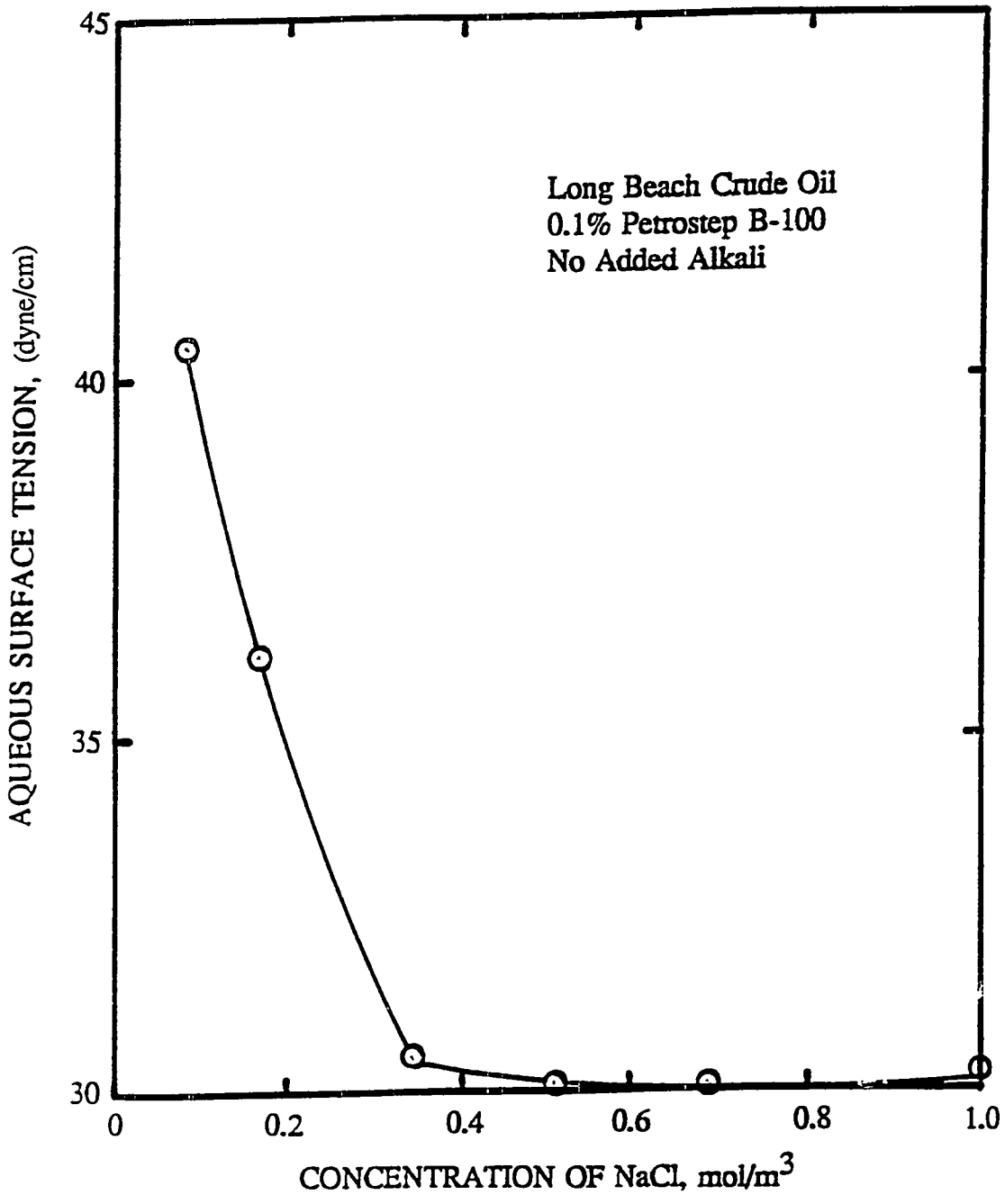

Figure 1-11. Contacted Aqueous Surface Tension as a Function of Ionic Strength and No Added Alkali with Petrostep B-105.

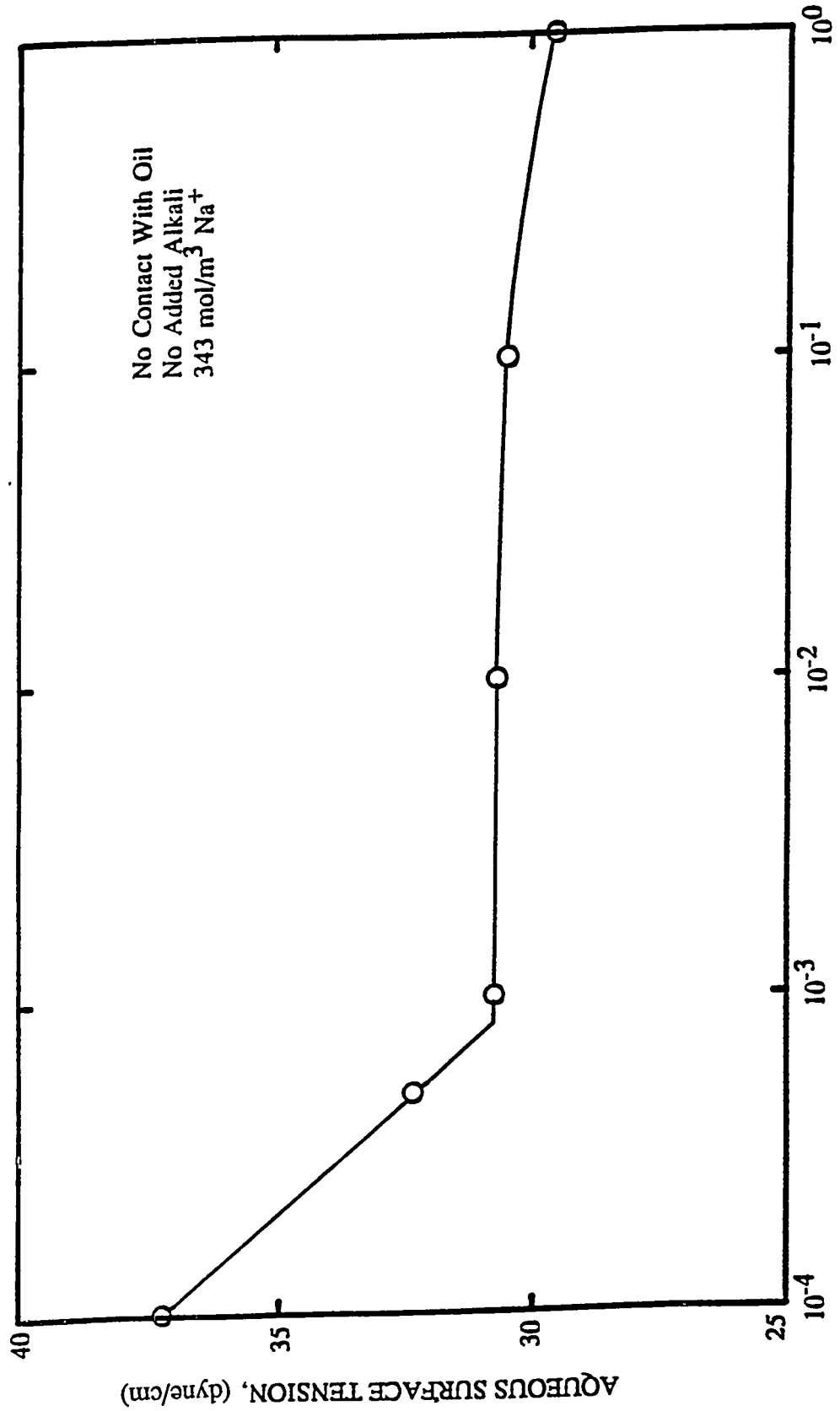

Figure 1-12. Adsorption Isotherm for Non-Contacted Aqueous Surface Tension of Petrostep B-105.

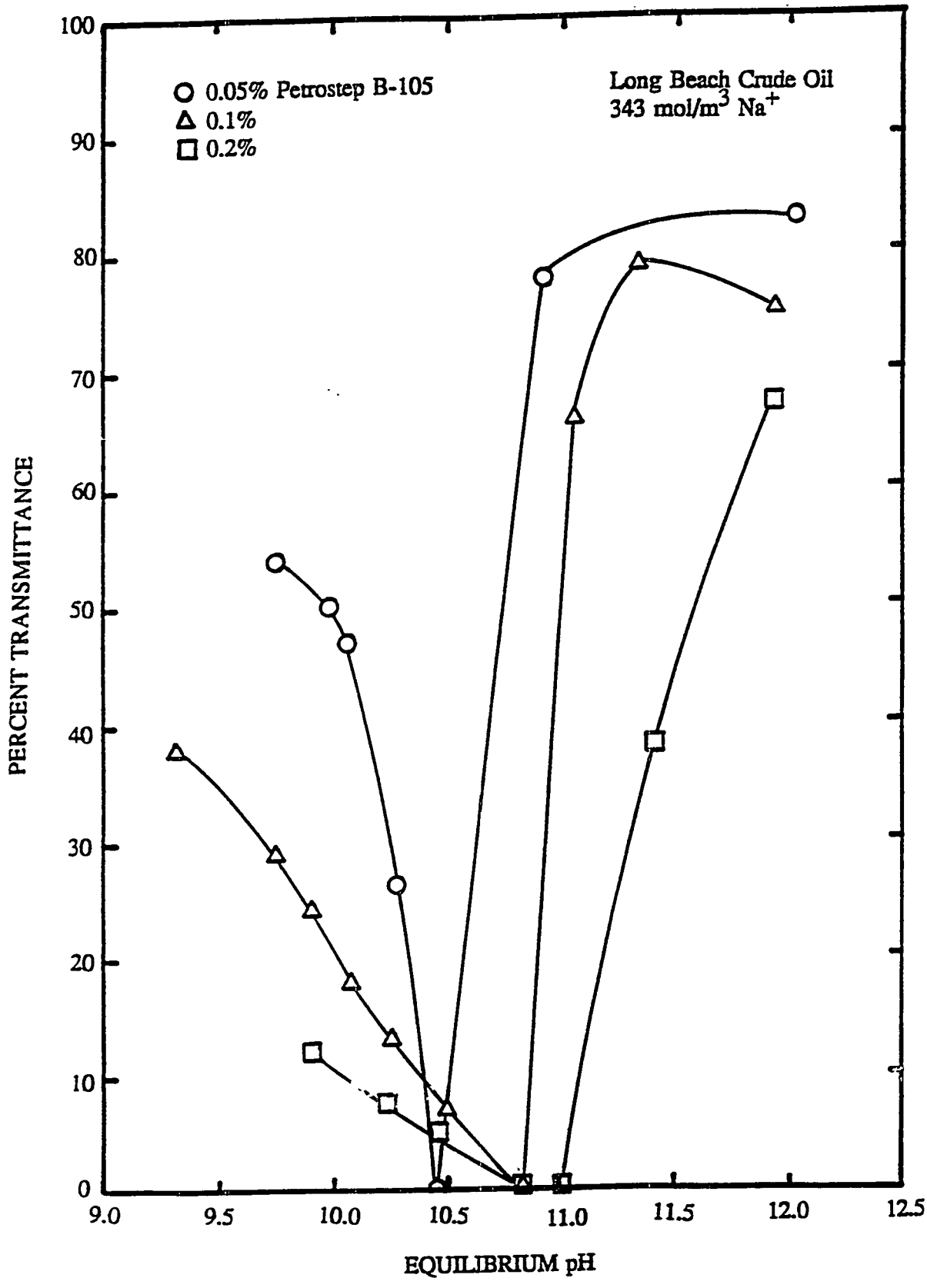

Figure 1-13. Effect of pH on the Extent of Emulsification with Various Levels of Petrostep B-105.

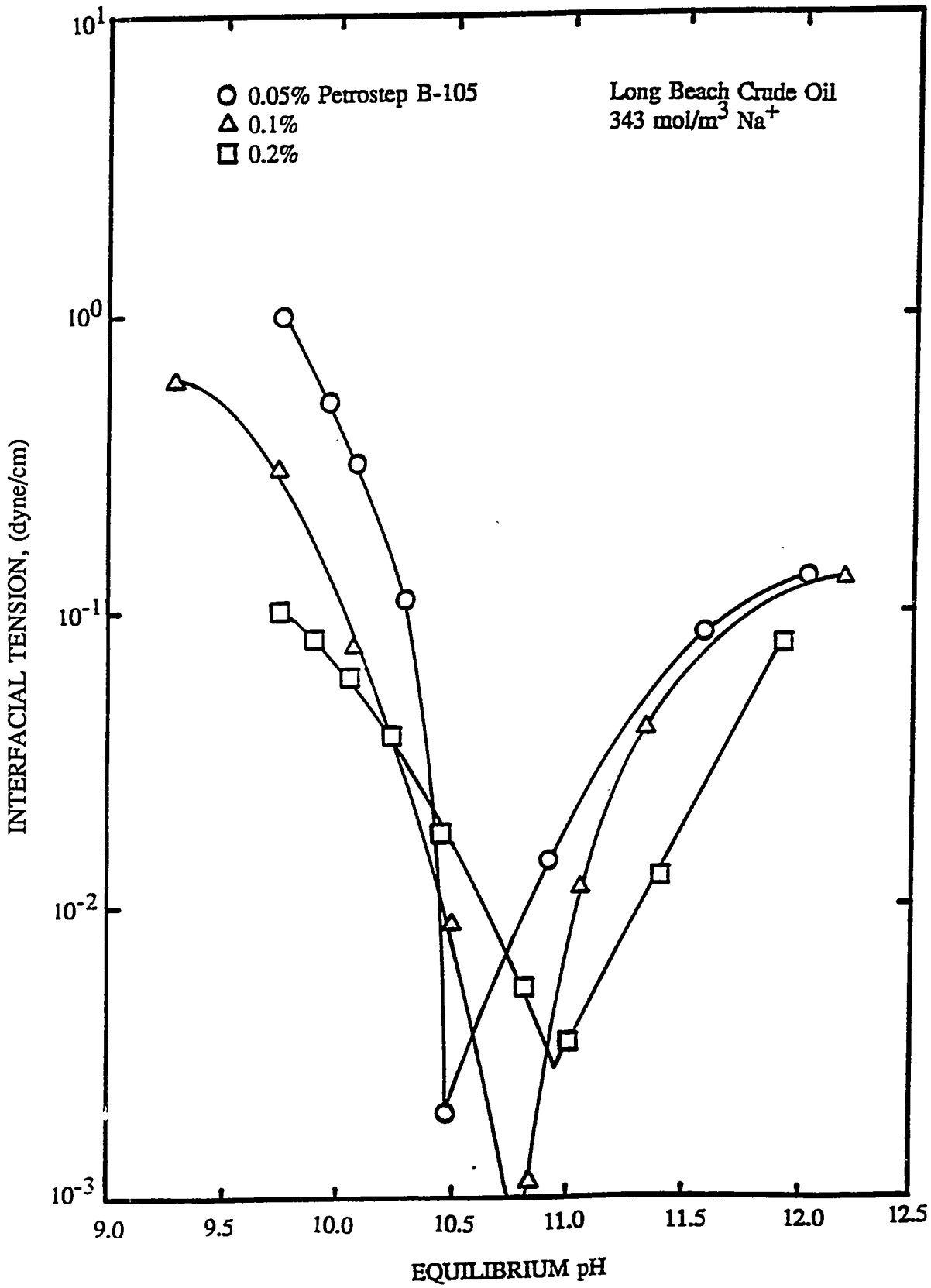

Figure 1-14. Effect of pH on the Equilibrium Interfacial Tension with Various Levels of Petrostep B-105.

Not only is the interfacial tension shifted, but it is also generally lower over a wider pH range. It seems more and more reasonable that the formation of mixed micelles is controlling the monomer concentrations and therefore interfacial tension. There is a competition in the mixed micelle between the added surfactant and the ionized acid. As more surfactant is added, more ionized acid is needed to compensate this increase, resulting in a shifting of the minimum in interfacial tension to higher pH.

Although interfacial tension and phase behavior were not optimized with respect to surfactant type, the effect of surfactant type should be mentioned here for completeness. By taking a mixture of surfactants with different molecular weights, one is able to tailor the surfactant-enhanced alkaline solution to that particular crude oil. This tailoring is possible because the interfacial tension is sensitive to the hydrophile-lipophile balance of the system. In doing so, the interfacial tension becomes ultralow, and the system may have an associated middle phase. Surfactant concentration and type along with pH and ionic strength can then be used to optimize the system for ultralow interfacial tension. The petroleum sulfonates used in this study, Petrostep B-100 and B-105 in combination with ionized acid did not produce any apparent middle phase. There was, however sedimentation of the spontaneously produced oil-in-water emulsions, but we do not consider this as a middle phase.

Effect of alcohol

The effect of isobutanol on the adsorption kinetics is shown in Figure 1-15. One effect of adding isobutanol (IBA) is to reduce the time needed to achieve equilibrium interfacial tension after a new interface is created. The reduction in time is about 10 minutes. This more

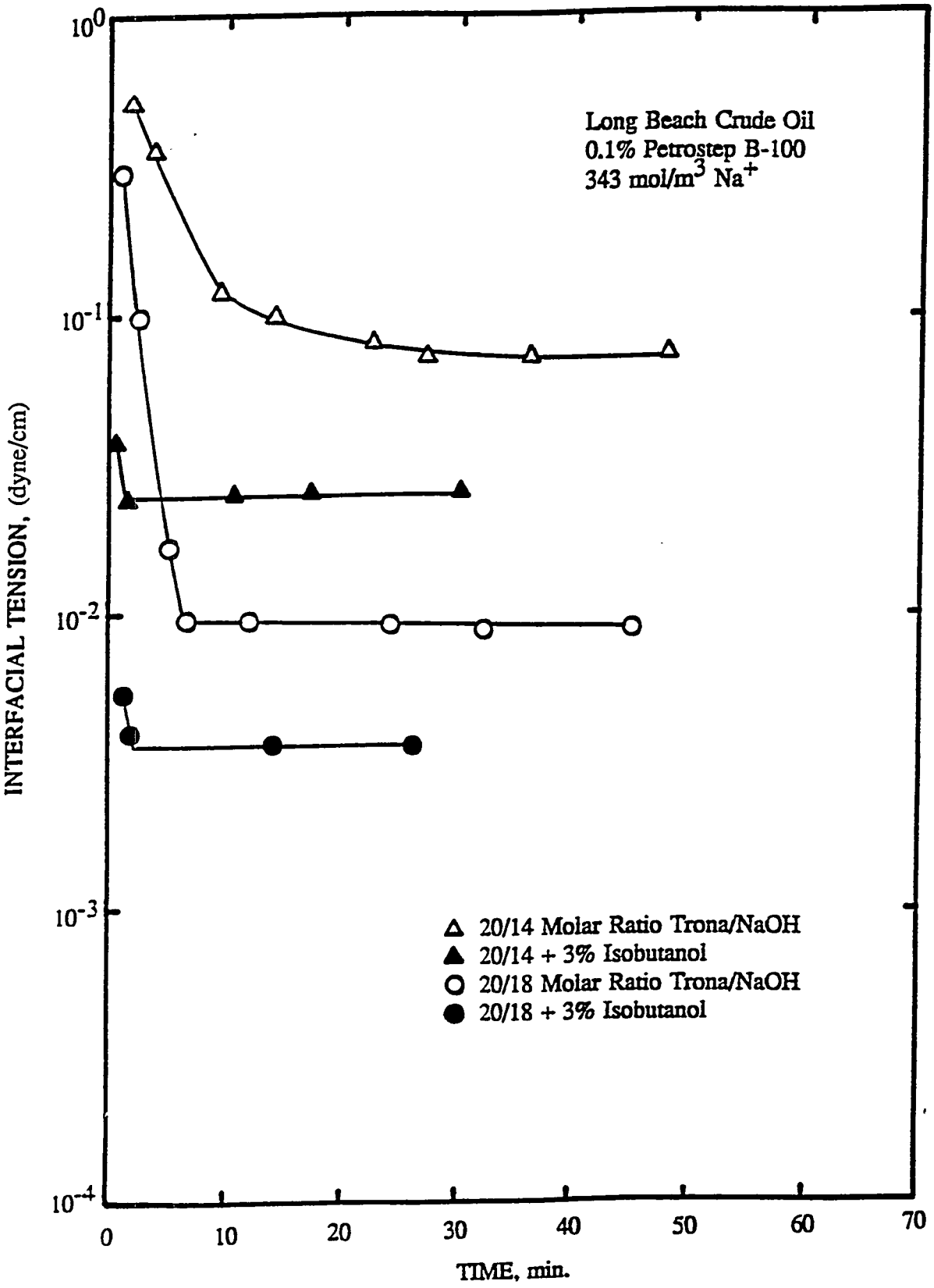

Figure 1-15. Equilibrium Interfacial Tension as a Function of Time with and without Isobutanol.

responsive adsorptive behavior has major practical ramifications when one considers the dynamic processes occurring during a reservoir flood as new interface is created or destroyed when oil droplets snap-off of oil ganglia or coalesce to form an oil bank.

As seen in Figures 1-16 and 1-17, the shifting of the minimum in interfacial tension or the percent transmittance is very slight upto 3.0 wt% IBA, however, 6.0 wt% IBA causes a significant reduction of interfacial tension and shifting of the minimum. This shifting is likely caused by the short chain length alcohol altering the solvent properties of the water to in-effect cause the CMC to increase and/or more surfactant to stay in the water instead of partitioning into the oil. That is why the trend observed here is the same as that when added surfactant is increased as seen in Figure 1-14. It can also be seen that with an increase in alcohol, the width of the minimum for both interfacial tension and percent transmittance becomes wider.

Effect of different oils

Shown in Figure 1-18 is the minimum in transient interfacial tension as a function of pH for both the Adena and Long Beach Crude oils. The long beach crude oil has a minimum at a typical pH of 10.7 for most acidic crude oils. However, the Adena oil has a minimum at a pH of 13, which is considerably higher than the Long Beach crude oil. Since the Adena oil does not have much organic acids, the minimum likely results from saponification of esters. Figure 1-19 shows that the alkaline reaction with the Adena oil does have interfacial activity. The minimum with the Adena oil occurs at a much shorter time than the Long Beach Crude oil.

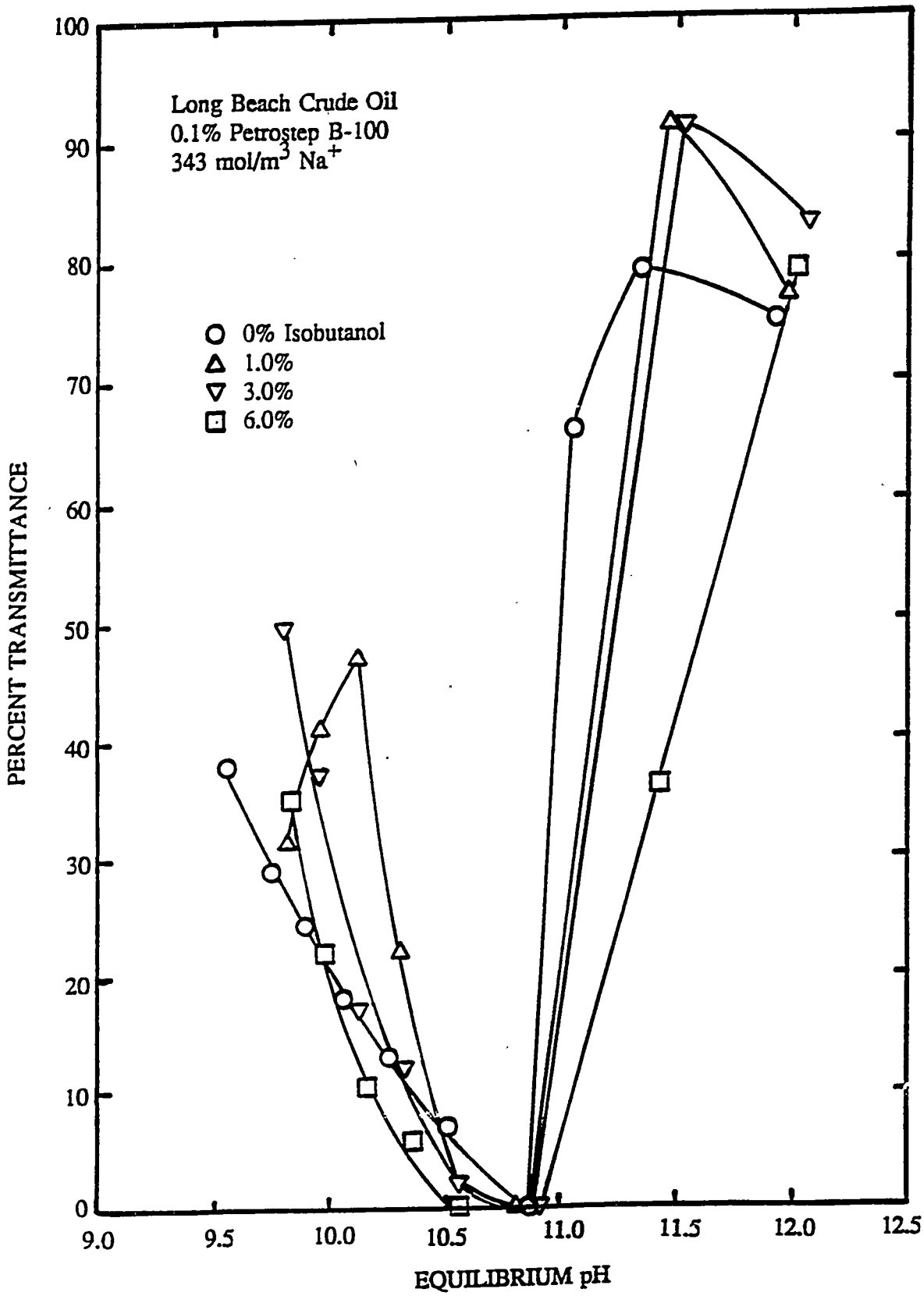

Figure 1-16. Effect of pH on the Extent of Emulsification with Petrostep B-105 at Various Levels of Isobutanol.

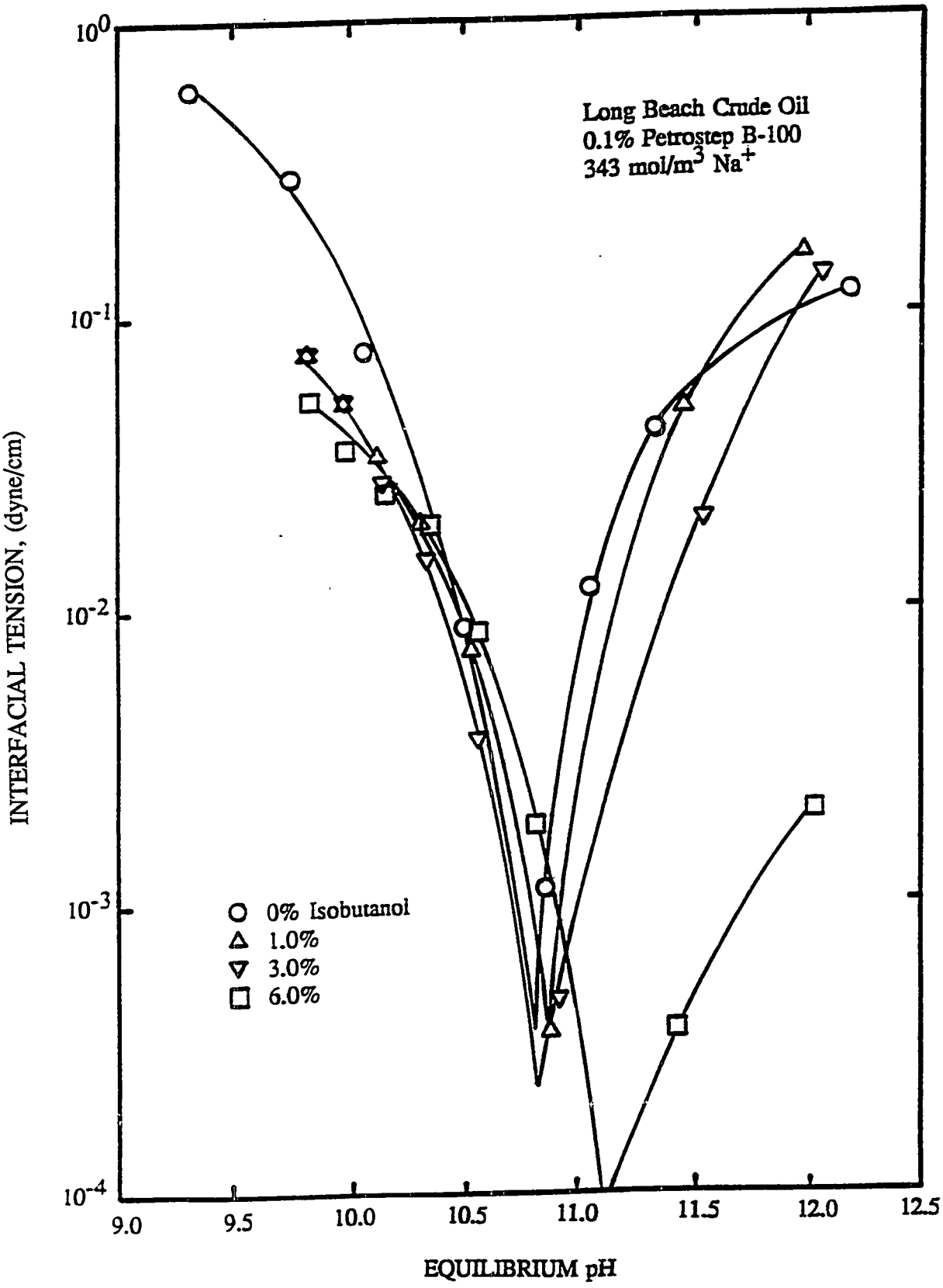

Figure 1-17. Effect of pH on the Equilibrium Interfacial Tension with Petrostep B-105 at Various Levels of Isobutanol.

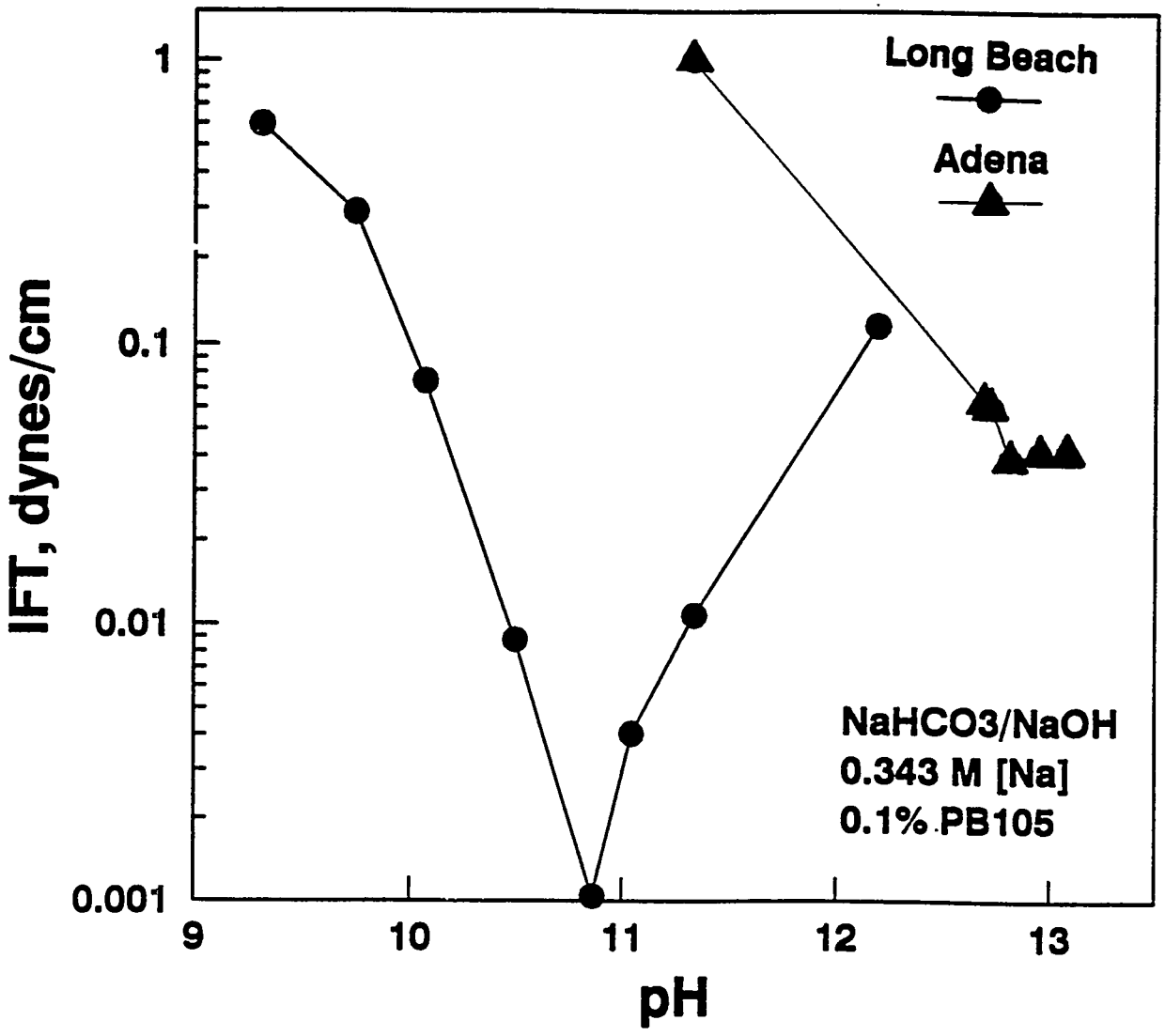

Figure 1-18. Effect of pH on the Transient Interfacial Tension Minimum.

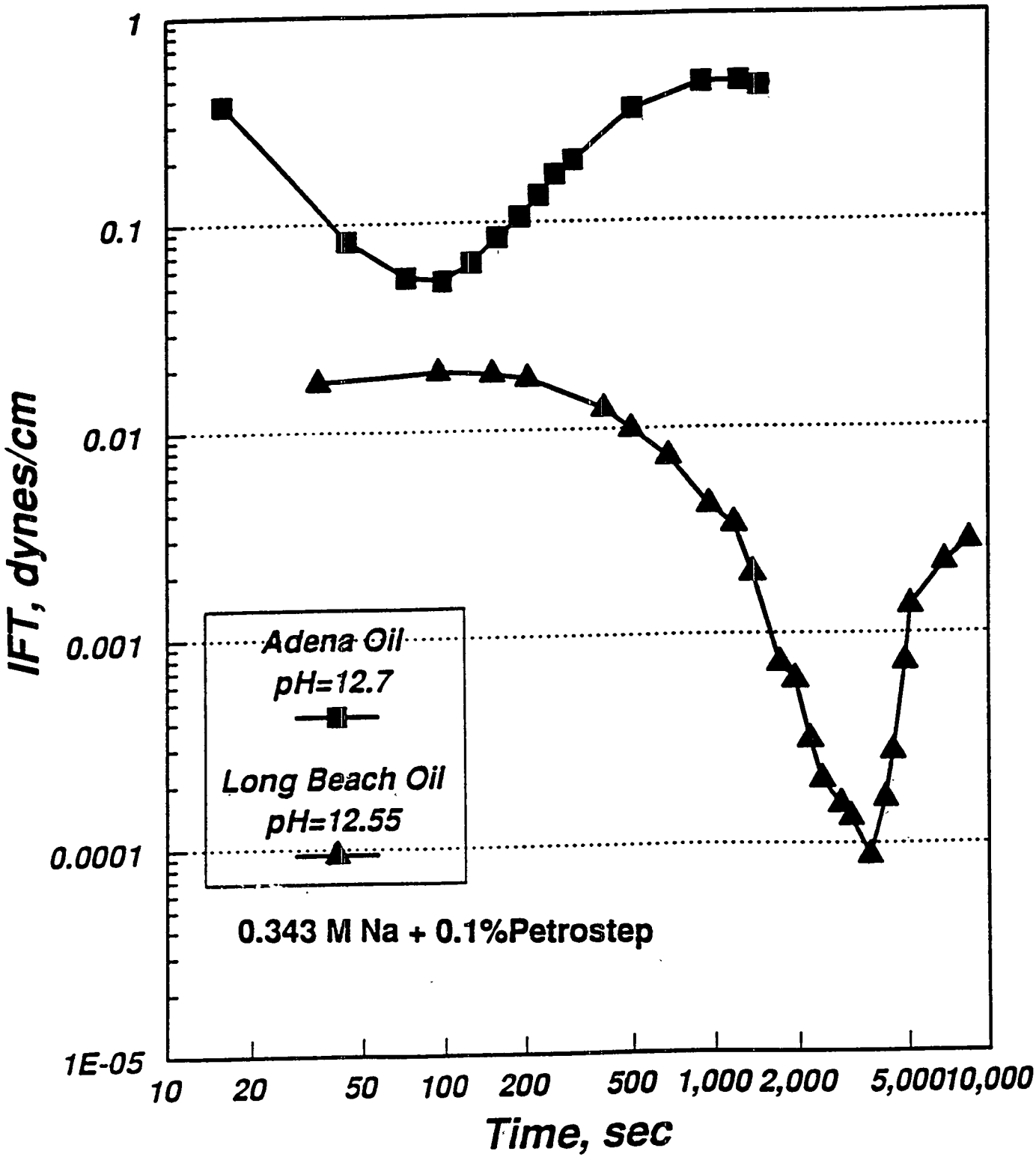

Figure 1-19. Transient Interfacial Tension for Adena and Long Beach Oil.

Effect of sodium and surfactant concentration on middle phase

Figure 1-20 shows that 0.684 M sodium has two minimums. The first minimum results from monolayer behavior of ionized and unionized acid. The second minimum results from middle phase formation. The spontaneous formation of middle phase was observed by us under the microscope. Also seen in Figure 1-20 is that the middle phase is increased by an increase in sodium concentration. The increase in surfactant concentration also causes more middle phase to form as seen in Figure 1-21.

SIGNIFICANT FINDINGS

1. With the use of inexpensive mixed alkalis such as carbonates, buffering the aqueous phase pH against changes in alkali concentration will also buffer the interfacial tension and extent of spontaneous emulsification against changes in the amount of alkali, even with the addition of a preformed surfactant.
2. By adding surfactant, the equilibrium interfacial tension becomes ultralow, the pH region for ultralow interfacial tension and for spontaneous emulsification is widened, and these regions are shifted to higher or lower pH depending on the surfactant type. This shifting is likely dependent upon the micelle monomer equilibria between the added surfactant, ionized and unionized acid.
3. The addition of surfactant causes a higher interfacial resistance to mass transfer which reduces the rate of acid ionization, resulting in lower transient interfacial tension for longer periods of time. The transient interfacial tension can also be maintained for longer periods of time by optimizing with respect to ionic strength and pH.

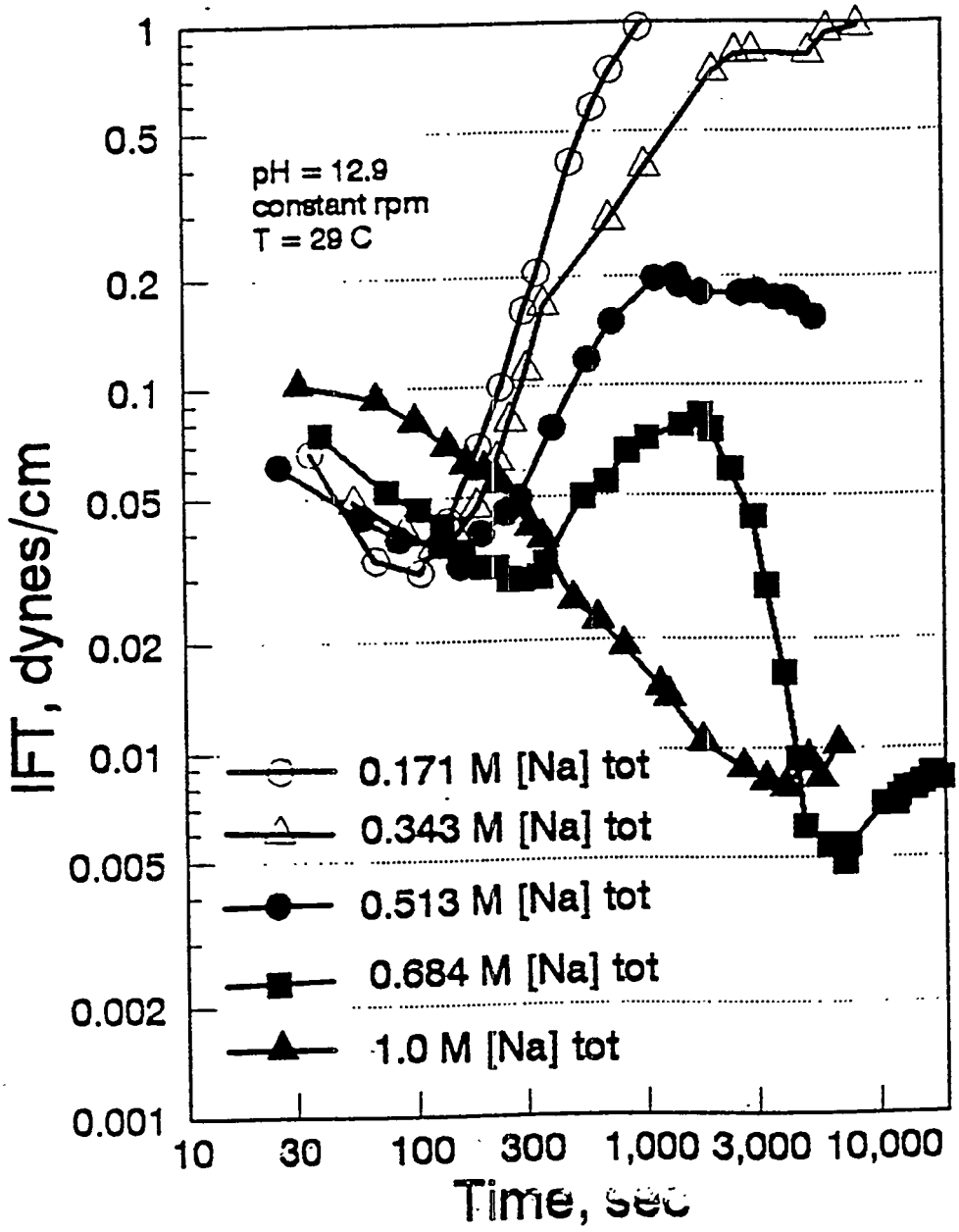

Figure 1-20. Effect of sodium concentration on Transient Interfacial Tension for Adena Oil.

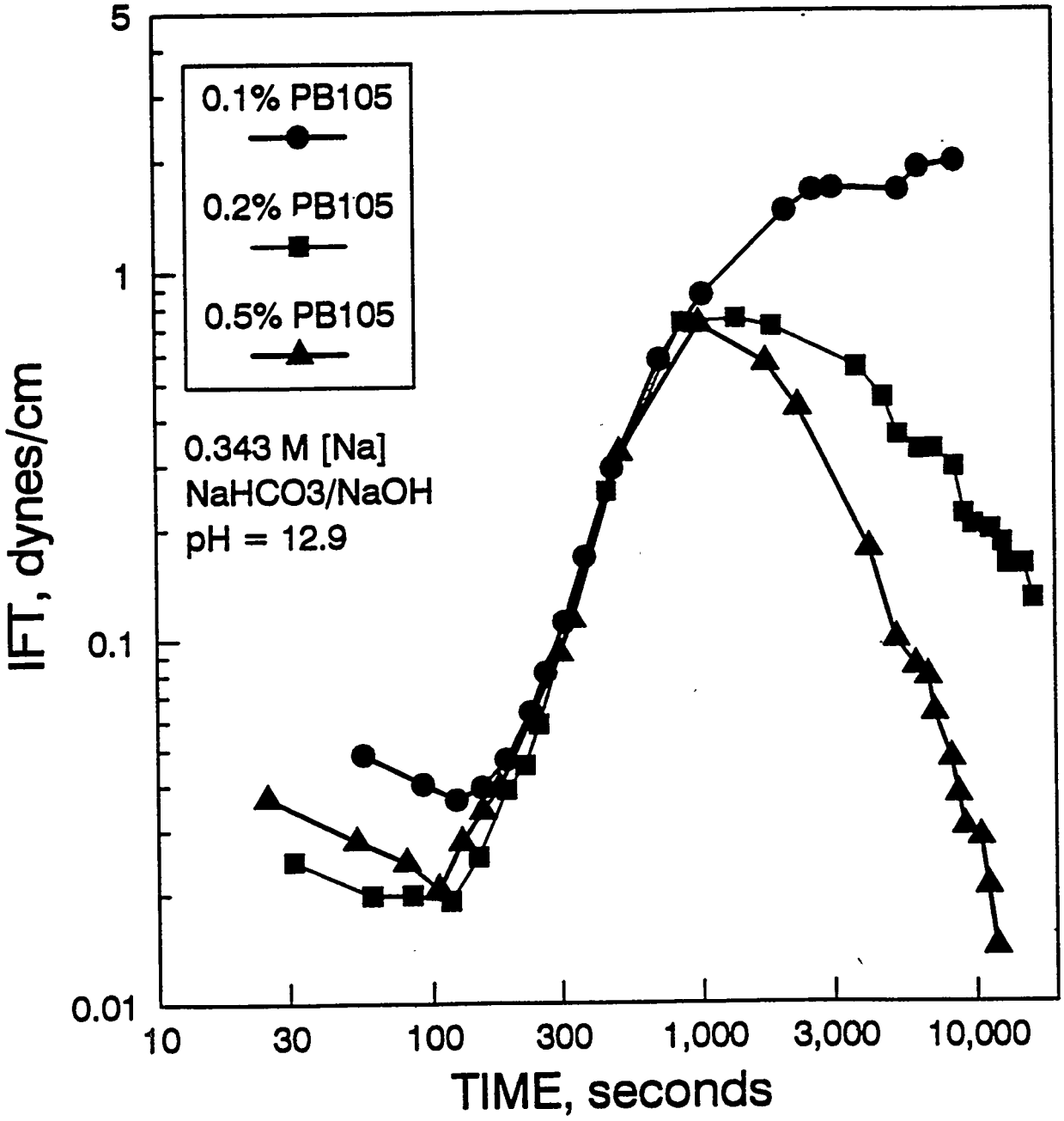

Figure 1-21. Effect of Added surfactant on Transient Interfacial Tension for Adena Oil.

4. The proper choice of ionic strength, pH, surfactant concentration, and surfactant type will optimize the aqueous/crude oil interactions to produce ultralow interfacial tension and the desired phase behavior.
5. Increasing surfactant concentration causes a shifting of the minimum in interfacial tension to higher pH. This shifting indicates the importance of the ionized acid in balancing the micelle monomer equilibria for optimization of interfacial tension and phase behavior.
6. The addition of isobutanol at low concentrations has little or no effect on the position of the minimum with respect to pH, however at high concentrations the interfacial tension is significantly reduced by the alteration of the aqueous phase solvent properties.
7. The addition of isobutanol reduces the time needed to achieve equilibrium interfacial tension after a new interface is created.
8. A direct correlation between transient interfacial tension, extent of emulsification, and equilibrium interfacial tension was found. This finding implies that observation of emulsification is sufficient to determine where equilibrium and transient interfacial tension are low, without making time consuming interfacial tension measurements. These phase behavior tests are not useful in this regard in the absence of added surfactant.
9. An increase in sodium or surfactant concentration can cause an increase in middle phase formation.

SUMMARY

We have shown how an important property of the system, namely interfacial tension is affected by pH, ionic strength, alkali concentration, added surfactant concentration and type, and

the presence of a cosurfactant. In particular, interfacial tension goes through a minimum with pH as well as ionic strength, and the presence of a small amount of added surfactant can cause interfacial tension to be ultralow both in transient and at equilibrium conditions.

By controling equilibrium pH, equilibrium ionic strength, and equilibrium surfactant concentrationa more effluent flood can be conducted. However, this controling these variables is not easily accomplished due to the harsh environment that the flood is subjected to. So the most obvious parameters that can be controlled are initial pH, initial ionic strength, alkalinity (alkali concentration) and initial surfactant concentration and type. How these variables change during the flood depends upon alkali/surfactant/rock interactions, alkali/surfactant/crude oil interactions, and crude oil/rock interactions.

REFERENCES

1-1. Falcone, J.S.; Krumrine, P.H.; Schweiker, G.C. "The Use of Inorganic Sacrificial Agents in Combination with Surfactants in Enhanced Oil Recovery", *JAOCS*, 1982, 59, 826-832.

1-2. French, T.R.; Burchfield, T.E. "Design and Optimization of Alkaline Flooding Formulations", paper presented at the SPE/DOE Seventh Symposium on Enhanced Oil Recovery held in Tulsa, OK on April 22-25, 1990.

1-3. Holm, L.W.; Robertson, S.D. "Improved Micellar/Polymer Flooding with High-pH Chemicals", *J. Pet. Tech.* 1981, January, 161-172.

1-4. Isaacs, E.E.; Smolek, K.F. "Interfacial Tension Behavior of Athabasca Bitumen/Aqueous Surfactant Systems", *Can. J. Chem. Eng.* 1983, 61, 233-240.

1-5. Krumrine, P.H.; Falcone, J.S.; and Campbell, T.C. "Surfactant Flooding 1: The Effect of

Alkaline Additives on IFT, Surfactant Adsorption, and Recovery Efficiency", *Soc. Pet. Eng. J.* 1982a, August, 503-513.

1-6. Krumrine, P.H.; Falcone, J.S.; Campbell, T.C. "Surfactant Flooding 2: The Effect of Alkaline Additives on Permeability and Sweep Efficiency", *Soc. Pet. Eng. J.* 1982b, December, 983-992.

1-7. Lau, H.C. "Alkali-Enhanced Steam Foam Oil Recovery Process", U.S. Patent No. 4,609,044, 1986.

1-8. Lawson, J.B.; Thigpen, D.R. "Staged Preformed-Surfactant-Optimized Aqueous Alkaline Flood", U.S. Patent No. 4,502,541, 1985.

1-9. Martin, F.D.; Oxely, J.C.; and Lim, H. "Enhanced Recovery of a "J" Sand Crude Oil with a Combination of Surfactant and Alkaline Chemicals", presented at the 60th Annual Technical Conference and Exhibition of the Society of Petroleum Engineers held in Las Vegas, NV on September 22-25, 1985; paper SPE 14293.

1-10. Mehdizadeh, A.; Handy, L.L. "Further Investigation of High-Temperature Alkaline Floods", presented at the 59th annual Technical Conference and Exhibition held in Houston, TX on September 16-19, 1984; paper SPE 13072.

1-11. Nelson, R.C. "Chemically Enhanced Oil Recovery: The State of the Art", *Chem. Eng. Prog.* 1989, March, 50-57.

1-12. Nelson, R.C.; Lawson, J.B.; Thigpen, D.R.; Stegemeier, G.L. "Cosurfactant-Enhanced Alkaline Flooding", presented at the SPE/DOE Fourth Symposium on Enhanced Oil Recovery held in Tulsa, OK on April 15-18, 1984; paper SPE/DOE 12672.

1-13. Rudin, J. "Surfactant-Enhanced Alkaline Flooding", Ph.D. Thesis, Illinois Institute of

Technology, Chicago, Illinois, December, 1991.

1-14. Rudin, J.; Wasan, D.T. "Mechanisms for lowering of interfacial tension in Alkali/Acidic Oil Systems, Part I: Experimental studies", *Colloids and Surfaces* 1992a, 68, 67-79.

1-15. Rudin, J.; Wasan, D.T. "Mechanisms for lowering of interfacial tension in Alkali/Acidic Oil Systems, Part II: Theoretical Studies", *Colloids and Surfaces* 1992b, 68, 81-94.

1-16. Rudin, J.; Wasan, D.T. "Mechanisms for lowering of interfacial tension in Surfactant-Enhanced Alkali/Acidic Oil Systems: Effect of Added Surfactant", *Industrial and Engineering Chemistry Research* 1992c, 31, 1889-1906.

1-17. Rudin, J.; Wasan, D.T. "Surfactant-Enhanced Alkaline Flooding: Buffering at Intermediate Alkaline pH", *SPE Reservoir Engineering* 1993, November.

1-18. Schuler, P.J.; Lerner, R.M.; Kuehne, D.L. "Improving Chemical Flood Efficiency with Micellar/Alkaline/Polymer Processes", presented at the Fifth Symposium on Enhanced Oil Recovery held in Tulsa, OK on April 20-23, 1986; paper SPE/DOE 14934.

1-19. Southwick, J.G.; Nelson, R.C. "Process for Preparing Alkaline Flooding Solutions that Avoid Silica Dissolution", U.S. Patent No. 4,458,755, 1984.

1-20. Surkalo, H. "Enhanced Alkaline Flooding" *J. Pet. Tech.* 1990, January, 6-7.

CHAPTER 2

Fluid-Solid Interaction: Optical imaging by differential and common interferometry

Structure and Dynamics of the Film/Meniscus Transition Region

The three phase contact angle is an important macroscopic characteristic of a capillary system and provides information about the interfacial energy of different surfaces, adhesion, wetting, and spreading. The rapid progression of studies on contact angle measurements is represented by the works of Neumann and Good 1979; Derjaguin et al., 1987; de Gennes 1985; Cutler and Kissa 1987; and, more recently, Kao et al., 1989; Dimitrov et al., 1990; Debacher and Ottevil 1991; Cazabat et al., 1991; Good 1994, Lee 1994, and Hirasaki 1994. The three phase contact angle is defined as one of the angles subtended by three (or more) interfaces at their line of intersection. Usually this is the angle between the interfaces of the choosing liquid (See Figure 2-1 a,b). It should be noted that the three phase contact angle define by the Neumann Young equation: $\sigma_{s/o} = \sigma_{s/w} + \sigma_{o/w} \cos \Theta_{mac}$ is a based on macroscopic concept, and the three-phase contact angle kinetic depends on the tangential balance between the three interfacial tensions: solid/oil-$\sigma_{s/o}$, solid/water-$\sigma_{s/w}$, and oil/water-$\sigma_{o/w}$, and if $\sigma_{s/w} - \sigma_{s/o} > \sigma_{o/w}$ the oil drop will spread on the solid (See Figure 2-1a) and when $\sigma_{s/w} - \sigma_{s/o} < \sigma_{o/w}$ the oil will separate from the solid (See Figure 2-1b). One can imagine that the drop size is also important for the three-phase contact angle kinetics (time for the contact angle to reach its equilibrium value).

The drop excess pressure is given by the Laplace equation and for the drop with the spherical surface : $P_\sigma = 2\sigma_{o/w} / R_d$ where R_d is drop radius. The drop excess pressure affects the contact angle kinetics and the smallest droplets on the solid surface will reach their equilibrium value of the three-phase contact angle faster than the larger droplets.

CONTACT ANGLE CONCEPT

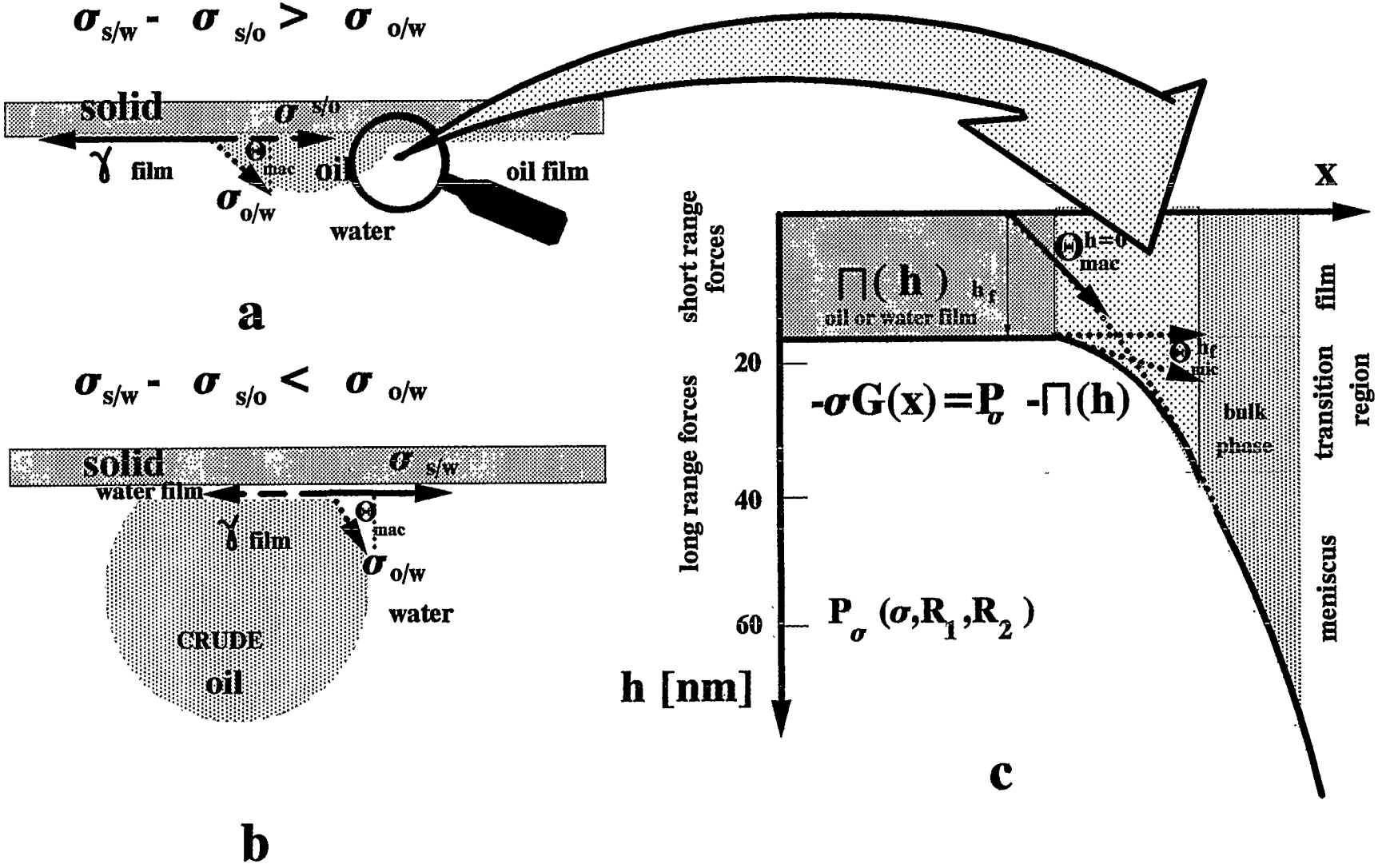

Figure 2-1.

Moreover, in the presence of hysteresis (typical for $\Theta > 20°$), the large drops may never reach their equilibrium contact angle.

In the real system sketched in Figure 2-1c there is a microscopic transition region between a wetting liquid film or a multi-layer adsorbed film and the meniscus, whereas on a microscopic scale the film could change its thickness gradually or by steps. The contact angle region between a liquid film and meniscus is determined by the nature of long and short range intermolecular forces. The equilibrium film thickness h_f depends on the nature of these forces and is given by the disjoining pressure isotherm $\Pi(h)$. The region between the film and drop meniscus is called the transition region, which is like a "wedged" film as shown in Figure 2-1c. The profile of the wedged film obeys the relationship

$$-\sigma G(x) = P_\sigma - \Pi(h) \qquad (1)$$

where G(x) is a local mean curvature, σ is the surface tension, P_σ is the capillary pressure and $\Pi(h)$ is the disjoining pressure. Generally the disjoining pressure is represented by three major terms: $\Pi=\Pi_{wv.}+\Pi_{rep.}+\Pi_{st.}$, where $\Pi_{wv.}$ represents a short-range van der Waals forces, $\Pi_{rep.}$ represents a short-range forces which are of the electrostatic or stearic nature. These two terms account for the interactions between the fluid surface and soil/liquid interface. The last one $\Pi_{st.}$ represents a long-range structural forces (See Chu et al. 1995).

The crude oil contains a submicron asphaltine and resin particles which interact with the film surfaces forming a particle layering structure inside the oil film. The

formation of particle layering inside the film leads to the stepwise film thinning behavior when a oil emulsion film is formed. The stepwise film thinning behavior is shown in Figure 2-2. The oil emulsion film was formed for a model system containing 7 wt% asphaltine dissolved in a 1:1 solution of benzene and heptane. In the presence of solid surface, one can expect that the effect of particle structuring phenomenon is stronger and up to several particle layers are formed close to the solid surface. Indeed for the wedged film bounded by solid surface in the presence of latex particles, Piaranski 1983 observed not only a layering formation but also a in-layer structuring: the first layer containing one layer of particles has a 2-D hexagonal structure, the two-layer has a 2-D cubic structure, but the three-layer has a 2-D hexagonal structure. Recently, using the capillary force balance technique, we have observed a step-wise transition phenomenon of particle layering inside the wedged film (See Figure 2-3).

This in-layer structural transition phenomenon in the film/meniscus region is newly discovered and it depends on the effective particle concentration, polydispersity as well as on the distance between the fluid surfaces bounding this region.

The macroscopic approach for the equilibrium film/meniscus was first developed by Frumkin 1938 and was subsequently used by Derjaduin, Landau and Lifshitz. The contact angle in the transition region is expressed via an integral over the excess disjoining pressure in the liquid film. At equilibrium the relation between contact angle film thickness and drop size (capillary pressure) is given by the equation:

$$\sigma_{o/w}\cos\theta = \sigma_{o/w} + P_c h + \int_{\infty}^{h} \Pi(h)dh \qquad (2)$$

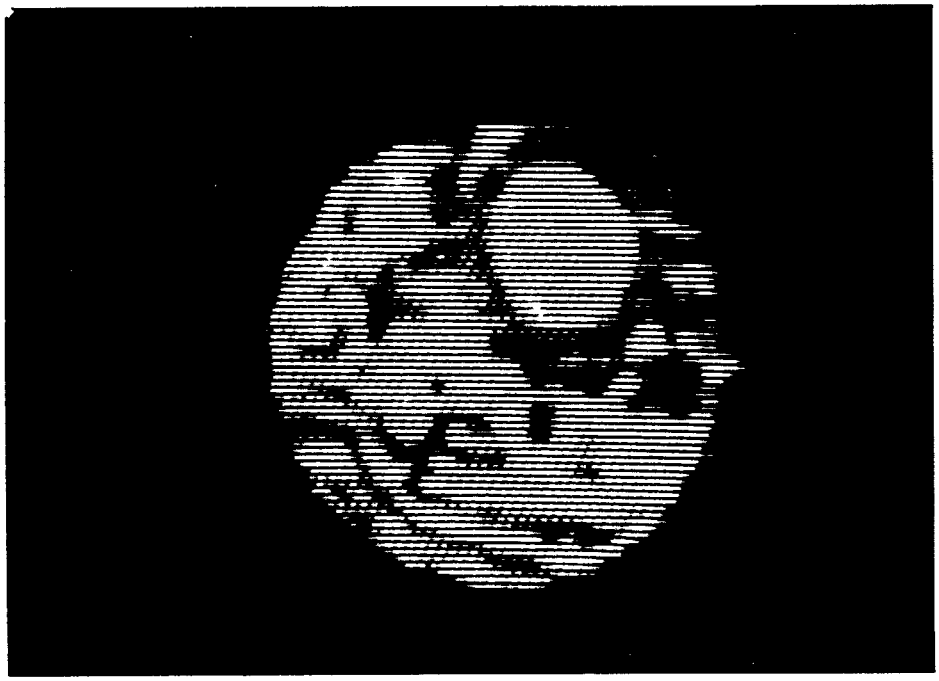

Figure 2-2.

Photomicrograph depicting the stepwise thinning of oil emulsion film in the presence of 7 V% asphaltene.

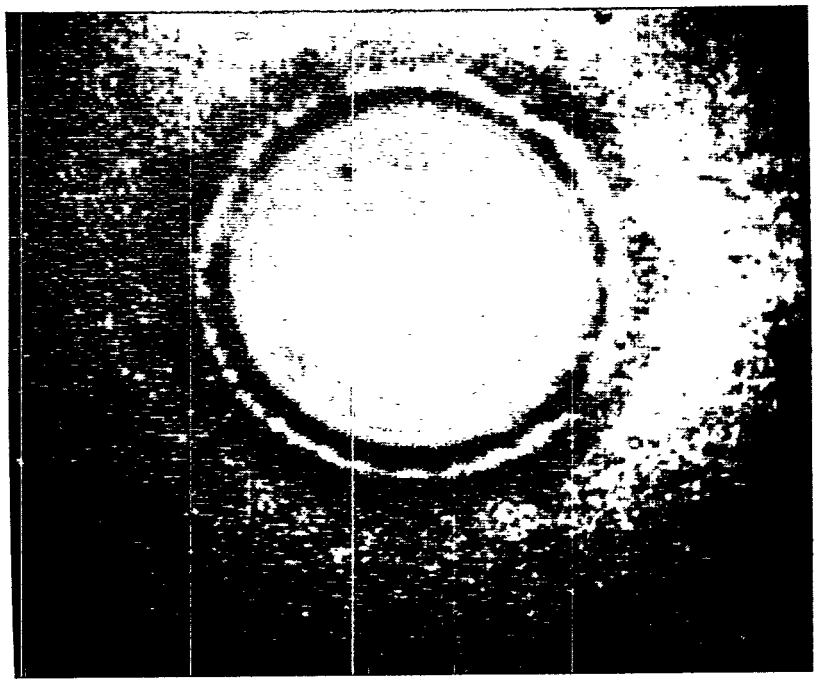

Figure 2-3.

Photomicrograph depicting the particles layering inside the wedged film.

Where Π(h) - is the isotherm of disjoining pressure of the wetting film. Simply by changing the drop size (capillary pressure) the equilibrium film thickness changes and one can use the above relation to study the film thickness stability, disjoining pressure and film elasticity on solid surfaces. The film elasticity is defined as:

$$E_{film}=h_{film}\frac{d\gamma_{film}}{dh_{film}} \tag{3}$$

As illustrated in Fig. 1c, the macroscopic contact angle Θ_{mac} is, by definition, subtended by the extrapolated meniscus surface which satisfies the Laplace equation applied to a solid surface or film h_f=0. This contact angle, $\Theta_{mac,}$ corresponds to a macroscopic model which represents the film as a membrane of zero thickness (the so called membrane model). The conditions for mechanical equilibrium at the contact line provide boundary conditions for the Laplace equation. In the membrane model, the transition region of the film meniscus is replaced by a single contact line, where the mechanical equilibrium is determined by the horizontal balance of forces. To understand the condition for equilibrium drop-film it is preferable to use a detailed model, which represents the film as a layer of finite thickness, h_f, film tension, γ_{film}, contact angle, $\Theta_{mic}{}^{h}$. The film tension is given by:

$$\gamma_{film}^{h}=\left(\frac{\sigma_{o/w}\,\sigma_{o/s}}{\sigma_{o/w}+\sigma_{o/s}}\right)\cos\theta_{h}+P_{o}h_{film} \tag{4}$$

The detailed model is particularly appropriate in the case of very small contact angles (spreading phenomenon), because the extrapolated meniscus surfaces may not intersect the solid surface. For the case of small droplet on the solid surface or when the oil drop is moving into tiny capillary a three phase contact line is formed with very small curvature 1/r, where the mechanical equilibrium is determined by the horizontal balance of four forces:

$$\gamma+\sigma_{o/w}\cos\Theta_{mac}+\sigma_{o/s}+\kappa/r=0 \qquad (5)$$

where γ is the film or interfacial tension solid /water,κ is the line tension and r is the radius of curvature of the contact line.

Usually, the term κ/r is negligible, however, for a meniscus with a small three-phase contact line (penetration of fluid inside the pore structure), the last term in above equation could play a significant role on the contact angle value and meniscus curvature.

Methods of Measuring Meniscus Profile

The equations (1, 2, 4 and 5) provide a suitable basis for determination of, contact angle, and surface and interfacial tensions. However, we emphasize that these equations are valid only when the contact angle is defined correctly as described above. Experimentally, the contact angles are usually measured by determining, by some optical method, the shape of the surfaces at some distance away from the contact line and then by extrapolating them until they intersect. The first problem that is encountered when this procedure is carried out in practice is that the minimum distance, from the three-phase

contact line, at which point one can obtain accurate experimental information about the shape of surfaces, is limited by the microscope's resolution power. The second problem is related to the transition region. In order to obtain the right value of the contact angle, all experimental points used for the extrapolation should lie outside the transition region, where the drop shape boundary satisfies the Laplace equation with the macroscopic value of the surface tension.

A. Side-View Method

The simplest way to determine the contact angle is to take side-view pictures of the system (side-view or goniometric method) (See Smolders and Overbek, 1961; Good, 1979; Chen et al., 1990) Dimitrov et al., 1991.

The major shortcoming of the side-view method is that the region close to the contact line cannot be seen and the extrapolation of the surfaces could result in considerable error. The side-view observation would give correct results only if the contact line and the transition region are determined accurately and the correct definition of the contact angle is used. That is why, very often, the experimental interpretation of contact angle is not correct. Therefore, interferometric methods which provide more accurate information about the shape of the meniscuses close to the three-phase contact region are the subject of this study.

B. Imaging Profile of a Fluid Layer by Light Interference Phenomena

The interference phenomenon occurs when the thickness of a transparent liquid film is comparable to the wavelength of the light and has a wedge-shaped profile. The fringes are due to differences in the optical paths, Δ, between light beams which are reflected (or refracted) by two interfaces. If light of wavelength λ is used, the fringes of maximum or minimum intensity are loci of points satisfying the requirement

$$\Delta = i\lambda/2, \quad i=0,1,2...,$$

where i is the order of interference. There are two optical ways to originate interference patterns. These are:

Reflection Interferometry

The physical principle of the interference by reflection is illustrated in Figure 2-4a. The light beams, reflected from interface $Z_1(x,y)$, interfere with the beams reflected from the interface $Z_2(x,y)$ (Nikolov and Wasan 1995). If n_1, n_2 and n_3 are the refractive indexes of the three neighboring phases, then $\Delta=2(Z_1-Z_2)n_2$.

When $n_2>n_1$ or n_3, then i is odd for the bright and even for the dark fringes. The position of the interference patterns in combination with the Laplace equation can be used successfully to obtain information on the profile of the meniscus interfaces. Practical applications of the method, such as calculating the meniscus profile and the three-phase contact angle have been published elsewhere (Dimitrov et al. 1990). When the fluid interface has a high radius of curvature, the distance between the interference patterns is

too small to be measured. In that case, differential interferometry can be used for imaging the interface profile.

Differential Interferometry

The basic principle of differential interferometry consists of splitting the original image into two images (Dimitrov et al. 1990; Lobo et al. 1990; Nikolov and Wasan 1995).

In the so-called shearing method, horizontal splitting is used, so that the two images are shifted at a distance **d** at which the beams reflected by the interfaces $Z_1(x,y)$ and $Z'_1(x,y)$ with the same y and x, $x+d$, respectively, interfered (See Figure 2-4b). Then $\Delta=2(Z_1-Z'_1)n_1$ and **i** is odd for the dark fringes and even for the bright ones. Thus, the use of differential interferometry in reflected light is only critical to the transparency of the phase with the refractive index n_1 (See the phase configuration shown in Figure 2-4b). For more information on the experimental technique, see Nikolov et al. 1986 and Nikolov and Wasan 1995. Figure 2-5 shows a photograph of the interference patterns produced from a floating crude oil lens at the water/air interface, obtained by reflected light, under the differential microscope. A schematic of the experimental arrangement is given in Figure 2-6. We studied oil/solid interactions, both in the presence of air and in the presence of a water solution, using a reflected light differential interference micrscope (Epival Interphako, Jena). We used the differential interference method to determine the light profile of the oil droplets at the solid/air surface, but the usual refleted light interferometry to determine the profile of the crude oil droplet at solid/water solution.

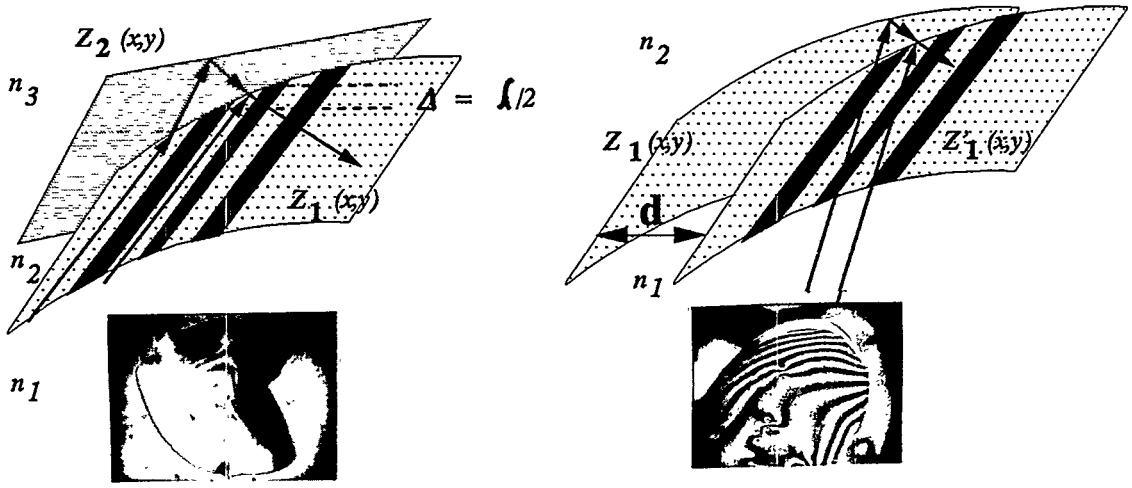

Figure 2-4.

Physical principe of intererence by reflectiona: usual interferometry; b- diferantial interferometry

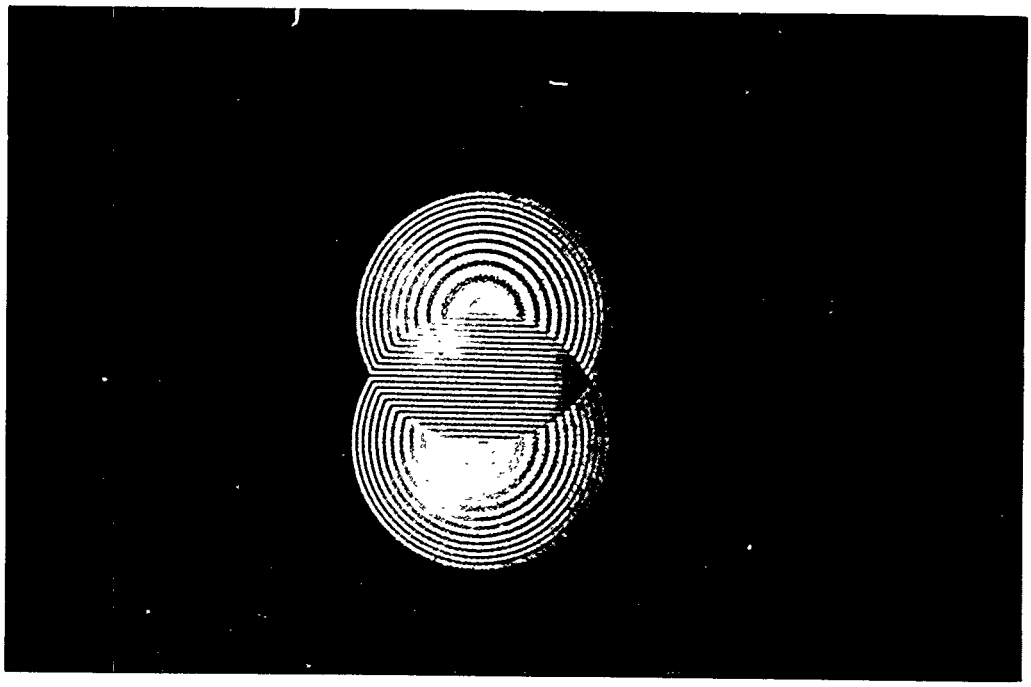

Figure 2-5.

Photomicrograph depicting the difference patterns in light reflected from the cap of a floating oil lens at the water/air interface.

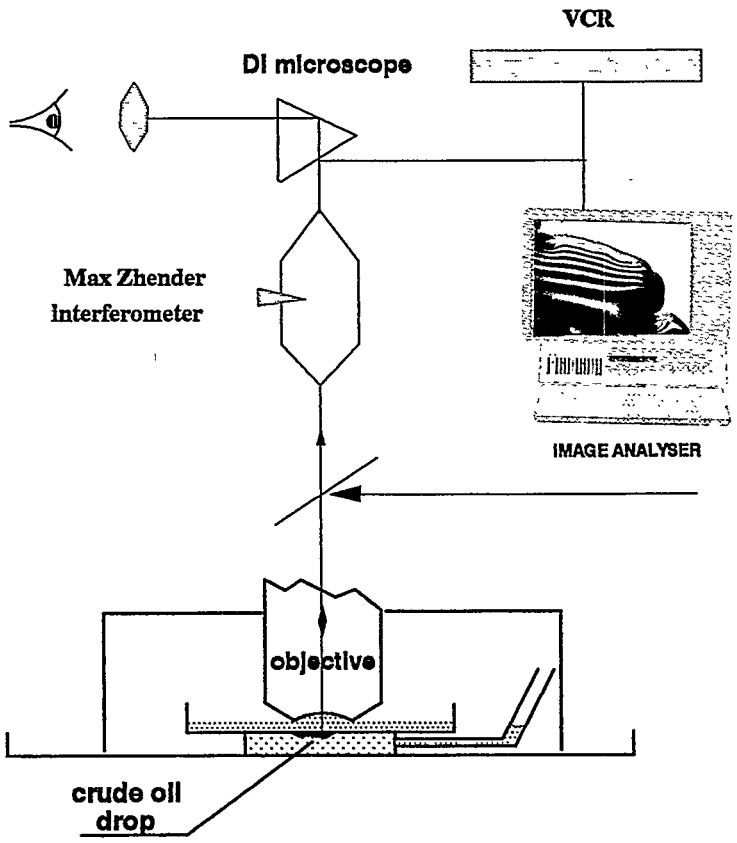

Figure 2-6.

Schematic of the experimental set-up used for microscopic studies of crude oil silica surface interactions

Contact angle kinetics at low concentration of Na^+

The three-phase contact angle kinetics of preequilibrated Long Beach crude oil with alkali solution (Na^+=0.085mol/l at pH=10.01) is shown in Figure 2-7, and the contact angle kinetics are presented in Table 2-1. The interferometric microphotograph clearly depicts the contact angle kinetics. Figure 2-7a shows a microphotograph taken in common interferometry of an oil drop on the silica surface in the presence of air with size 500 μm. The drop has an irregular shape indicating the contact angle hysteresis. The circular interference patterns seen in the microphotograph (See Figure 2-7a) have been used to estimate the value of the contact angle (See Table 2-1). Immediately after adding the water solution to the system, the three-phase contact angle begins to shrink irregularly (See Figure 2-7b) and the contact angle increases its value to 15-40°. After 1-2 hours the oil drop has a spherical shape (See Figure 2-7c) with a macroscopic contact angle from 110-140°. One can note a formation of a speckled bright band inside the dark oil area. The specks show the formation of small water lenses between the oil and solid surface. From a microscopic point of view, two contact lines have been established: the first is between the oil drop, solid surface and water film (outer line), and the second is between the oil drop, solid surface/water film (inner line). After several hours, the oil drop is separated from the solid by the water film (See Figure 2-7d).

Contact angle kinetics at low concentration of Na^+ and in the presence of surfactant B-105

We also studied the three-phase contact angle kinetics of preequilibrated Long

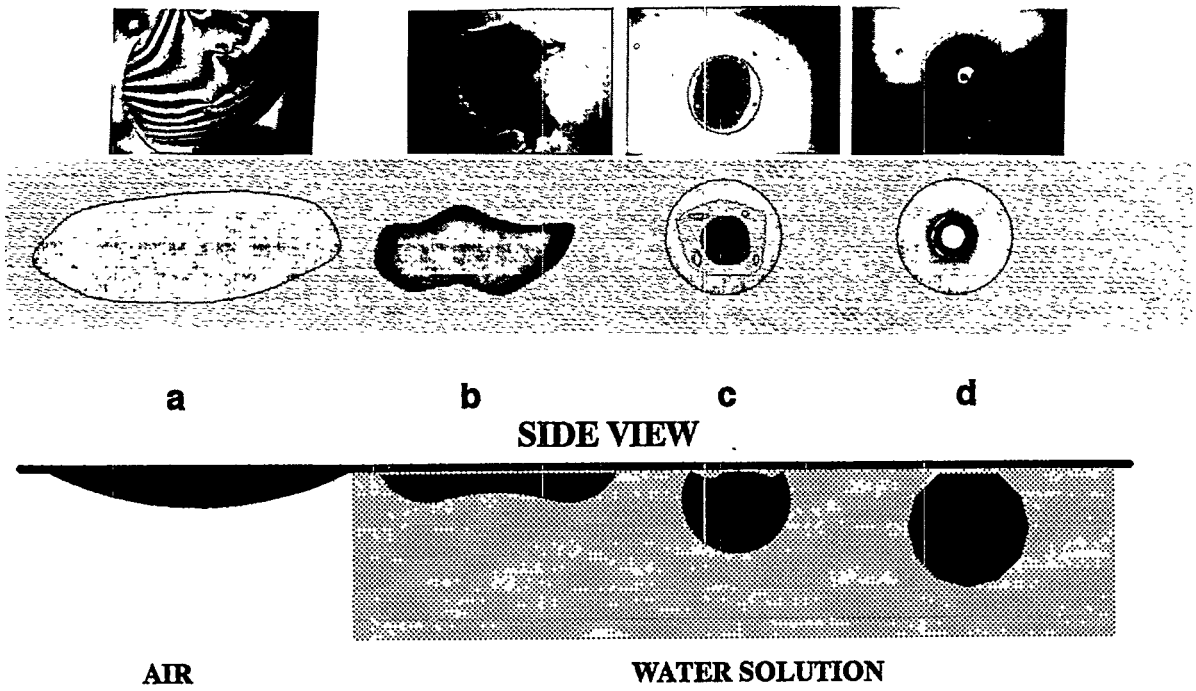

Figure 2-7.

Long beach crude oil silica surface interactions vs. time, a/ oil on solid surface in the presence of air, b/ oil in the presence of watre solution, Na = 0.085 mol/l, pH=1(after 1/2 h, c/ after 1-2 h, oil begins to separate from solid, d/after 3-4 h drop is separated from the solid with watre film.

Table 2-1. For drop size from 400-700 microns

Sample	Na=0.085 mol/l, pH=10.01			
Time (hour)	0	0.5	1-2	3-4
Contact Angle (^{o})	5-10	15-40	110-140	175
Sample	Na=0.085 mol/l, pH=10.01, 0.1% Petrostep B-105			
Time (hour)	0	1-2	5-6	10-14
Contact Angle (^{o})	5-10	10-30	110-150	170
Sample	Na=1.0 mol/l, pH=10.20			
Time (hour)	0	0.5	4-5	18-20
Contact Angle (^{o})	5-10	1-3	0.1-0.5	0-0.1
Sample	Na=1.0 mol/l, pH=10.03, 0.1% Petrostep B-105			
Time (hour)	0	1-2	8-10	
Contact Angle (^{o})	5-10	20-40	70-120	

Beach crude oil with water solution (Na^+=0.085mol/l and 0.1 wt% B-105 at pH=10.03). Figure 2-8 shows interferometric microphotographs depicting the contact angle kinetics and its hysteresis. The contact angle kinetics are presented on Table 2-1. Figure 2-8a shows a microphotograph taken in usual interferometry of an oil drop on silica surface in the presence of air. The drop size is about 700 μm. The small dark spots inside the oil drop are small air bubbles trapped inside the oil. The drop three-phase contact line has an irregular shape, indicating the contact angle hysteresis. The circular interference patterns seen in the microphotograph (See Figure 2-8a) have been used to estimate the value of the contact angle and its hysteresis (See the data presented in Table 2-1). After adding water solution (Na^+=0.085mol/l and 0.1 wt% B-105 at pH=10.03) to the system, the three-phase contact line begins to shrink irregularly (See Figure 2-8b) and the contact angle slowly increases its value to 10-30°. Compared with the previous case without surfactant, the contact angle kinetics are much slower and even after several hours (see Figure 2-7c) the drop has an irregular shape. Note in the previous case, for that period of time, the oil drop has been separated from the solid surface. In this case, the drop is separated from the solid (See Figure 2-8d) after 10-14 h. The detailed examination of the microphotograph in Figure 2-8d shows that the water film separating oil drop from solid surface is much thinner (See and compare the intensity of the central bright spot of Figure 2-7d and 2-8d).

Contact angle kinetics at high concentration of Na^+ without surfactant

In order to study the effect of electrolyte on the three-phase contact angle kinetics,

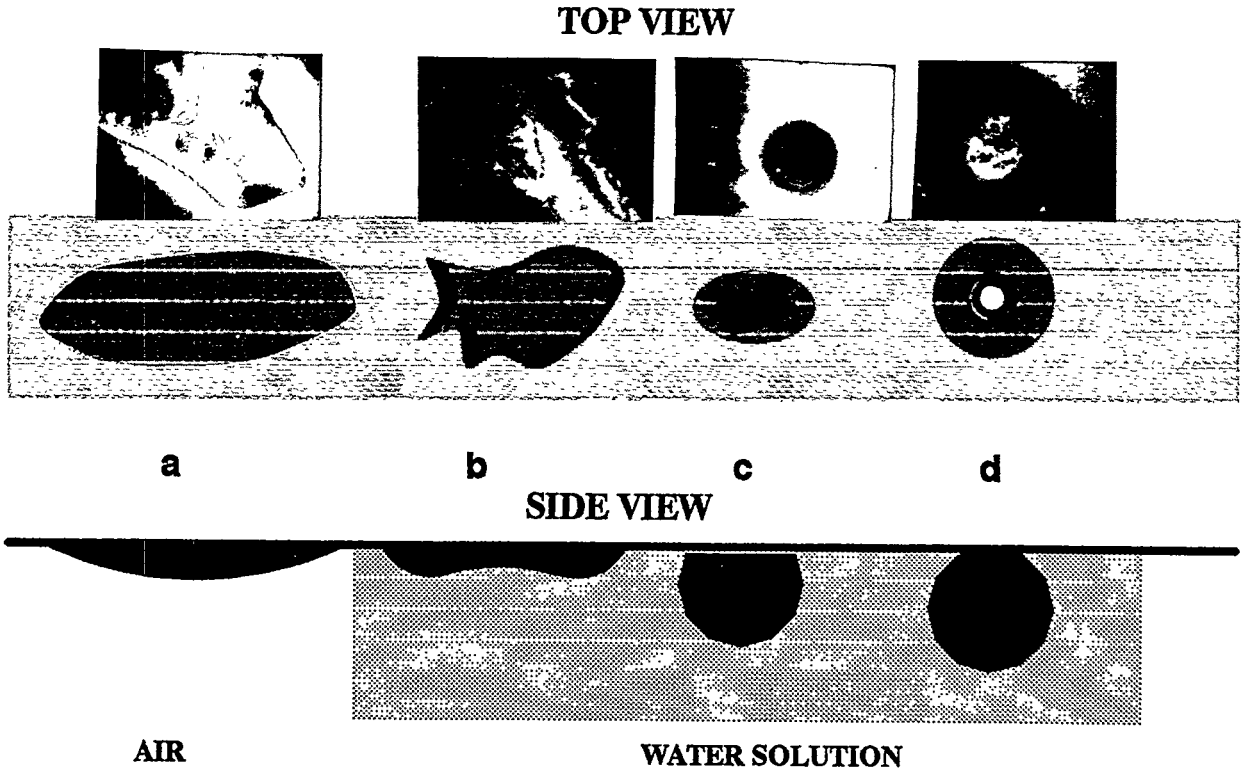

Figure 2-8.

Long Beach crude oil silica surface interactions vs. time a/ oil on solid surface in the presence of air, b/ oil on solid surface in the presence of water solution Na^{+}= 0.085 mol/l, 0.1 wt% B-105 and pH=10.03 after 1-2 h, c/ after 5-6 h, oil begins to separate from solid, and d/ after 10-14 h some of the smaller oil drops are separated from the solid with water film.

the Long Beach crude oil was preequilibrated with water solution (Na^+=1.0 mol/l and pH=10.20). Figure 2-9 shows interferometric microphotographs depicting the contact line kinetics, and the contact angle kinetics are presented in Table 2-1. Figure 2-9a shows a microphotograph taken in usual interferometry of an oil drop on a silica surface in the presence of air. The drop size is about 600 μm. After adding water solution (Na^+=1.0 mol/l at pH=10.20) to the system, the three-phase contact line begins to spread, and an oil film is formed on the solid surface (See Figures 2-9b and 2-9c). The value of the contact angle decreases. Note that the distance between the interference patterns versus time increases (See and compare Figures 2-9b and 2-9c) which shows that the contact angle between film and oil drop decreases, and almost all of the oil spreads on the solid. The oil film thickness is about 100 to 200 nm (See Figure 2-9d), and the values of macroscopic contact angle versus time are presented in Table 2-1.

Contact angle kinetics at high concentration of Na^+ with surfactant

The three-phase contact angle kinetics of preequilibrated Long Beach crude oil with water solution (Na^+=1.0 mol/l with 1 wt% B-105 at pH=10.03) are shown in Figure 2-10. The macroscopic contact angle kinetics are presented in Table 2-1. The interferometric microphotograph in Figure 2-10a shows an oil drop on the solid silica surface in the presence of air. The macroscopic contact angle is from 5-10° as in the previous case. In the presence of alkali solution (Na^+=1.0 mol/l with 1 wt% B-105) we observed that the three-phase contact line begins to shrink irregularly (See Figure 2-10b) and contact angle increases its value after 1-2 h to 20-40°. After 8-10 hours the oil splits

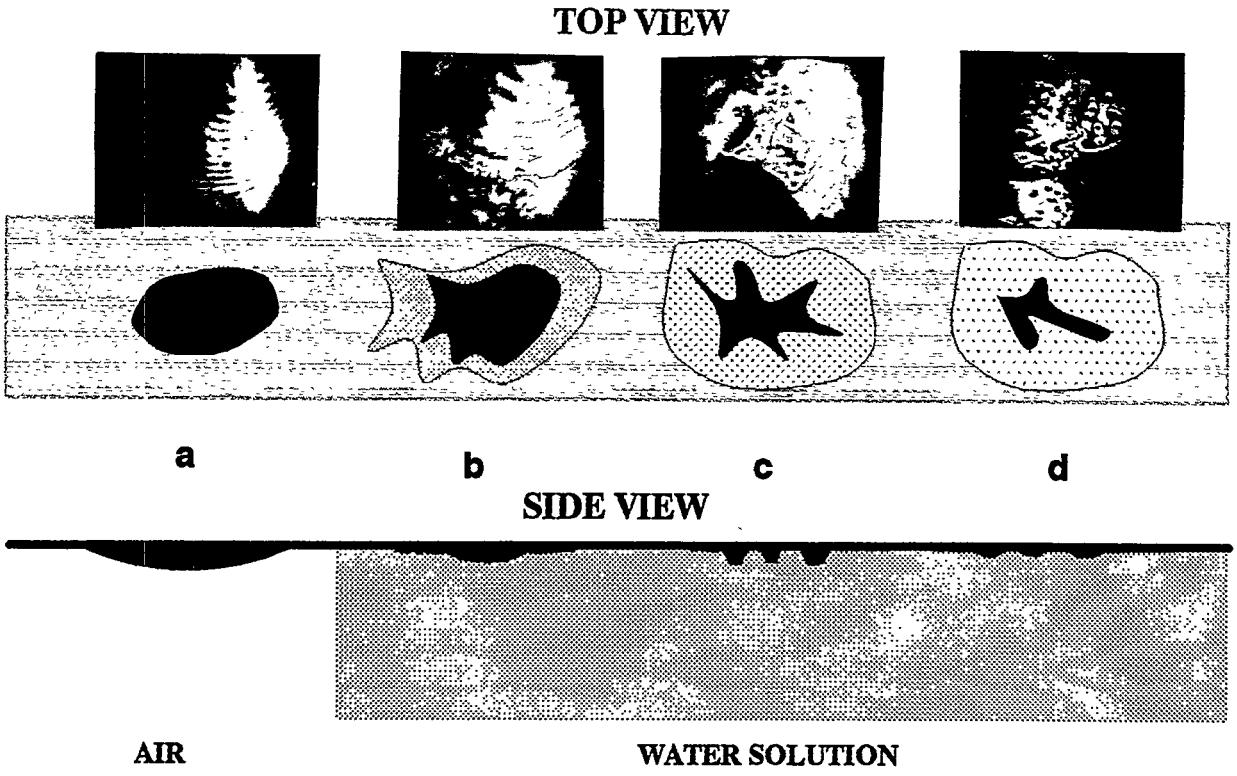

Figure 2-9.

Long Beach crude oil silica surface interactions vs. time a/ oil on solid surface in the presence of air, b/ oil on solid surface in the presence of water solution Na^{+}= 1.0 mol/l, and pH=10.20 after 1/2 h, oil begins to spread on the solid c/ after 4-5 h around the intial oil drop a thin oil film is formed, d/ afte 18-20 h oil film thicknes is 100 to 200 nm.

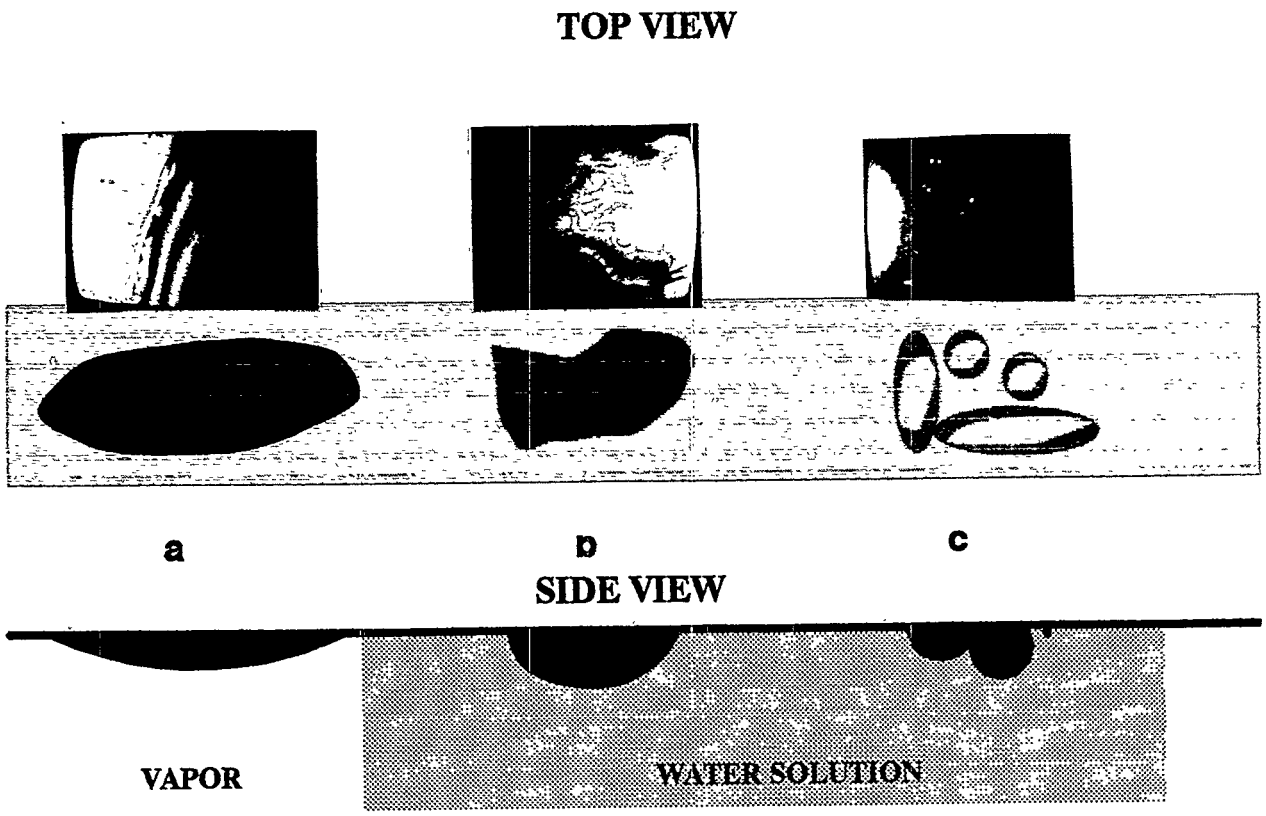

Figure 2-10.

Long Beach crude oil silica surface interactions vs. time a/ oil on solid surface in the presence of air, b/ oil on solid surface in the presence of water solution Na^{+}= 1.0 mol/l, 0.1 wt% B-105, pH=10.03 after 1-2 h, c/ after 8-10 h the contact region shrinks and smaller drops are formed having biger contact angle.

into smaller drops (See Figure 2-10c).

Calculation of film elasticity

We observed, when the crude oil droplets are placed on the dry silica surface and then a water solution with low concentration of Na^+ and surfactant B-105 is added, after several hours the oil droplets began to separate from the solid surface with small amounts of water. One can imagine that in the real enhance oil recovery process that the interactions between the crude oil droplets with the solid surface in the presence of water solution with low concentration of Na^+ and surfactant B-105 also took place. To model the interactions between the crude oil drop with the silica surface in the presence of low concentration of Na^+ and surfactant B-105 we conducted the following experiment. After the oil drop was separated from the solid with the thin water film, a tangential to the silica solid surface, water flow is created. The small oil droplet (with size about 200 μm) begins to roll up on the silica surface and a thick water film is formed. Sloping the water flow the oil drop stops to roll up and the thick water film begins to drain. In Figure 2-11a a film thickness transition is occurring, with a thick film region apparent in the top right of the frame and thin film region apparent in the top left of the frame. In Figure 2-11b the entire film has accomplished the thickness transition and has achieved a thickness of 5 nm. Some simple, asymptotic expansions for the meniscus profile is used to fit the position of interference patterns and to calculate the contact angle and film thickness. The calculated film parameters are presented in Table 2-2.

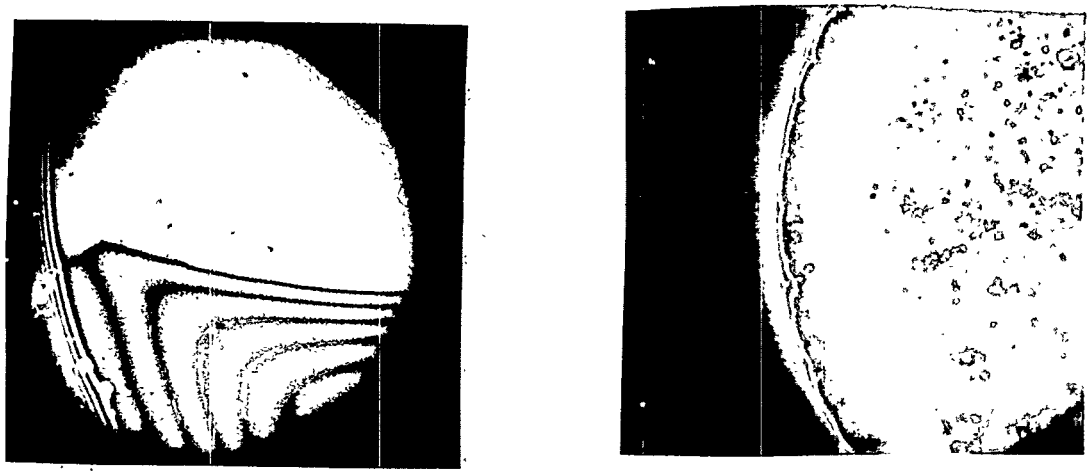

Figure 2-11.

Photomicrographs depicting the film thickness transition of water film on silica surface: a. thick , b. thin film.

Table 2-2. **Calculated Film Parameters**

FILM THICKNESS (Å)	CONTACT ANGLE (deg)	FILM ELASTICITY† dyne/cm
220	0.52	$2.1 * 10^{-4}$
50	1.08	$4.9 * 10^{-5}$

† FOAM FILM ELASTICITY ~ 10^{-3} dyne/cm !

DISCUSSION

The experimental observations show that the concentrations of electrolyte and surfactant are important factors in affecting the macroscopic contact angle kinetics and oil drop separation from the solid surface.

In Figures 2-7d and 2-7d, microscopic photographs depict the initial stages of crude oil droplet separation from a silica solid surface in the presence of low concentration of electrolyte and pH=10. The speckled band between shows the formation of small water lenses (seen as white spots) between the oil and solid surface. Note that at pH=10 on the crude oil/water interface begins the formation of soap. The concentration of soap locally increases, specially inside the three phase contact region where the diffusion is restricted. The surfactant suppressed interfacial tensions provide the driving force for oil removal, and "diffusional" mechanism, in which water and surfactant molecules diffuse between the oil and solid surfaces ahead of the moving three phase contact region (See Kao, et al. 1989). For this purpose, in the future similar experiments should be performed, investigating the efficiency of oil droplet removal in relation to micellar type and presence, solid surface type, oil type and salt concentration.

Increasing the electrolyte concentration we observed an oil spreading phenomenon on the solid silica surface. For silica surface at higher pH and electrolyte, it is known that the surface charge density increases and porous gel layer is formed with low diffuse potential (R. Hunter 1987, p 381, V1). The gel layer diffuse potential decreases with an increase in the electrolyte concentration and from that one can expect that the interfacial tension ($\sigma_{s/w}$) to increase. The oil/water interfacial tension - $\sigma_{o/w}$ also decreases with

increase in electrolyte concentration. Because of this, one can expect a spreading of the oil phase on the solid surface and, indeed, in the presence of high electrolyte concentration, we observed oil spreading on the solid surface (See Figure 2-10d and Table 2-1). It is well known that in the presence of surfactant the interfacial tension of oil/water is reduced and surfactant may also reduce the surface energy (interfacial tension) of solid/water. To predict the effect of surfactant on the contact angle, it is also important to know the orientation of surfactant molecules on solid and oil/water surface. Because of negative surface charge of the gel layer formed on the solid surface, one can imagine that the surfactant molecule orientation on the solid surface is with the carbon chain on the solid surface. The orientation of surfactant molecule on the water/oil interface is well-known; the surfactant polar part is in the water. Assuming the above described surfactant molecular orientation, one can predict that in the presence of surfactant the contact angle of an oil drop will increase. However, the three-phase contact angle kinetics also depend on the drop size and interfacial tension. With a smaller drop, the drop excess pressure is higher, and the three-phase contact angle reaches its equilibrium value faster. By that reason at high surfactant concentration even the small droplets can not reach its equilibrium contact angle value.

In Table 2-2 are presented the calculated film parameters: contact angle and film elasticity at two film thicknesses of the water pseudo-emulsion film: 22nm and 5nm. The calculated film elasticity for the water pseudo-emulsion film is at least one order of magnitude smaller than the elasticity of a foam film where the solid surface is not present. We believe a possible reason for that difference is the strong long range forces

of the solid surface, which induces a structure inside the water pseudoemulsion film. Such effect of the water structuring between two solid surfaces has been reported by Isrealchvili and co-worker (1985).

REFERENCES

2-1. Neumann, A.W. and Good, R.J., "Techniques of Measuring Contact Angles", Surface and Colloid Science, (Eds.) R.J. Good and R.R. Strober, Vol.11, Plenum, N.Y., pp.31-92, (1979).

2-2. Derjaguin, B.V., Churaev, N.V. and Muller V.M.,"Surface Forces", Consultant Bureau, N.Y.,pp.363-380, (1987).

2-3. de Gennes, P.G., *Rev.Mod.Phys.* **57**, 827, (1985).

2-4. Cutler, W.G. and Kissa, E. (Eds.), "Detergency-Advances", M. Dekker, 1987.

2-5. Kao,R., Wasan, D.T., Nikolov, A.D. and Edwards, D.A, *Colloids and Surfaces*, **34**, 389 (1988).

2-6. Dimitrov, A.S., Kralchevsky, P.A., Nikolov, A.D. and Wasan, D.T., *Colloids and Surfaces*, **47**, 299 (1990).

2-7. Debacher, N.A. and Ottewill, R.H., *Colloids and Surfaces*, **52**, (1991).

2-8. Cazabat, A.M., Fraysse. N and Heslot, F., *Colloid and Surfaces*, **52**, 1 (1991).

2-9. Good, R.J., Contac angle, wetting, and adhesion: a critical review "in Contact Angle, Wettability and Adhesion", Ed K.L. Mittal, VSP, pp.3-36, (1993).

2-10. Lee, L.H., Roles of molecular interactions in adhesion, adsorption, contact angle

and wettability "In Contact Angle, Wettability and Adhesion", Ed K.L.Mittal, VSP, pp.45-96, (1993).

2-11. Hirasaki, G.J., Structural interactions in wetting and spreading of van der Waals fluids "In Contact Angle, Wettability and Adhesion", Ed K.L.Mittal, VSP, pp.183-220, (1993).

2-12. Chu, X., Nikolov, A.D., Wasan D.T., *Langmuir*, (1995, in press).

2-13. Pieranski,P.,*Contemp. Phys.*, **24**, 25, (1983).

2-14. Frumkin, A.,N., *J. of Physical Chemistry*, **12**, 337, (1938) (in Russian)

2-15. Smolders, C.A. and T.G.Overbeek, *Rec. Trav. Chim.*, **80**, 635 (1961).

2-16. Good, R.J., "Contact Angles and the Surface Energy of Solids", Surface and Colloid Science, (Eds.) R.J. Good and R.R. Strober, V.11, Plenum, N.Y. pp. 1-30, (1979).

2-17. Dimitrov A.S.,Kralchevsky,P.A.,Nikolov, A.D.,Noshi H.,Matsumoto M., *J. Colloid and Interface Sci.*, **145**, 279, (1991).

2-18. Lobo, L.A., Nikolov, A.D., Dimitrov, A.S., Kralchevsky, P.A. and Wasan, D.T., *Langmuir*, **6**, 995, (1990).

2-19. Nikolov A.D., Wasan D.T.,"Fluid-Fluid Interfaces: Optical Imaging of Capillary Systems". "in Handbook of Surface Imaging and Visualization" Ed A. Hubbarded, CRC Press, Inc. 1995 (in press).

2-20. Nikolov, A.D., Dimitrov, A.S. Kralchevsky, P.A., *Optica Acta*, v.33, No.11, p.1359, (1986).

2-21. Kao, R., Wasan, D.T., Nikolov, A.D. and Edwards, D. A., *Colloids and Surfaces*,

34, 389-398, (1988).

2-22. Israelachvili J. "in Intermolecular and Surface Forces" Academic press, London, pp 194-212, (1985).

2-23. Hunter R. "in Foundations of Colloid Science" Volume 1, Clarendon press, Oxford, p 381, 1987.

CHAPTER 3

Interactions in Acidic Oil/Alkaline-Surfactant Solutions: Theoretical Studies

INTRODUCTION

Surfactant enhanced alkaline floods have been shown to be more effective than alkaline floods alone. It has been shown that insitu generation of surfactant occurs when an acidic oil is contacted with an alkaline flood solution. In the presence of added surfactant, interaction between the added and generated surfactant is expected to effect the interfacial tension. The increase in micellar hold-up due to the generation of the acid, causes a drop in the equilibrium sodium ion concentration in the aqueous phase due to counter-ion binding. In this chapter, we have studied the effect of the interaction between the generated soap-acid and the added surfactant on the equilibrium interfacial tension in the presence of high sodium ion concentration.

A model which accounts for the interaction between the surface active species (soap, acid and surfactant) was developed. It has been shown that mixtures of soaps (similar to the generated surfactant), and dodecyl benzene sulphonate (added surfactant) show positive deviations from ideality in their mixed cmcs, but not in the mixed adsorbed monolayer formed at the interface (Rosen, 1989). The predictions from this model were compared to experimental data. The effect of interaction parameters on the predictions was studied, to determine their optimum values.

EXPERIMENTAL

The experimental system used was similar to that used by Rudin & Wasan (1992) in their studies of the effect of alkali on interfacial tension of acidic oil/alkaline solution systems. The oil used was Decane, certified grade obtained from Fisher scientific. Oleic acid at a concentration of 20 mol/m^3 was mixed to the oil phase. The aqueous phase was prepared by

dissolving NaCl, certified grade from Fisher scientific, in deionized filtered water. Sodium hydroxide, reagent grade, was added to the aqueous phase at various concentrations. The amount of added NaCl was varied to keep the total added Na+ constant at 171 mol/m^3 (from NaCl and NaOH). 0.1 wt % Sodium Dodecyl Benzene Sulphonate was added to all the aqueous samples. Linear alkyl aryl sulphonates have been experimentally shown to reduce IFT more than several other types of surfactants. The aqueous phase and the oil phases were equilibrated by gentle mixing an contact over a period of 30 days. The interfacial tension of the equilibrated oil and aqueous phase was measured using a spinning drop tensiometer.

MODEL

An equilibrium model was developed for the system. Both the pseudophase separation approximation for micellization as well as the Mass Action Model for micellization were applied. Non-ideality in the mixed micellar phase was approximated by the regular solution approximation (Hall and Huddleston, 1985).

Pseudo-phase separation model

An identical system without the added surfactant has been modeled by Ramakrishnan (1985). However, several equations arising due to the addition of the surfactant were added to the existing model. These were the equations describing the equilibrium material balance for the surfactant, chemical potential balances for the surfactant, ionized acid (soap) and acid in the aqueous, oil and micellar phases. Equations for the activity coefficients of the different surface active components, based on the regular solution approximation for the mixed micelles were

added to the model (Holland and Rubingh, 1983). Mixed micellization for ionic surfactants has been studied by Kamrath and Frances (1983).

The above system of equations were reduced to 4 equations in 4 variables which were,

$$c_S - \frac{c_S^{P^{2-\alpha}}}{c_{Na}^{1-\alpha}} \frac{M_S}{M} \exp\left[\beta_{SA}\left(\frac{M_A}{M} - M_2 c_{HA}\right)^2 + \beta_{SH}(M_2 c_{HA})^2 + (\beta_{SA}+\beta_{SH}-\beta_{AH})\left(\frac{M_A}{M} - M_2 c_{HA}\right)M_2 c_{HA} \right] = 0 \quad (1)$$

$$c_A - \frac{c_A^{p(2-\alpha)}}{c_{Na}^{(1-\alpha)}} \left(\frac{M_A}{M} - M_2 c_{HA}\right) \exp\left[\beta_{SA}\left(\frac{M_S}{M}\right)^2 + \beta_{AH}(M_2 c_{HA})^2 + (\beta_{SA}+\beta_{AH}-\beta_{SH})\frac{M_S}{M} M_2 c_{HA} \right] = 0 \quad (2)$$

where $M_2 = M_1/k_D$ and M is the total micellar phase hold-up.

$$M_A = V_o \left[c_{HA,i} - c_{HA} - 2k_d c_{HA}^2 - \frac{c_{HA}}{k_D V_R} - \frac{c_A}{V_R}\right]$$

$$M_S = V_w \left[c_{Si} - c_S - \frac{V_R c_{Na} c_S (c_o + k_d c_{HA}^2)}{k_s (c_w + c_2)}\right]$$

$$-\frac{c_2 V_w}{\alpha} + \frac{V_w}{\alpha}\left(c_{Na} - c_S - c_A + \frac{k_A c_{HA}}{k_D c_A} - \frac{k_w k_D c_A}{k_A c_{HA}}\right) - V_o c_{HA,i} + V_o c_{HA} + 2k_d V_o c_{HA}^2 + \frac{V_w c_{HA}}{k_D} + V_w c_A - V_w c_{Si} + V_w c_S + \frac{V_o c_{Na} c_S (c_o + k_d c_{HA}^2)}{k_s (c_w + c_2)} = 0 \quad (4)$$

These equations were solved by using a first order technique which may be written as

$$x^{n+1} = x^n - [\, J(x^n)]^{-1} F(x^n) \quad (5)$$

Where, x is the vector of variables,

J is the Jacobian matrix

F is the vector of functions.

and the superscripts n and n+1 represent the values of functions at the previous and current iteration. The above equations yield, the aqueous phase concentrations of the surfactant monomer, ionized acid monomer, the free sodium ions and the oil phase concentration of the acid. All other concentrations were computed from these.

Mass Action Model

The Mass Action Model (MAM) (Jones and Bury, 1927; and Murry and Hartley, 1935) has been applied to the formation of micelles and mixed micelles of two anionic surfactants by Kamrath and Frances (1984). They have extended their model to account for change in the counter-ion binding parameter (Kamrath and Frances, 1985), which makes it applicable to

mixtures of ionic and non-ionic surfactants. This approach views mixed micelle formation as a reversible reaction which may be written as,

$$x_A N\ A^- + x_S N\ S^- + \beta N\ Na^+ \rightleftharpoons M(micelle)$$

where K_M is the equilibrium constant for the above equation. This yields an equation relating the chemical potentials of the products to those of the reactants. Since the stoichiometric coefficients of the reaction appear in the potential balance, the finite aggregation number of the micelles are explicitly taken into account. These equations can be applied to the formation of micelles in pure surfactant solutions also. When only individual surfactant species are present we get

$$N\ A^- + \beta\ N\ Na^+ \rightleftharpoons M_A$$

and

$$N\ S^- + \beta N\ Na^+ \rightleftharpoons M_S$$

where K_A and K_S are the equilibrium constants. Since both A- and S- are anionic, the aggregation number in micelles formed by the mixture of the two is expected to be same as the aggregation number of the pure micelles. In the mass action model, since a finite concentration of micelles is present even at very low surfactant concentrations, the critical micelle concentration has to be defined. The cmc is that concentration of surfactant, at which only a very small fraction of it is in the micellar form. All equations from the phase separation model, except the

chemical potential balances between the micellar and aqueous phase apply here. The reaction equilibrium equations were added to these, to complete the mass action model. These equations were reduced to 4 equations in 4 variables to give the following dimensionless equations.

$$\frac{c_{HAi}}{c_S^*} - \frac{c_{HA}}{c_S^*}(1+2k_d c_{HA} + \frac{1}{k_D V_R}) - \frac{c_S x_A}{V_R c_s^*(1-x_A)} (\frac{1}{d})^{\frac{1}{N}} \exp\,[w(1-2x_A)] - Q\,(\frac{c_{Na}}{c_S^*})^{\beta N} (\frac{c_S}{c_S^*(1-x_A)})^{N} \frac{x_A}{V_R} \exp[-Nwx_a^2] = 0 \quad (6)$$

$$\frac{c_{S,i}}{c_S^*} - \frac{Bc_{Na}c_S(c_o + k_d c_{HA}^2)}{c_S^*} - \frac{c_S}{c_S^*}\left(1 + Q\,(\frac{c_S}{c_S^*(1-x_A)})^{(N-1)}(\frac{c_{Na}}{c_S^*})^{\beta N} \exp[-Nwx_a^2] \right) = 0 \quad (7)$$

$$\frac{c_1 + c_{N,i} + c_{S,i}}{c_S^*} - \frac{c_{Na}}{c_s^*} - \frac{Bc_{Na}c_S(c_o+k_d c_{HA}^2)}{c_S^*} - \beta Q(\frac{c_S}{(1-x_A)c_S^*})^N(\frac{c_{Na}}{c_S^*})^{\beta N} \exp[-Nwx_A^2] = 0 \quad (8)$$

$$\frac{c_{Na}}{c_S^*} + \left(\frac{K_A}{K_D}\right)\frac{d^{\frac{1}{N}}}{c_S^*}\frac{(1-x_A)}{x_A}\frac{c_{HA}}{c_S}\exp[-w(1-2x_A)] - \left(\frac{k_W k_D}{k_A}\right)\left(\frac{1}{d}\right)^{\frac{1}{N}}\frac{c_S x_A}{c_S^* c_{HA}(1-x_A)}$$

$$\exp[w(1-2x_A)] - \frac{c_{N,i}}{c_S^*} - \frac{c_S}{c_S^*} - \frac{\left(\frac{1}{d}\right)^{\frac{1}{N}}}{c_S^*}\frac{x_A}{(1-x_A)}c_s\exp[w(1-2x_A)] - \tag{9}$$

$$(1-\beta)Q\left(\frac{c_S}{(1-x_A)c_s^*}\right)^N\left(\frac{c_{Na}}{c_S^*}\right)^{\beta N}\exp[-Nwx_A^2] = 0$$

where

$$Q = \frac{\varepsilon}{(1-\varepsilon)^N(1-\beta\varepsilon)^{\beta N}}$$

$$B = \frac{P}{k_s\,(\,c_w + c_{n,i}\,)}$$

$$d = \left(\frac{c_S^*}{c_A^*} \right)^{(N(\beta+1)-1)}$$

The above 4 equations were solved by a first order technique same as the one used for solving the phase separation model. These equations yield the concentration of surfactant monomers in the aqueous phase, concentration of sodium ions, the concentration of acid in the oil phase and the fraction of acid in the micelles. All other concentrations were computed from these.

Adsorption

The equations used for obtaining the specific adsorption of all the surface active compounds are similar to those used earlier (Rudin and Wasan, 1992), with some modifications. Since the bulk concentrations are known from the previous section, we get 3 equations in as many variables. The variables here are the moles per unit area of the interface of the unionized acid, the ionized acid and the surfactant. The kinetic and electrical contributions to surface pressure were computed from these variables. The equilibrium IFT was computed based on the equation of state (for the adsorbed layer) approach (Ramakrishnan, 1985). The computed surface pressure is subtracted from the IFT for the clean interface to get the final IFT. In the following equations n_S refers to the moles of surfactant per unit area of the interface at equilibrium, while n_A and n_{HA} refer to the moles per unit area of the ionized and unionized acid at the interface.

$$n_A - d_A c_A (1-f) \exp\left[\frac{W_1}{RT} - 2\sinh^{-1}\left(\frac{(n_A+n_S)\varepsilon N}{2\sqrt{2\varepsilon_m RTc_{Na+}}}\right)\right] = 0 \qquad (10)$$

Where W_1 is the energy required to move a mole of A- from the oil water interface into the bulk water, d_A is the length of the surfactant in the aqueous phase and f, the fractional surface covered is defined as,

$$f = \frac{n_A}{n_{A,\max}} + \frac{n_S}{n_{S,\max}} + \frac{n_{HA}}{n_{HA,\max}} \qquad (11)$$

The adsorption of the acid from the oil phase is quantified by,

$$n_{HA} - d_{HA} c_{HA} (1-f) \exp\left[\frac{W_2}{RT}\right] = 0 \qquad (12)$$

where W_2 is the energy required to move a mole of acid from the interface to the bulk oil and d_{HA} is the length of the acid in the oil phase. The adsorption of surfactant from the aqueous phase is quantified by,

$$n_S - d_S c_S (1-f) \exp\left[\frac{W_3}{RT} - 2\sinh^{-1}\left(\frac{(n_A+n_S)\varepsilon N}{2\sqrt{2\varepsilon_m RTc_{Na+}}}\right)\right] = 0 \qquad (13)$$

where W_3 is the energy required to move a mole of surfactant from the interface to the bulk aqueous phase and d_S is the length of the surfactant in the aqueous phase.

These adsorption equations were solved for the three variables n_A, n_S and n_{HA} using the first order scheme described by equation 5. The fractional surface covered and the resulting surface pressure were computed based on the values of specific adsorptions.

$$\pi_K = RT\, n_{\max} \ln (1-f)$$
$$where \quad n_{\max} = \frac{n_A + n_S + n_{HA}}{f} \tag{14}$$

The above is the kinetic contribution to the surface pressure. The electrical contribution to the surface pressure comes from the Gouy-Chapman theory which accounts for the repulsion in the adsorbed monolayer of ionic surfactants (Ramakrishnan, 1985).

$$\pi_E = \frac{4\sqrt{2}}{\varepsilon} (kT)^{\frac{3}{2}} \sqrt{RT\varepsilon_m c_{Na}} \left[\cosh(\frac{\varepsilon\phi(0)}{2kT}) - 1 \right] \tag{15}$$

where,

$$\phi(0) = -\frac{2kT}{\varepsilon} \sinh^{-1}\left[\frac{(n_A+n_S)\varepsilon N}{2\sqrt{2\varepsilon_m RTc_{Na}}} \right] \tag{16}$$

RESULTS AND DISCUSSION

The main improvement of this model over previous models, is that it accounts for the non-ideality of the micellar pseudo-phase. This implies that the activity coefficient of the surface active species is greater or less than one depending on whether the deviation from ideality is positive or negative. Thus the bulk phase concentrations of the surface active species may be more than or less than the values predicted by a model which does not account for non-ideality. The surface tension reduction is a function of the maximum adsorption and the bulk phase activity. But since the system is always above the mixed cmc, the maximum adsorption does not change significantly and the contribution of the bulk activities to the surface tension reduction has to be considered. Interfacial tension variation beyond cmc are very small, as they are in this system (IFT varies between 1 dyne/cm and zero). The total adsorption which has a stronger effect on IFT also varies with the composition of the interfacial layer.

Figure 3-1 shows a comparison of the experimental data and the predicted IFT from the pseudo-phase separation model, for an ideal and non-ideal micellar phase. The values of the constants defining the surfactant properties are also shown in the figure. Figure 3-2 shows the computed variation of the concentrations of ionized acid (soap) monomers, surfactant monomers in the aqueous phase and that of the acid in the oil phase. It is clear that the acid is practically all in the ionized from at high alkali concentrations. Beyond the point of complete ionization the soap and surfactant concentrations do not change with alkali as no new micelles are formed.

Figure 3-3 shows the variation of the specific adsorptions of the various surface active species with alkali concentration. It is clear that the surfactant adsorbed at the interface is replaced by the soap. Also the acid adsorbed decreases gradually and becomes negligible at high

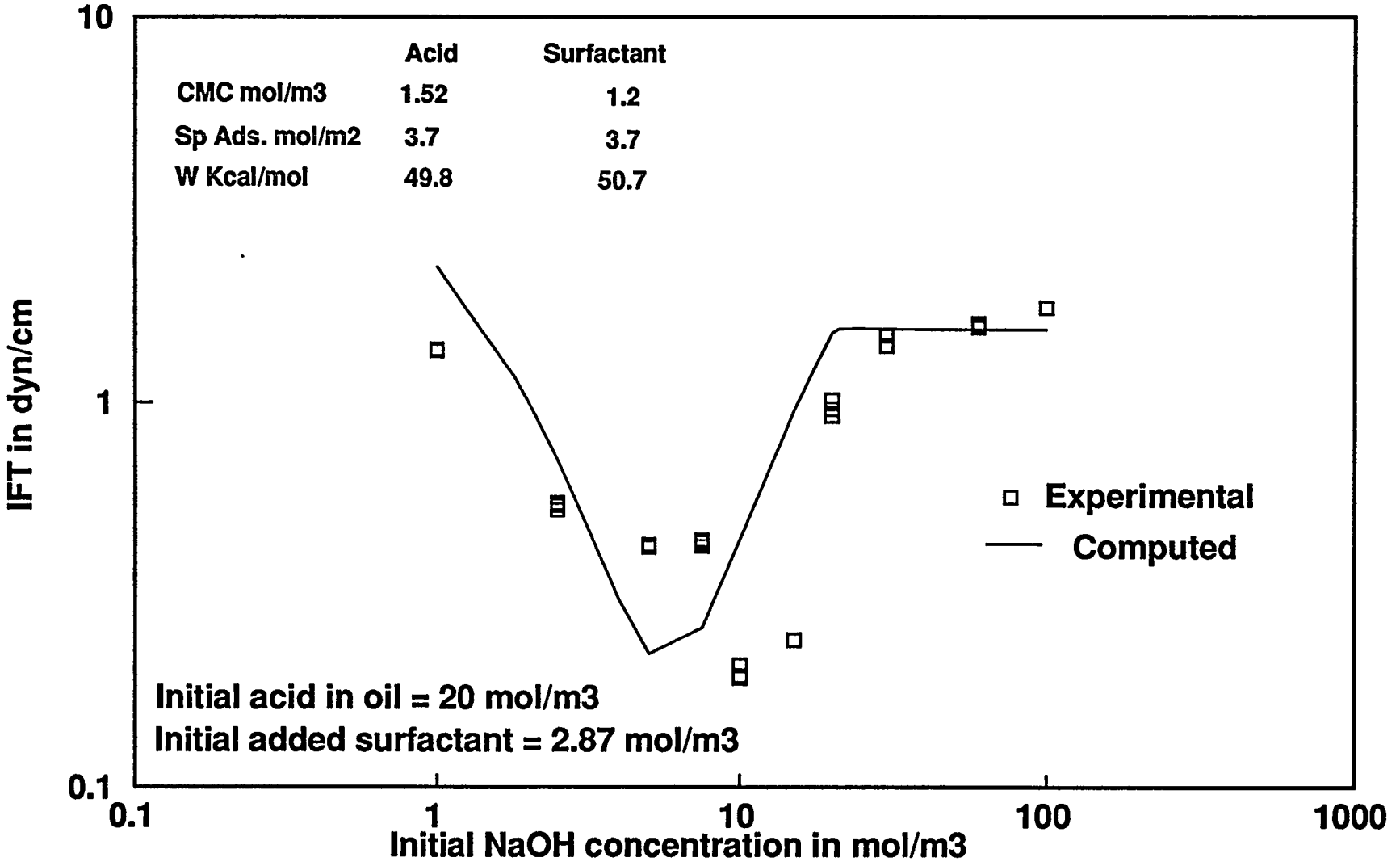

Figure 3-1. **Predicted IFT, based on the pseudo-phase separation model and its comparison to experimental data.**

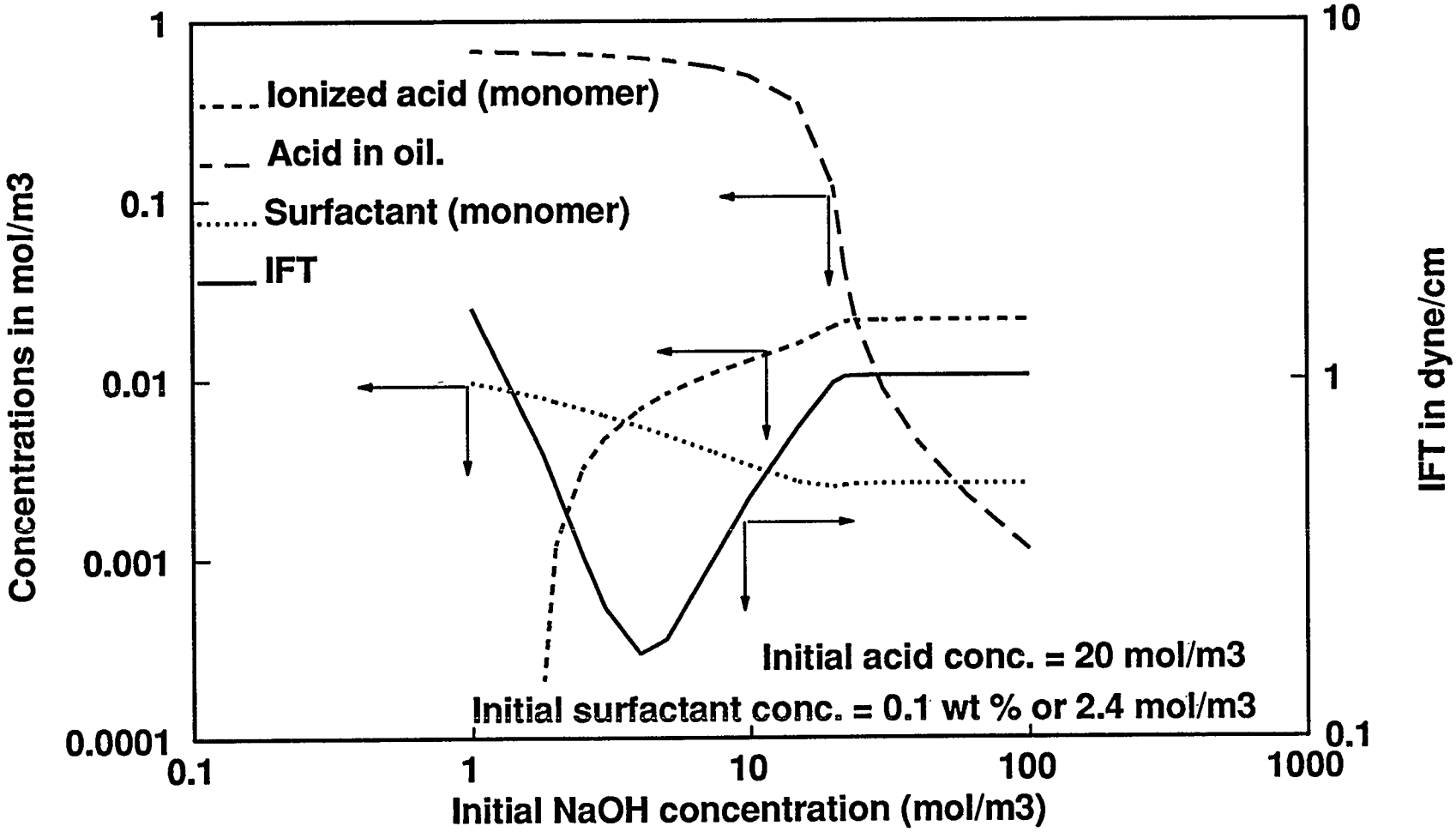

Figure 3-2. **Predicted bulk phase concentrations of the various surface active components.**

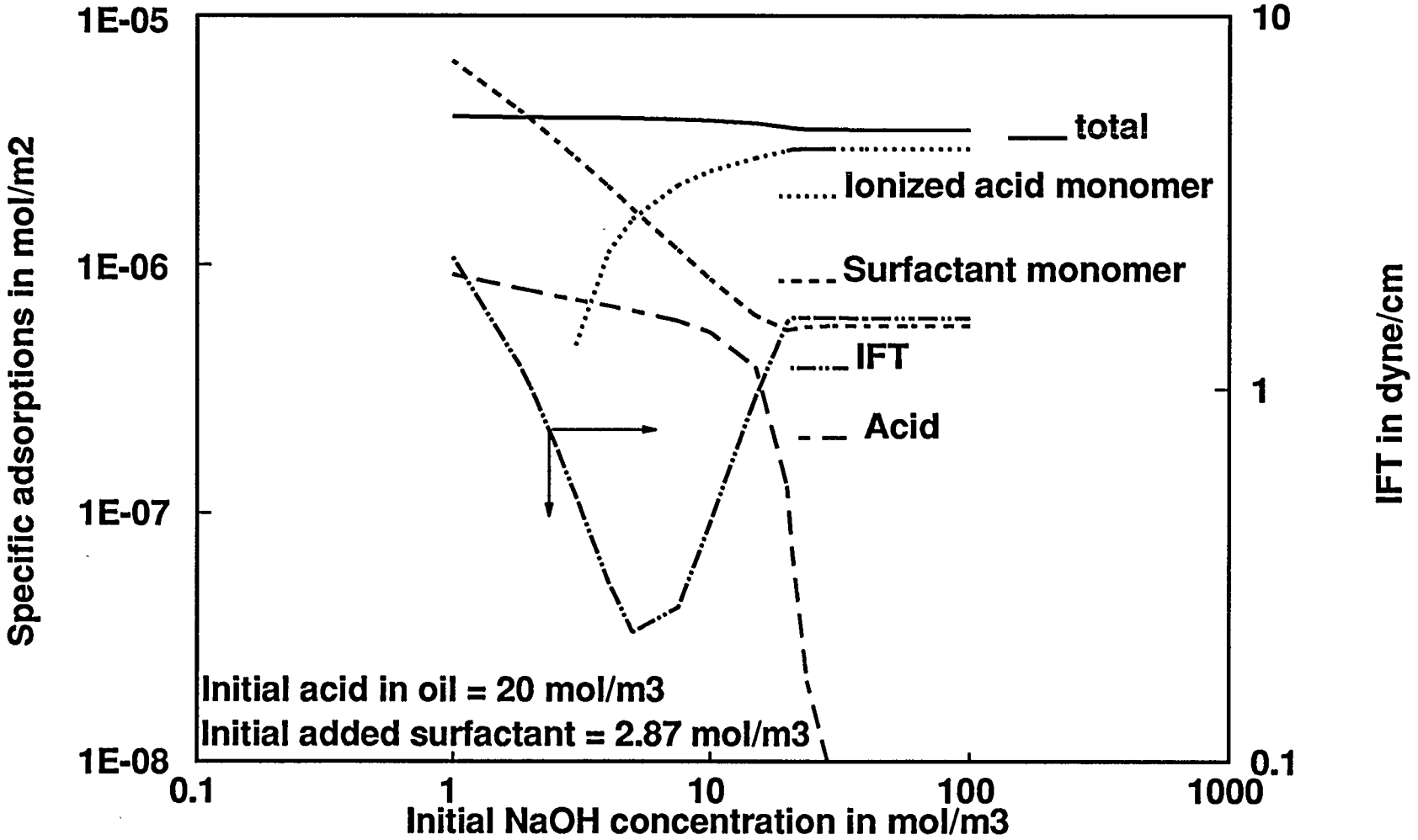

Figure 3-3. **Predicted specific adsorptions of the various surface active components present in the system.**

alkali concentrations. Figure 3-4 shows the respective contributions of adsorption and the electrostatic term to the surface pressure. In this system the total adsorption, decreases gradually which would cause an increase in IFT. However the electrostatic contribution increases with alkali causing the surface pressure to increase.

Figure 3-5 shows that the position of the IFT minima occurs when both the adsorption and the electrostatic contributions are significant. Figure 3-6 shows the variation of the total sodium ion concentration and the electrostatic term to surface pressure. At high sodium ion concentration the electrostatic repulsion between the anionic surface active species at the interface is low due to stronger double layers. As alkali concentration is increased, soap is generated, more micelles are formed, which causes the removal of Na+ from the aqueous phase due to counter-ion binding. The Na+ ion concentration does not change after all the acid is ionized, because beyond this point no more micelles are formed. Figure 3-7 shows the mole fractions of the total acid (including soap) and surfactant in the micellar phase. Since a regular solution model was used to account for non-ideality, the effect of non-ideality will peak when the mole fraction of the two are similar. The regular solution approximation to mixed micelles of anionic and non-ionic surfactants have been criticized on fundamental grounds (Rudin, 1991). However when both surface active components are anionic, the number of possible configurations in a mixed micelle is not much different from that of pure micelles having the same aggregation number. Hence the assumption of negligible entropy change due to mixing is justified. The limitation however remains due to the presence of the small amount of unionized acid in the micelles, which has been shown to have a significant contribution to the observed IFT minima. Figure 3-8 shows the mole fraction of the surface active species at the interfacial layer. Here

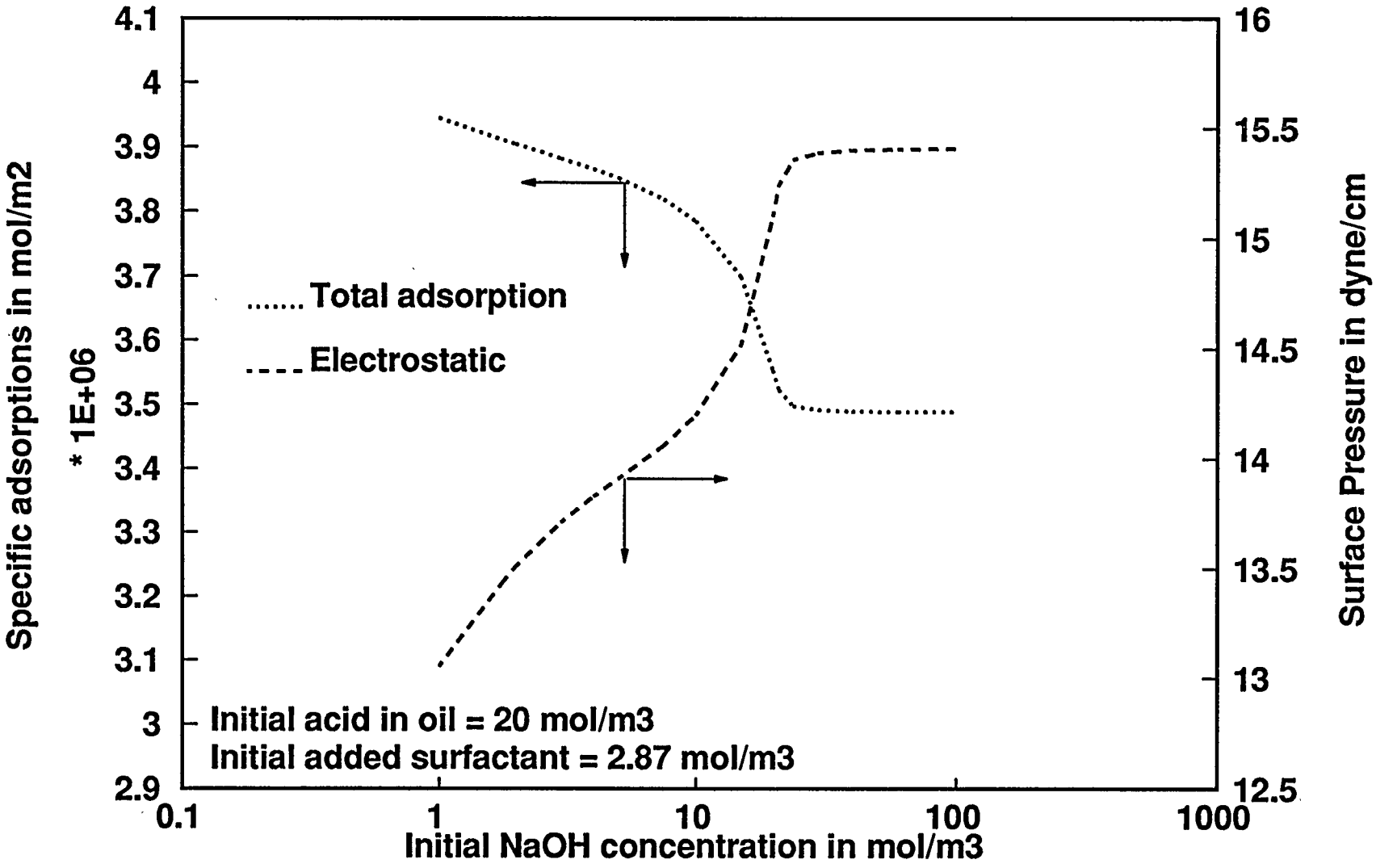

Figure 3-4. **Predicted total specific adsorption and the electrostatic component of surface pressure.**

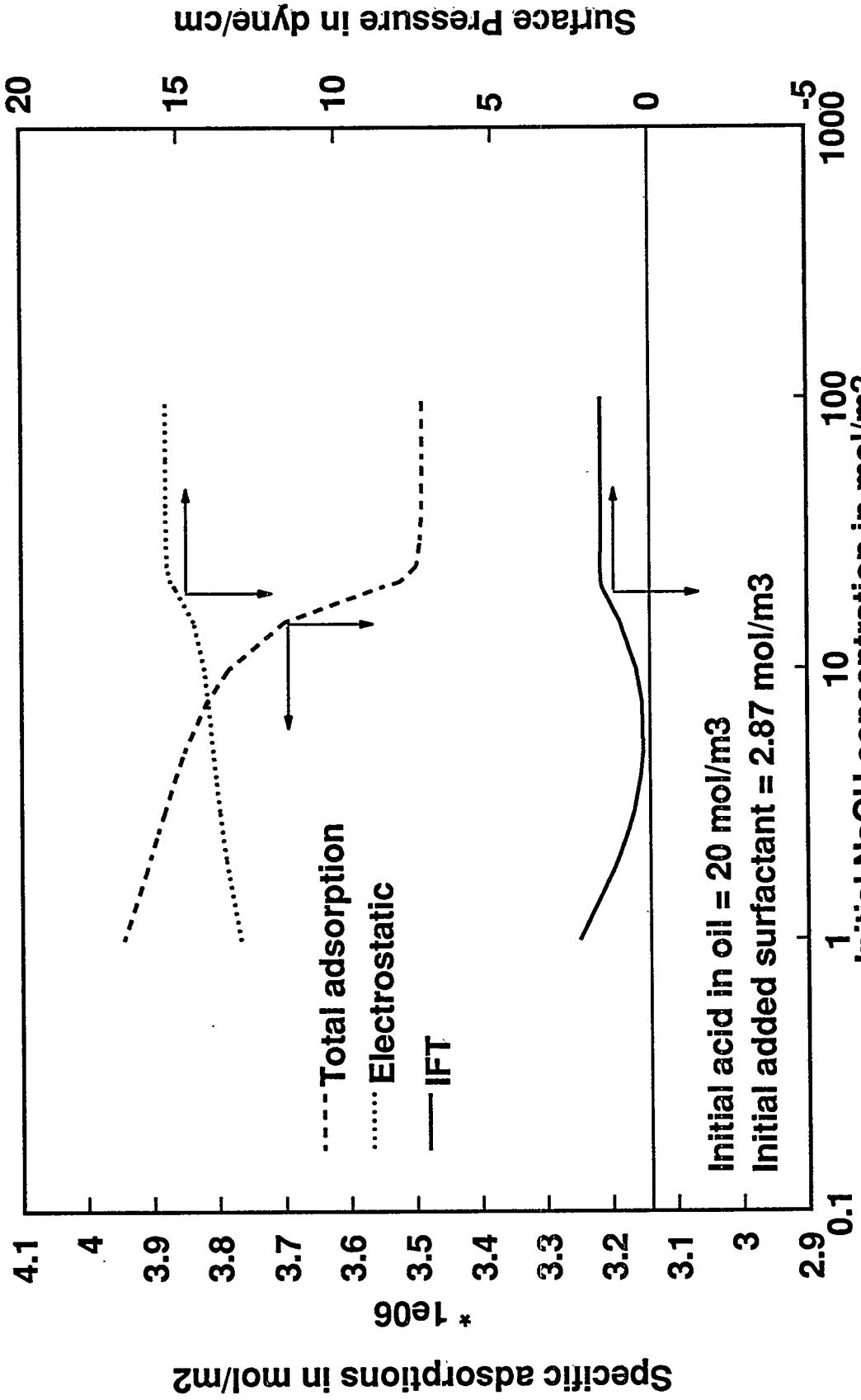

Figure 3-5. **Predicted IFT, total adsorption and the electrostatic contribution to surface pressure.**

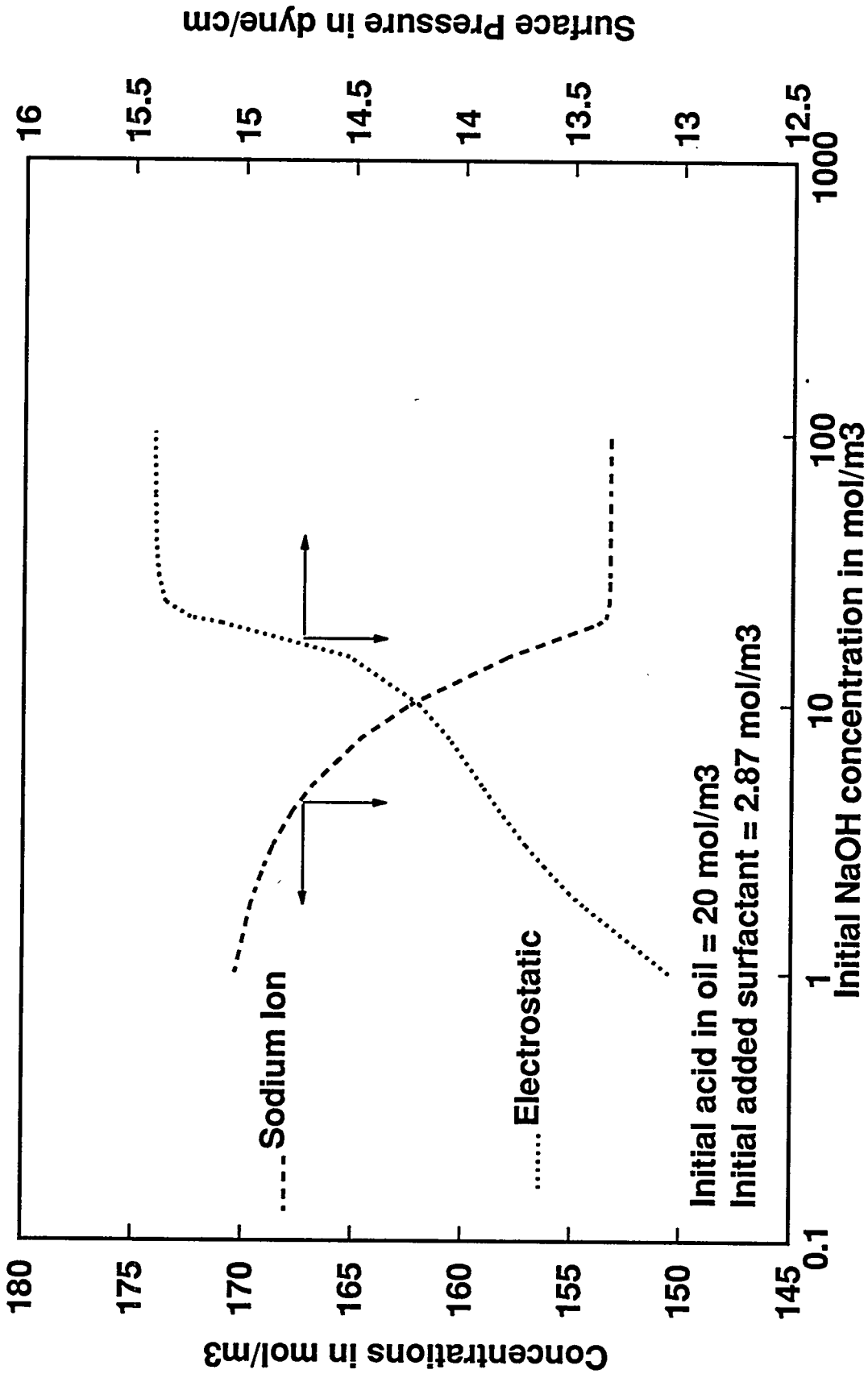

Figure 3-6. **Predicted variation of sodium ion concentration over initial alkali concentration and the electrostatic contribution to surface pressure.**

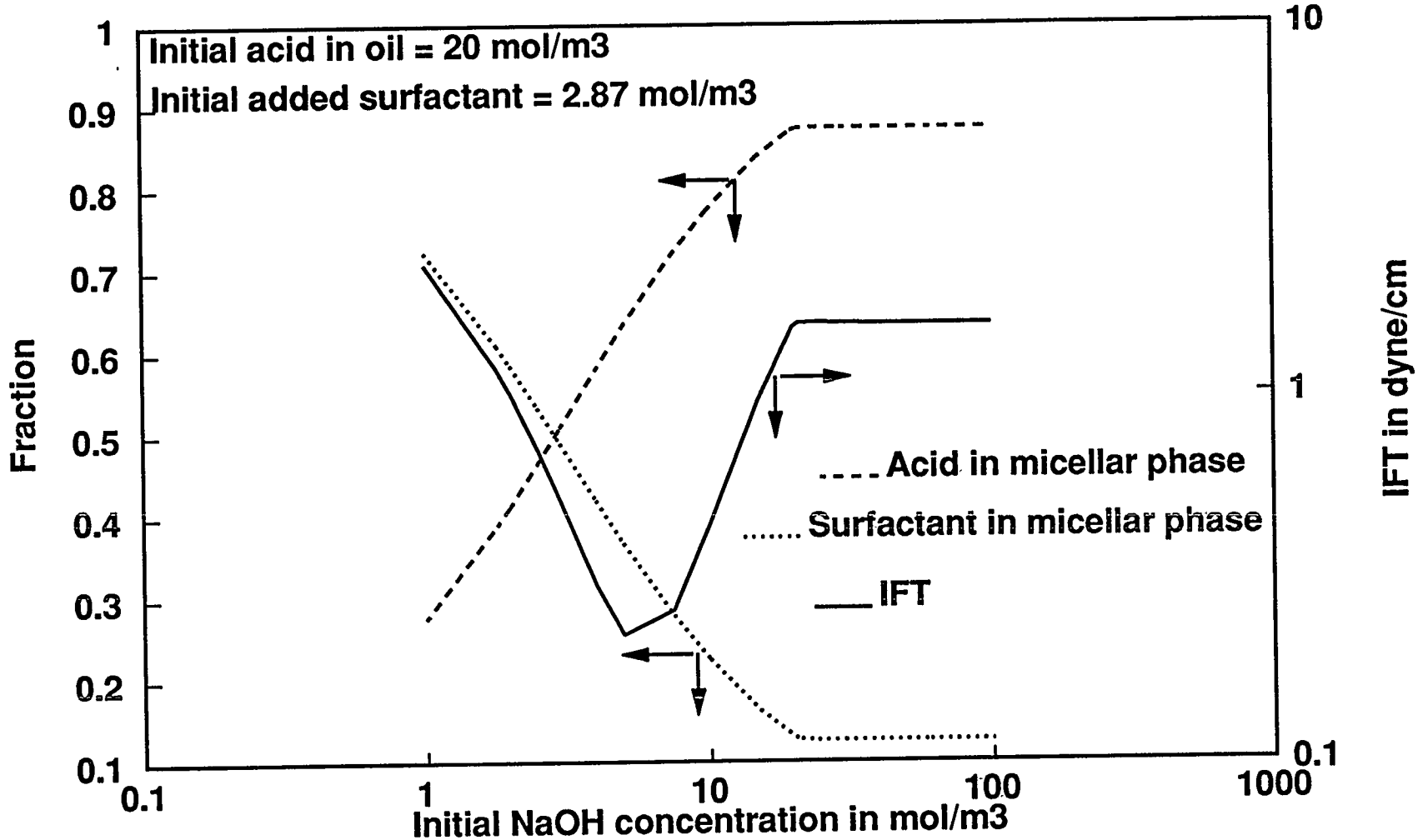

Figure 3-7. **Predicted variation of the mole fraction of surface active components in the micellar phase with initial alkali concentration.**

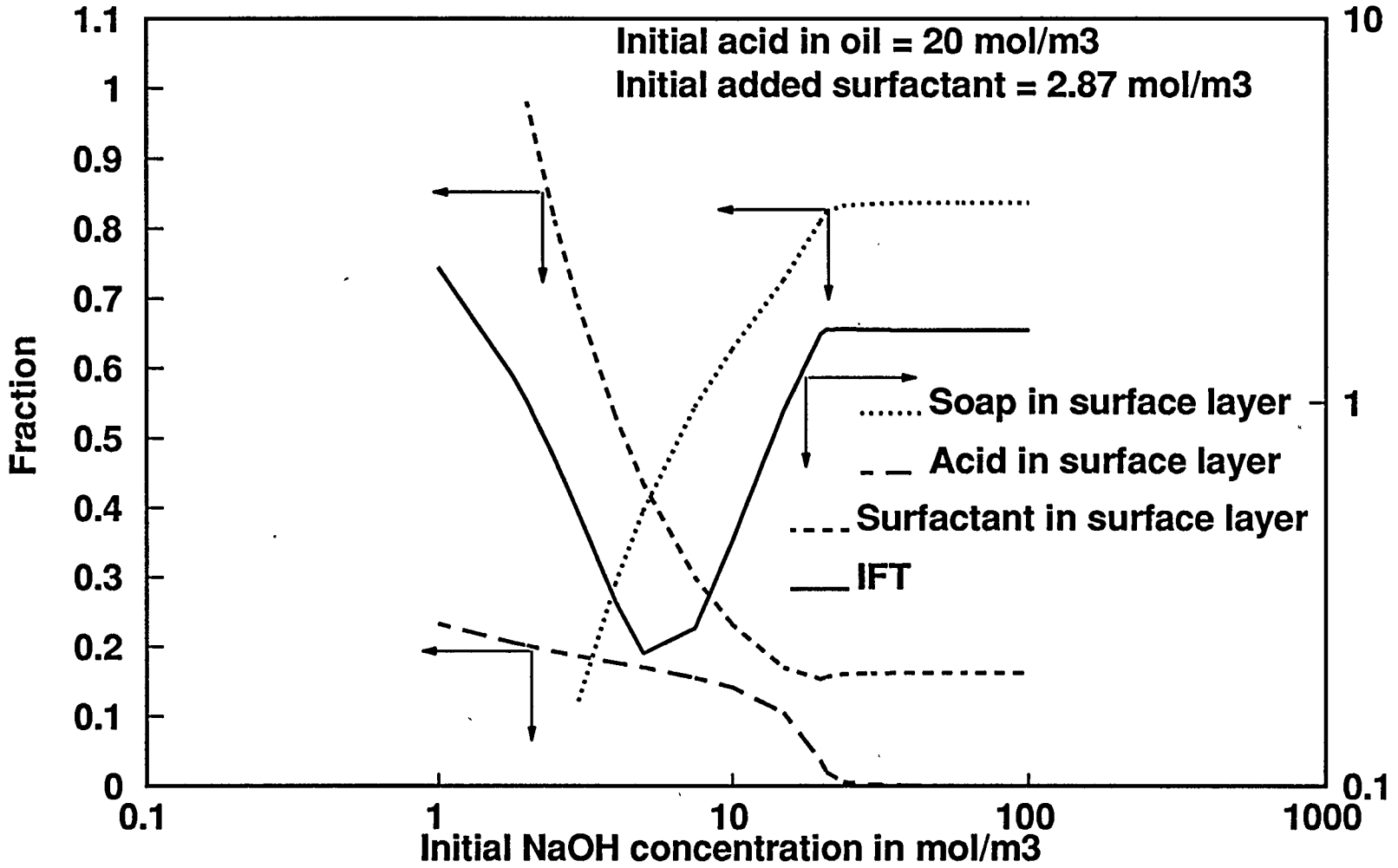

Figure 3-8. **Predicted variation of the mole fraction of surface active components in the interfacial monolayer with initial alkali concentration.**

clearly, the minima in the interfacial tension occurs when the mole fractions are similar.

Figure 3-9 shows the effect of the various interaction parameters on the computed IFT curve. It can be seen that the minima in the IFT is predicted by several combinations of the interaction parameters. Figure 3-10 shows the effect of a change in the acid partition coefficient, which is a very critical parameter, on the position of the minima.

CONCLUSIONS

The minima in IFT observed over added alkali concentration, when an acidic oil is contacted with an alkaline surfactant solution in which the total added Na^+ concentration is kept constant, is due to a combination of two factors.

The first factor appears to be the decrease in total adsorption but increase in the electrostatic contribution to surface pressure with the increase in initial alkali concentration. This is because though the added Na^+ concentration is constant, the equilibrium Na^+ decreases as alkali is increased, because of the increase in the total micellar phase. The micellar hold-up clearly increases with increase in alkali. At very high Na^+ concentration adsorption at the interface is high but the electrostatic contribution is low. At low Na^+ concentration adsorption is low but the electrostatic contribution is high. The minima occurs at a point between the two where the net effect of the two peaks.

Mixtures of surfactants have been known to show lower IFTs than either alone. There is evidence to suggest that the cmcs in mixtures of soaps and sodium dodecyl benzene sulphonates are higher than what is predicted by assuming that the micellar phase behaves ideally (Rosen, 1989). Thus, if a similar positive deviation is absent in the adsorbed layer, the interfacial

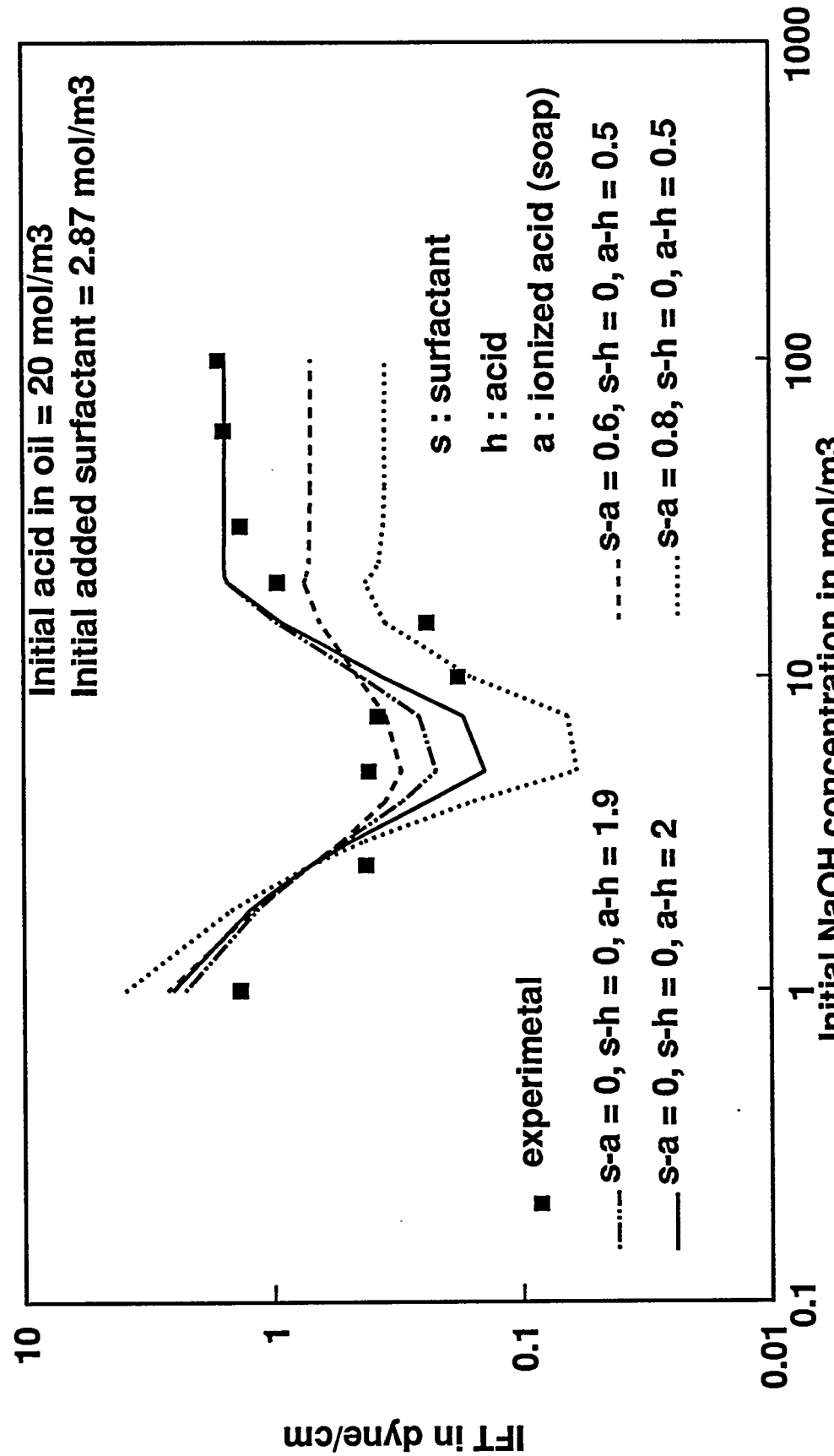

Figure 3-9. **The effect of the micellar phase interaction parameters on the predicted IFT and its comparison to experimental data.**

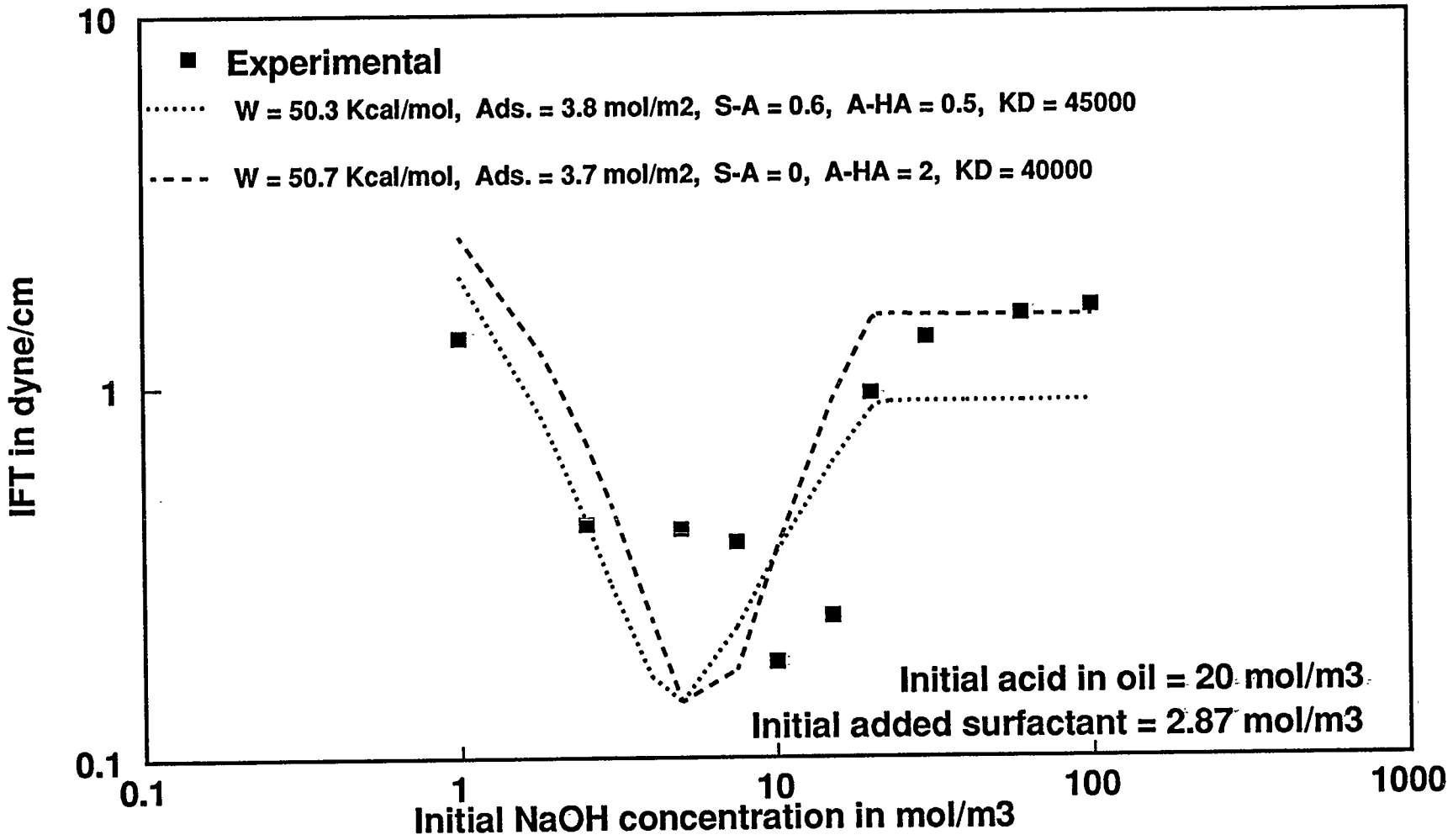

Figure 3-10. **The effect of the acids partion coefficient (KD), surfactant parametrs and the interaction parameters on the predicted IFT.**

tension in a mixture of these two types of surfactants, would be lower than achievable by either alone. It has been suggested (Rosen, 1989) that the net interaction in the adsorbed layer between these two types of surfactants amounts to a negative deviation from ideality. Thus clearly a mixture of these two surfactants would cause additional lowering of IFT. A similar mechanism appears to be occurring in this system. The alkali concentration controls the ratio of the surface active compounds in the micelles and consequently at the interface. The effect of this non-ideality would peak at the point where the fractions of the surface active compounds are similar.

NOMENCLATURE

M	Micellar phase hold-up
K_D	Acid oil/water partition coefficient
α	Fraction of unbound sites on a micelle
x	mole fraction in the micelle
N	Aggregation number of the micelle
ß	Counter-ion binding parameter
τ	activity coefficient in the micellar phase
c	concentrations
w	micellar interaction parameter
K	reaction equilibrium constant
$ß_{SA}$	Micellar interaction parameter between soap and surfactant
$ß_{SH}$	Micellar interaction parameter between acid and surfactant
$ß_{AH}$	Micellar interaction parameter between acid and soap

V Volume

K_d Dimerization equilibrium constant

K_s Surfactant oil/water partition coefficient

V_R Oil/water volume ratio

K_A Acid dissociation constant

K_w Water dissociation constant

$n_{A,max}$ Maximum adsorption of soap

$n_{S,max}$ Maximum adsorption of surfactant

$n_{H,max}$ Maximum adsorption of acid

R Universal gas constant, J/molK

T Absolute temperature

εm Dielectric constant of the aqueous phase

ε electronic charge in coulombs

N' Avogadro number

k Boltzmann's constant

Φ surface potential

Subscripts

o oil

w water

i initial amount

S surfactant

A ionized acid

Na+ Sodium ion

N,2 NaCl

1 NaOH

HA unionized acid

MA micelle of A

MS micelle of S

M mixed micelle of A and S

w water

o oil

Superscripts

p Pure surfactant cmcs

* Pure surfactant cmcs

REFERENCES

3-1. Rosen M. J., "Surfactants and Interfacial Phenomena", Wiley Interscience, 1989, 401.

3-2. Rudin J. and Wasan D. T., "Mechanism for lowering of Interfacial tension in Alkali/Acidic Oil Systems: Effect of Added Surfactant", *Ind. Eng. Chem. Res.*, Vol. **31**, No 8, 1992, 1899-1906.

3-3. Ramakrishnan T. S., PhD Thesis, Illinois Inst. of Tech., (1985).

3-4. Holland P. M., Rubingh D. N., "Nonideal multicomponent mixed micelle model", *J. Phys. Chem.*, **87**, (1983), 1984-1990.

3-5. Kamrath R.F., Frances E.I.,"Thermodynamics of mixed micellization. Pseudo-phase separation models.", *Ind. Eng. Chem. Fundam.*, **22**, (1983), 230-239.

3-6. Jones E. R., Bury C. R., *Philos. Mag.*, (1927), **4**, 841.

3-7. Murray R. C., Hartley G. S., *Trans. of Faraday Soc.*, (1935), **31**, 183.

3-8. Kamrath R. F., Frances E. I., *J of Phys. Chem.*, (1984), **88**, 1642- 1648.

3-9. Kamrath R. F., Frances E. I., "Phenomena in mixed surfactant systems", ACS symposium series.

3-10. Rudin J., Wasan D.T., "Mechanisms for lowering of IFT in alkali/acidic oil systems,2. Theoretical studies.", *Colloids and Surfaces*, **68**, (1992), 81-94.

3-11. Rudin J., PhD Thesis, Illinois Inst. of Tech., (1991).

3-12. Osborne-Lee I. W., Schechter R. S., Wade W. H., Barakat Y., *J. of Colloid Interface Sci.*, Vol. **108**, 1, (1985), 60-73.

3-13. Hall D. G., Huddleston R. W., "A regular solution treatment of the micelle point in surfactant mixtures of different types.", *Colloids and Surfaces*, **13**, (1985), 209-219.

☆U.S. GOVERNMENT PRINTING OFFICE: 1995 - 660-029/20008